

Thesis

presented for the

Degree of Doctor of Philosophy

in the

University of Southampton

entitled

COMPLEXES OF TERVALENT

VANADIUM AND CHROMIUM

by

P.T. Greene, B.Sc., A.R.I.C.

June 1967

## FOREWORD

The research described in this thesis was carried out in the chemical laboratories of the Universities of Southampton and Reading between October 1964 and May 1967.

I should like to express my sincere thanks to my supervisor, Professor G.W.A. Fowles, for his advice, guidance and encouragement throughout the course of this work.

I should also like to thank Dr. J.S. Wood for his invaluable assistance with the crystallographic work and many helpful discussions, and my wife for her advice and help with computer programming and her constant support and encouragement.

The assistance of the technical staffs at Southampton and Reading is gratefully acknowledged and I wish to record my appreciation to my colleagues for useful discussions and many enjoyable times.

Finally, I thank the Science Research Council for the award of a maintenance grant.

ABSTRACT

FACULTY OF SCIENCE

CHEMISTRY

Doctor of Philosophy

COMPLEXES OF TERVALENT  
VANADIUM AND CHROMIUM

by Peter Townsend Greene

A summary of the coordination chemistry of vanadium is followed by a consideration of the theoretical principles underlying the physical methods used for structure determination. The various experimental techniques employed during the course of the work are discussed in the appendices.

The reactions of vanadium(III) chloride and bromide (or their trimethylamine and acetonitrile complexes) with pyridine, 2,2'-bipyridyl and 1,10-phenanthroline have been studied. With pyridine, the adducts  $VX_3 \cdot 3py$  are isolated, but the products obtained when the bidentate ligands are used depend on the reaction conditions and starting materials. With excess ligand, compounds of the type  $VX_3 \cdot 2B$  (B = phen, X = Cl, Br; B = bipy, X = Br) are formed and are

characterized as the cationic species cis  $[VX_2B_2]X$ . The adduct  $2VCl_3, 3bipyr$  is assigned the ionic structure  $[VCl_2(bipyr)_2][VCl_4(bipyr)]$ . Several neutral species e.g.  $VCl_3, bipyr, CH_3CN$  are also obtained. Spectroscopic data are consistent with the presence of a six coordinate vanadium(III) species in all these complexes.

The reaction of tetrahydrofuran (THF) and 1,2-dimethoxyethane ( $C_4H_{10}O_2$ ) with vanadium(III) chloride and bromide yield the complexes  $VX_3, 3THF$  ( $X = Cl, Br$ ) and  $VX_3, 1.5C_4H_{10}O_2$ ; thermal decomposition of the latter compounds gives the adducts  $VX_3, C_4H_{10}O_2$ . The spectroscopic and magnetic properties of these compounds have been interpreted on the basis of six coordinate vanadium(III) species.

In addition to the previously reported five coordinate complexes  $VX_3, 2N(CH_3)_3$  ( $X = Cl, Br$ ) and  $VCl_3, 2S(CH_3)_2$ , some new compounds, namely  $VBr_3, 2S(CH_3)_2$ , the tetrahydrothiophen ( $C_4H_8S$ ) adducts  $VX_3, 2C_4H_8S$  ( $X = Cl, Br$ ) and  $CrCl_3, 2N(CH_3)_3$  have been synthesized. A variety of physical data indicates that all the complexes are five coordinate in benzene solution; in the solid, the sulphide adducts appear to contain six coordinate vanadium(III) species,

whereas the trimethylamine adducts retain their five coordinate geometry.

A molecular structure determination of  $\text{CrCl}_3 \cdot 2\text{N}(\text{CH}_3)_3$  by single crystal X-ray diffraction confirms that the molecule is pentacoordinate in the solid state with  $\text{C}_{2v}$  symmetry.

TABLE OF CONTENTS

	Page
<u>PREFACE</u>	
<u>CHAPTER ONE - The Chemistry of Vanadium</u>	1-15
Introduction	1
The binary halides of vanadium	2
Coordination chemistry of vanadium	4
<u>CHAPTER TWO - Theoretical Principles Underlying the Physical Methods used for Structure Determination</u>	16-46
A. Molecular weight measurements	16
B. Measurement of conductivity	17
C. Spectroscopic methods	
I Infrared spectra	19
II Visible and ultraviolet spectra	26
D. Magnetic properties	35
E. Crystal structure analysis using X-rays	43
<u>CHAPTER THREE - Complexes of Vanadium(III) Halides with Tertiary Heterocyclic Nitrogen Donors</u>	47-72
Introduction	47
I - Reaction of $VX_5 \cdot 2NMe_3$ (X = Cl, Br) with pyridine	48
Discussion	49

	Page
II - Reaction of vanadium(III) halides (or their derivatives) with 2,2'-bipyridyl and 1,10-phenanthro- line	55
Discussion	60
<u>CHAPTER FOUR - Complexes of Vanadium(III) Halides with Ether Donor Molecules</u>	73-84
Introduction	73
Preparation of the complexes	73
Results and Discussion	75
Discussion of the Charge-Transfer spectra of six-coordinate vanadium(III) complexes	82
<u>CHAPTER FIVE - Five-coordinate Complexes</u>	85-102
Introduction	85
Experimental	
1. Reaction of vanadium(III) chloride and bromide with dimethylsulphide	86
2. Reaction of vanadium(III) chloride and bromide with tetrahydrothiophen	87
3. Reaction of chromium(III) chloride with trimethylamine	87
Results and Discussion	92

	Page
<u>CHAPTER SIX - Crystal and Molecular Structure of trichloro- bistrimethylamine- chromium(III)</u>	103-113
Introduction	103
Experimental data	104
Determination of the structure	105
Results and Discussion	108
<u>APPENDIX A - Starting Materials and Analytical Methods</u>	114-121
I - Preparation and purification of starting materials	
a) gases	114
b) liquids	114
c) halides	116
d) solid ligands	118
e) complex compounds	118
II - Analytical procedures	
a) vanadium analysis	119
b) chromium analysis	120
c) halogen analysis	120



	Page
<u>APPENDIX B - Experimental Techniques</u>	122-142
I - Vacuum line techniques	122
II - Experimental aspects of structural investigations	
a) molecular weight determination	127
b) measurement of conductivity	128
c) magnetic susceptibility measurement	
(i) room temperature susceptibility	130
(ii) measurement of variation of magnetic susceptibility with temperature	133
d) spectral measurements	
(i) infrared spectra	135
(ii) visible and ultraviolet spectra	136
e) X-ray diffraction techniques	139
<u>APPENDIX C - Observed and Calculated Structure</u>	143
<u>Amplitudes for trichlorobistri-</u> <u>methylaminechromium(III)</u>	pp(i)-(viii)

REFERENCES

## PREFACE

The work described in this thesis forms part of a research programme (under the direction of Professor G.W.A. Fowles) the aim of which is the elucidation of the complex chemistry of the early transition elements.

This research is concerned with the preparation and characterisation of some complex compounds of vanadium(III) chloride and vanadium(III) bromide, and emphasis is placed on the measurement of their spectroscopic and magnetic properties. The range of known six-coordinate vanadium(III) complexes is extended, and five-coordinate adducts with organo-sulphur donors are prepared and characterised. The synthesis of trichlorobis(trimethylamine)chromium(III) is described and a single crystal X-ray study shows that the molecule possesses pentacoordinate geometry in the solid state.

The experimental results are preceded by a survey of the existing chemistry relevant to the work, and a discussion of the physical methods used for structure determination.

CHAPTER ONE

THE CHEMISTRY OF VANADIUM

## Introduction

Vanadium is a typical transition element belonging to the first transition series, which, for the purpose of this thesis embraces those elements lying between scandium and zinc in the periodic table. The element possesses a ground state with an incomplete "d" shell, namely  $[\text{Ar}]3d^34s^2$ , it has the ability to form complex compounds in formal oxidation states ranging from +5 to -1, and many of its complexes are paramagnetic, exhibiting a wealth of colours.

## The Chemistry of Vanadium

In common with other first row elements, the chemistry of vanadium differs from the other members of its sub-group, which belong to the second and third transition series. Whereas with vanadium, the lower oxidation states +4 and +3 are readily accessible and more important than the +5 state, the known chemistry of the lower members of the sub-group VA, niobium and tantalum, is more or less restricted to the highest oxidation states, +5 and +4. Vanadium shows little resemblance to its immediate non-metallic neighbour, phosphorus, except in the +5 oxidation state. Both form, for example, covalent oxyhalides,  $\text{POCl}_3$  and  $\text{VOCl}_3$ , which

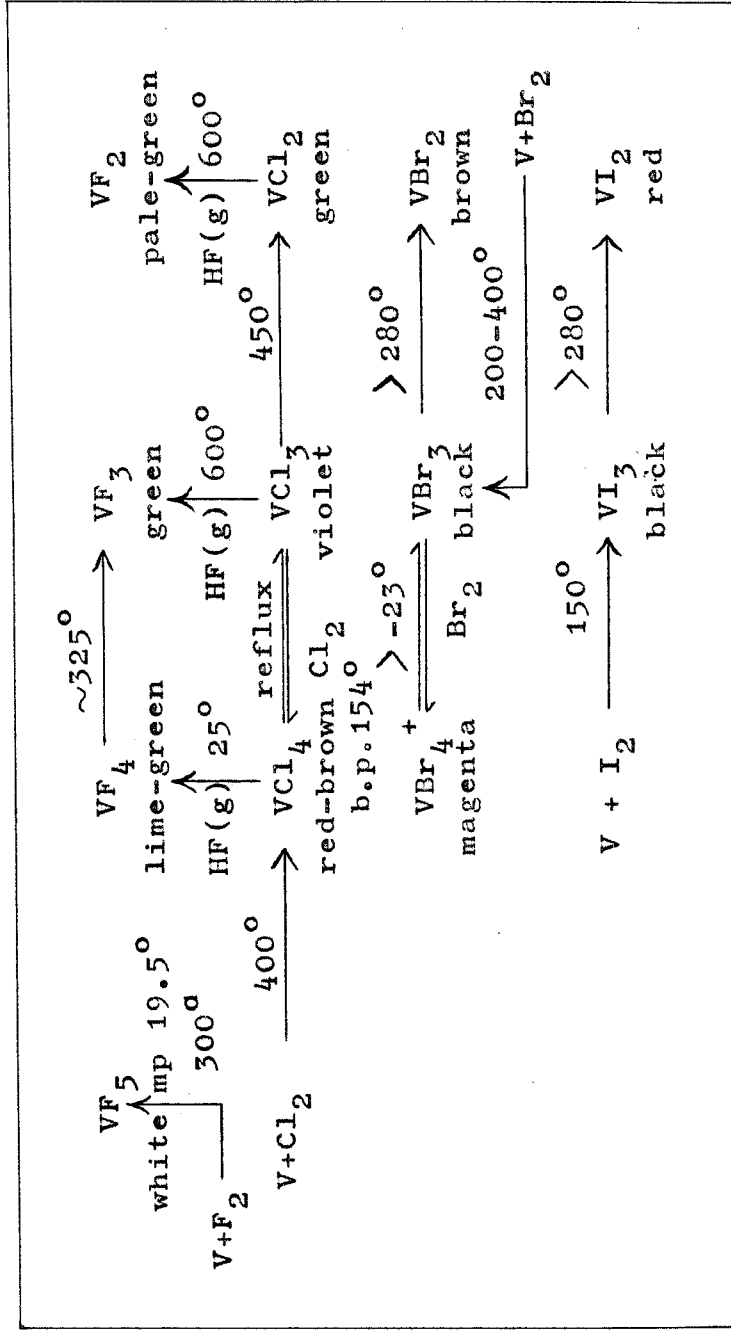
have similar physical properties, and a variety of anionic oxy-complexes such as vanadates and phosphates. However, the difference between the elements is more apparent when the chemistry of the lower oxidation states is examined. Phosphorus exists only in the +3 state, whilst vanadium behaves as a typical transition element, exhibiting multivalency and paramagnetism.

The discussion of the chemistry of vanadium which follows will be limited mainly to the halides and their complexes, since this is the most relevant background to the work described later in this thesis. A rigorous discussion of the aqueous chemistry of vanadium has been omitted, and no mention, except where relevant, has been made of complexes derived from the oxovanadium(IV) cation, whose extensive chemistry has been summarised recently in two reviews.<sup>1,2</sup> An account of the early work on vanadium chemistry has been given by Sidgwick,<sup>3</sup> and a comprehensive review on the coordination chemistry of vanadium has recently been published.<sup>4</sup>

(i) The Binary Halides of Vanadium

The preparative routes to these halides are summarised in table 1.1. The only pentavalent halide is vanadium(V) fluoride, a low melting solid which is a powerful fluorinating and oxidising agent.<sup>5</sup> The existence of  $\text{VCl}_5$  has been discussed<sup>6</sup> and it has been concluded from

\*Table 1.1 Preparation and Properties of Vanadium Halides



+ ref. 7

\* ref. 12

thermodynamic considerations that its formation from the stable  $\text{VCl}_4$  would not be feasible. Of the halides in oxidation state +4, all but the iodide are known, but their stability to dissociation to the corresponding vanadium(III) halides decreases rapidly in the order  $\text{VF}_4 > \text{VCl}_4 \gg \text{VBr}_4$ .

$\text{VF}_4$  is a lime-green solid with a room temperature magnetic moment of 1.65 B.M.<sup>8</sup> The structure of the solid, which turns brown on exposure to air, is unknown, but vanadium probably achieves six coordination via fluorine bridging.  $\text{VCl}_4$  is a red-brown, oily liquid which is violently hydrolysed by water. An electron diffraction investigation<sup>9</sup> has confirmed earlier spectroscopic<sup>10</sup> and magnetic<sup>11</sup> measurements which demonstrated that  $\text{VCl}_4$  is monomeric and tetrahedral. A V-Cl bond length of  $2.138 \pm 0.002 \text{ \AA}$  was found.  $\text{VBr}_4$  is stable only below  $-23^\circ\text{C}$  at which temperature it spontaneously decomposes to  $\text{VBr}_3$  and bromine.<sup>7</sup>

All four trihalides are known.  $\text{VF}_3$  is a green solid melting above  $800^\circ\text{C}$ , and is insoluble in water, although a trihydrate is known.<sup>3</sup> In contrast,  $\text{VCl}_3$ ,  $\text{VBr}_3$  and  $\text{VI}_3$  are all readily hydrolysed by water and are thermally unstable, decomposing to the corresponding dihalides when heated (see table 1.1). Although  $\text{VCl}_3$ ,  $\text{VBr}_3$  and their titanium(III) analogues have the same hexagonal close-

packed  $\text{BiI}_3$  structures,<sup>13</sup> their magnetic properties are very different.<sup>14</sup>  $\text{VCl}_3$  and  $\text{VBr}_3$  follow a Curie-Weiss law behaviour with room temperature moments near 2.70 B.M. whilst their titanium analogues are strongly antiferromagnetic.

Little is known of the dihalides.  $\text{VCl}_2$ ,  $\text{VBr}_2$ , and  $\text{VI}_2$  have the hexagonal close-packed  $\text{CdI}_2$  structure<sup>13,15</sup> and are antiferromagnetic.  $\text{VCl}_2$  is an unreactive green, leaf-like solid, soluble with difficulty in water and stable in air.

(ii) The Coordination Chemistry of Vanadium

As the basicity of vanadium increases with decreasing oxidation number, the most stable complexes of vanadium(V) are anionic, whilst the known complexes of vanadium(II) are predominantly cationic, and the stabilities of complexes of vanadium(IV) and (III) lie between these two extremes.

(a) Oxidation state +5

The presence of oxygen or fluorine is required to stabilise the highest oxidation state of vanadium, which has an empty "d" shell, giving rise to diamagnetic compounds. The only binary halide known is  $\text{VF}_5$ , but the oxyhalides,  $\text{VOX}_3$  (where X = F, Cl, Br) have been prepared.<sup>3</sup> These compounds are readily hydrolysed liquids, whose infrared spectra<sup>16-18</sup> have been shown to be consistent



with their monomeric formulation with  $C_{3v}$  symmetry.

Neutral complexes of vanadium(V) are limited mainly to those formed by the oxyhalide  $VOCl_3$ .  $VOCl_3$  undergoes either addition reactions with donor molecules to produce complexes of the type  $VOCl_3 \cdot 2L$  ( $L =$  acetonitrile,  $\frac{1}{2}$ bipyr, for example),<sup>4</sup> or it may participate in a variety of solvolytic reactions with alcohols, phenols and carboxylic acids,<sup>4</sup> exemplified by the preparation of  $VO(OCH_3)_3$  from  $VOCl_3$  and methanol.<sup>19</sup> The structure of  $VO(OCH_3)_3$  has recently been deduced by X-ray analysis<sup>20</sup> to be a polymeric system of dimers linked by methoxyl bridges, in which the vanadium atom is six coordinate. This may be compared with  $VOCl_3$  in which vanadium is in an essentially tetrahedral environment.<sup>17</sup>

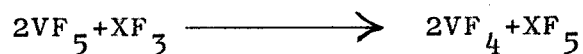
Interesting neutral adducts,  $2XeF_6 \cdot VF_5$  and  $2XeOF_4 \cdot VF_5$ , have been prepared by allowing the appropriate inert gas compound to react with  $VF_5$ ;<sup>21</sup> the structures of these adducts are unknown. Several anionic fluoro complexes, including the hexafluorovanadate(V) anion are known,<sup>3,4,12</sup> but the only other anionic halogeno complex reported, appears to be  $[VOCl_4]^-$ .<sup>3</sup>

(b) Oxidation state +4

The electronic configuration of vanadium in this oxidation state is  $[Ar] 3d^1$ ; complexes are therefore paramagnetic and of spectroscopic interest. This is the

most important and widely studied oxidation state of vanadium, which is dominated by the chemistry of compounds derived from the oxovanadium(IV) species whose properties will not be discussed here.

$\text{VF}_4$  forms 1:1 adducts with ammonia, pyridine and selenium(IV) fluoride.<sup>8</sup> The structures of these compounds are unknown, but the ammonia and pyridine derivatives are believed to be fluorine bridged polymers. If  $\text{VF}_5$  is allowed to react with  $\text{XF}_3$  (X = P, As, Sb) then the first product of the reaction is  $\text{VF}_4$ :<sup>8</sup>



$\text{VF}_4$  will then react with  $\text{XF}_5$ , and complexes formulated as  $\text{VF}_3^+ \text{XF}_6^-$  have been isolated. The anion  $\text{XF}_6^-$  was identified by its infrared spectrum, but the nature of the  $\text{VF}_3^+$  species is unknown; it may be a fluorine-bridged polymer.

Vanadium(IV) chloride may undergo addition, solvolytic or reduction reactions depending upon the nature of the ligand and the experimental conditions. Some nitrogen or sulphur donors cause reduction to vanadium(III),<sup>4</sup> but generally, this may be avoided if dilute solutions of ligands in inert solvents are used, and the reaction performed at low temperatures. A wide variety of complexes with bidentate and monodentate ligands has been reported,<sup>4</sup> and their spectroscopic and magnetic properties have been

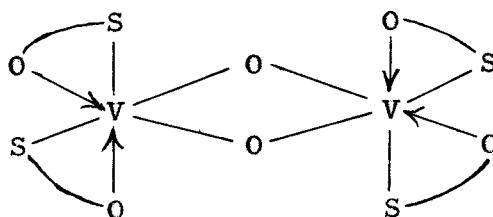
interpreted in terms of octahedral structures with tetragonal distortions. The complexes are very susceptible to hydrolysis.

Seven coordinate vanadium(IV) has been claimed recently to account for the properties of the complexes  $VCl_4 \cdot tas$  where *tas* is either of the terdentate arsenic ligands *o-tas* (bis(*o*-dimethylarsinophenyl)methylarsine) or *v-tas* (tris 1,1,1(dimethylarsinomethyl)ethane).<sup>22</sup> These compounds are monomeric and isomorphous with their titanium(IV) chloride analogues, whose N.M.R. spectra show that all the arsenic atoms are coordinated to the metal. The 1:2 adduct formed when  $VCl_4$  interacts with *o*-phenylenebisdimethylarsine (*diars*),<sup>23</sup> is isostructural with its titanium(IV) analogue, which has been shown by X-ray structure analysis<sup>24</sup> to possess an eight coordinate stereochemistry. It is interesting to note that the analogous *o*-phenylenebisdiethylarsine yields only a 1:1 complex when it reacts with  $VCl_4$ .<sup>25</sup>

Although vanadium(IV) chloride is violently hydrolysed to species containing oxovanadium(IV) with water, other protonic solvents cause incomplete solvolysis. Generally, two vanadium-chlorine bonds are solvolysed by primary and secondary amines,<sup>26</sup> and alcohols,<sup>27</sup> but no reduction to the trivalent state occurs.

A novel complex containing no halogens or oxo-

vanadium(IV) species has been synthesised by reacting  $\text{VOSO}_4$  with TTMBH ( $\text{C}_4\text{H}_3\text{SC}(\text{SH}) = \text{CHCOCF}_3$ ).<sup>28</sup> It is dimeric in nitrobenzene and has been assigned the following structure:



### Anionic Complexes

Hexahalogenovanadates(IV) have been isolated with fluorine and chlorine as donor atoms. Reaction of vanadium(IV) fluoride with potassium fluoride in selenium(IV) fluoride yields  $\text{K}_2\text{VF}_6$ <sup>8</sup> which obeys the Curie-Weiss law with a room temperature magnetic moment of 1.76 B.M. The hexachlorovanadate(IV) anion has now been stabilised with a variety of cations.<sup>29,30</sup> The dark-red solids have room temperature magnetic moments near 1.73 B.M. and their visible spectra contain a broad, asymmetric band at  $\sim 15,000 \text{ cm.}^{-1}$  assigned to the  ${}^2\text{E}_g \leftarrow {}^2\text{T}_{2g}$  transition. The asymmetry in the band is due to the presence of a Jahn-Teller distortion. Oxotetrachlorovanadate(IV) and oxotrichlorovanadate(IV) anions,  $[\text{VOCl}_4]^{2-}$  and  $[\text{VOCl}_3]^-$  have been precipitated from saturated ethanolic hydrogen chloride solutions of vanadium(IV) by addition of the

appropriate basic chloride. Their physical properties have been investigated,<sup>30,31</sup> but their structures are uncertain.

(c) Oxidation State +3

The configuration  $3d^2$ , which has been the subject of extensive theoretical treatment, is the electronic ground state of vanadium(III). The spectral<sup>32</sup> and magnetic<sup>14</sup> properties of many octahedral vanadium(III) complexes have been explained using a ligand field model which requires the presence of a trigonal distortion of the regular octahedral field. Vanadium(III) forms cationic, neutral and anionic complexes, with the metal attaining its usual coordination number of six; however, four and five coordinate compounds are also known.

Cationic Complexes

The most common cationic species is the green hexa-aquovanadium(III) ion whose spectral properties have been extensively studied in solution,<sup>33</sup> and its magnetic properties as the alum  $\text{NH}_4\text{V}(\text{SO}_4)_2 \cdot 12\text{H}_2\text{O}$ .<sup>34</sup> When ethylene and propylenediamine react with vanadium(III) chloride, compounds of stoichiometry  $\text{V}(\text{en})_3\text{Cl}_3$  and  $\text{V}(\text{pn})_3\text{Cl}_3$  are isolated in which the vanadium is believed to exist as the cationic species,  $\text{V}(\text{en})_3^{3+}$  ( $\text{V}(\text{pn})_3^{3+}$ ).<sup>35,36</sup>

### Neutral Complexes

$VCl_3$  and  $VBr_3$  both have polymeric structures and they react slowly with donor molecules. Comparatively few complexes with monodentate ligands have been reported and only the 3:1 adducts formed by reaction of the halides with nitriles<sup>68</sup> appear to have been well characterised. Clark<sup>22</sup> reports the preparation of the complexes  $VCl_3,otas$  and  $VCl_3,vtas$ , where *otas* and *vtas* are the terdentate arsenic ligands described earlier. The complexes are monomeric and low infrared spectral data indicate that the three chlorines possess a cis configuration.

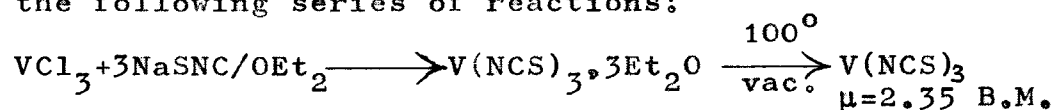
Alcohols do not solvolyse vanadium(III) chloride but form addition compounds such as  $VCl_3,3C_2H_5OH$ , which is a green solid.<sup>38</sup>

The interaction of liquid ammonia with  $VCl_3$ <sup>39</sup> or  $VBr_3$ <sup>40</sup> causes ammonolysis of one vanadium-halogen bond, and a mixture of solvolysis products is obtained.

Carboxylates of the form  $V(OOC.R)_3$  prepared from vanadium(III) chloride appear to be normal trivalent vanadium complexes with magnetic moments around 2.7 B.M.<sup>4</sup> However, if vanadium diboride ( $VB_2$ ) is allowed to react with acetic or benzoic acids, carboxylates of the form  $V(O_2CR)_3$  are produced, the acetate derivative being dimeric in freezing acetic acid. Although vanadium is in oxidation state +3, the magnetic properties of these compounds are

complicated as the room temperature magnetic moment is only 0.77 B.M. per vanadium. On the basis of magnetic, infrared and N.M.R. data, a dimeric structure with four bridging carboxylate molecules has been proposed,<sup>41</sup> by analogy with the known structure of the diamagnetic chromium(II) acetate dihydrate.<sup>12</sup>

The pseudo halide  $V(NCS)_3$  has been isolated by the following series of reactions:<sup>42</sup>



Recently, complexes of this Lewis acid have been prepared direct from vanadium(III) halides by reaction with alkali thiocyanates in various organic media.<sup>43</sup> In this way, complexes such as  $[V(NCS)_3, (CH_3CN)_3], 2CH_3CN$  and  $V(NCS)_3, 3THF$  were isolated from acetonitrile and tetrahydrofuran solutions respectively.

#### Anionic Complexes

Complexes of the type  $VX_6^{3-}$  have now been prepared when  $X = F,$ <sup>3</sup>  $Cl,$ <sup>44</sup>  $Br,$ <sup>44</sup>  $NCS,$ <sup>45</sup>  $NCSe,$ <sup>46</sup> and the spectral and magnetic properties of the hexahalogenosalts have been investigated. Several hydrated fluoro and chloro-anions such as  $VX_5, H_2O^{2-}$  and  $VX_4, 2H_2O^-$  are also known,<sup>4</sup> and their spectroscopic properties have been interpreted on the basis of six coordinate vanadium(III) species. The binuclear complex  $V_2Cl_9^{3-}$  has been isolated as its

tetraethylammonium salt,<sup>47</sup> which is isomorphous with its titanium(III) and chromium(III) analogues.<sup>48</sup>

Six coordinate anionic complexes of the type  $M^+[VX_4, 2L]^-$  have been synthesised with a variety of nitrogen donors.<sup>49</sup> Thus for X = Cl, ligands used include acetonitrile, pyridine and 2,2'-bipyridyl; for X = Br, I, only acetonitrile complexes were reported. The compounds  $Ph_3CH_3As[VX_4, 2CH_3CN]$  (X = Cl, Br) undergo thermal decomposition at 80°C in vacuo when the tetrahedral species  $VCl_4^-$  and  $VBr_4^-$  are isolated.

Trisoxalato complexes of vanadium(III) are well established,<sup>4</sup> but it is only recently that the structure of the potassium salt has been determined by X-ray analysis.<sup>50</sup> The vanadium atom is in a six coordinate environment with bidentate oxalate groups, giving the anion  $D_3$  symmetry. The salt is isomorphous with its chromium, iron and aluminium analogues.

A variety of five coordinate complexes of vanadium(III) halides is now known, but discussion of these adducts is deferred until a later chapter.

#### (d) Oxidation State +2

The chemistry of this oxidation state has received little attention and few complexes have been well characterised. Cationic, neutral and anionic species are known, but, as aqueous solutions of vanadium(II) are very



susceptible to atmospheric oxidation, most work has been limited to a study of complexes formed in fused melts, or non-aqueous solvents.

### Cationic Complexes

The violet hexaaquovanadium(II) cation is readily prepared by the zinc reduction of an acid solution of vanadium(V). Addition of a solution of 2,2'-bipyridyl and potassium iodide in methanol produces a green solution from which  $V(\text{bipyr})_3\text{I}_2$  is isolated.<sup>51</sup> Its magnetic moment of 3.7 B.M. confirms the presence of divalent vanadium, which has a  $3d^3$  configuration. Other cationic compounds of vanadium(II) of the type  $\text{VL}_n^{2+}$ , where n is 4 or 6 and L = oxygen or nitrogen donor, have been stabilised with the anion  $V(\text{CO})_6^-$ .<sup>52</sup> A recent X-ray crystal structure determination<sup>59</sup> of the Tutton salt,  $V(\text{NH}_4)_2(\text{SO}_4)_2 \cdot 6\text{H}_2\text{O}$ , has established that the vanadium atom is octahedrally coordinated by water molecules, with the axial vanadium-oxygen bonds slightly shorter than those in the equatorial plane.

### Neutral Complexes

These complexes are virtually unknown. Some complexes of vanadium(II) chloride with nitrogen donors have been isolated. For example,<sup>53</sup> the pyridine complex  $\text{VCl}_2 \cdot 4\text{py}$  is a cherry-red solid with a  $\mu_{\text{eff}}$  of 3.87 B.M., and addition complexes of vanadium(II) chloride with

ammonia and methylamine are known, but they are unstable in aqueous solution and lose ligand when heated to about 70° in vacuo.<sup>54</sup>

#### Anionic Complexes

Anionic complex chlorides of divalent vanadium have been isolated from potassium or caesium chloride melts,<sup>4</sup> and, from spectral measurements on  $VCl_2$  dissolved in a LiCl-KCl eutectic, the presence of  $VCl_6^{4-}$  has been inferred.<sup>55</sup>

#### (e) Oxidation States +1, 0, -1

These low oxidation states of vanadium have been stabilised by ligands of low electronegativity such as CO,  $PPh_3$ ,  $CN^-$ , and bipyridyl and phenanthroline.<sup>4</sup>

Vanadium(I) is present in the cation  $[V(CO)_4C_6H_6]^+$ , but when this is reduced with sodium borohydride, the neutral  $\pi$ -cyclohexadienyltetracarbonylvanadium(0) is isolated.<sup>56</sup> Vanadium hexacarbonyl itself is unique amongst hexacarbonyls in possessing one unpaired electron; however, as seen above, it readily forms the anion  $[V(CO)_6]^-$  with the diamagnetic  $d^6$  "inert gas" configuration.

Perhaps the most unusual complexes of vanadium isolated in recent years have been those with dithiolate ligands. Complexes of the type  $[VS_6C_6R_6]^z$  where

$R = CF_3$ ,  $z = -2, -1$ ,  $R = C_6H_5$ ,  $z = -2, -1, 0$  have been prepared, for example, but the exact designation of an oxidation state in these adducts is difficult. E.S.R. data support the view that the unpaired electrons appeared to be strongly delocalised on the ligand. A recent X-ray structure determination<sup>58</sup> of  $[VS_6C_6(C_6H_5)_6]^0$  has shown it to possess trigonal prismatic ( $D_{3h}$ ) symmetry, rather than the expected trigonal ( $D_3$ ) coordination.

#### The Complex Chemistry of Chromium

The coordination chemistry of chromium will not be discussed; any relevant chemistry will be developed as necessary when the chromium complexes which have been prepared are compared with their vanadium analogues.

CHAPTER TWO

THEORETICAL PRINCIPLES UNDERLYING  
THE  
PHYSICAL METHODS USED FOR STRUCTURE DETERMINATION

## Introduction

In this Chapter the various methods used to elucidate the structure of a complex compound, whose empirical formula has been determined by elemental analysis, are examined. The underlying theoretical principles of these methods are briefly outlined here, and the practical aspects of these measurements are described in appendix B.

### (A) Molecular Weight Measurements

If a complex is soluble in a non-donor solvent, molecular weight measurements in that solvent will indicate the degree of polymerization in solution, and thus a molecular formula may be deduced, given the empirical constitution determined by analysis.

Molecular weight data is particularly important when odd coordination numbers are suspected. Thus  $\text{TiCl}_4 \cdot \text{NMe}_3$  was shown to be monomeric,<sup>60</sup> and hence five coordinate, in benzene solution. Molecular weight measurements in donor solvents must be interpreted with caution because of the possibility of reaction between the complex and the solvent. Unfortunately, the majority of complexes prepared in this work were insoluble in solvents suitable for molecular weight determinations. Molecular weights of suitably soluble compounds were estimated by the cryoscopic

method in benzene.

(B) Measurement of Conductivity

Conductivity measurements will detect the presence of ions in a compound when it is dissolved in a suitable solvent. Acetonitrile and nitromethane are two such solvents, since they are easily purified and have fairly high dielectric constants. Various difficulties are inherent in the measurement of conductivities in non-aqueous solvents. Firstly, the complex should give ions which are large and spherical to avoid ion-pairing, a common phenomenon in non-aqueous systems which results from the low dielectric constant of the solvent medium, compared with that of water. Ion-pairing is important in fairly concentrated solutions and is detected by a lower conductivity than expected, and deviations from linearity of the Onsager plot,  $\Delta$  (conductivity) vs. (concentration)<sup>1/2</sup>. Secondly, the ions themselves must be inert to chemical reaction with the solvent.

It has been the practice to determine the ion type of an unknown electrolyte by comparison of its conductivity with that of a known electrolyte at a similar concentration (usually  $\sim 10^{-3}$  M.) in the same solvent. Walden and Birr<sup>61</sup> have measured the conductivities of the tetraethylammonium halides, which have been used as

standards, over a range of concentrations in acetonitrile, and found that, at  $10^{-3}M$ , the conductivities decrease from a value of  $\sim 175 \text{ ohm}^{-1} \text{ cm}^2$  for the iodide to  $\sim 160 \text{ ohm}^{-1} \text{ cm}^2$  for the chloride. They noted that, as a general trend, conductivities of salts with a common cation decreased as the size of the anion decreased; these findings have more recently been confirmed by Harkness and Daggett.<sup>62</sup> It was also found that the slopes of the  $\Delta$  vs. (concentration)<sup>1/2</sup> plots for a variety of 1:1 electrolytes lie in the range 350-500. Feltham and Hayter<sup>63</sup> point out that comparisons of conductivities at one concentration are not particularly meaningful since a molecular weight of the unknown electrolyte must be assumed. They suggest measuring the conductivity of the unknown over a range of concentration, constructing an equivalent conductivity vs. (equivalent concentration)<sup>1/2</sup> plot, and comparing its slope with the slope of the  $\Delta e$  vs  $\sqrt{Ce}$  plots of known electrolyte types. In this way, both the ion type and molecular weight of the complex may be deduced.

Conductivity determinations at one concentration are still useful measurements, since the presence or absence of ions in a complex may be quickly ascertained.

(C) Spectroscopic Methods

I Infrared Spectroscopy<sup>64,65</sup>

The region of electromagnetic radiation known as the infrared extends roughly from  $50 \text{ cm.}^{-1}$  to  $10,000 \text{ cm.}^{-1}$ . In this work two distinct regions, namely  $5000 - 500 \text{ cm.}^{-1}$  and  $500 - 200 \text{ cm.}^{-1}$  were used to characterize complexes, and it is convenient to discuss these areas of the infrared spectrum separately.

Any non-linear molecule of  $N$  atoms may have  $3N-6$  normal modes of vibration, of which only a certain number will be excited when infrared radiation of the appropriate frequency is absorbed. The selection rule is that a particular normal mode will only be excited if excitation leads to a change in dipole moment of the molecule. It may be shown that an infrared active mode is one which has identical transformation properties to one or several of the Cartesian coordinates in the particular point group to which the molecule belongs. Even with these restrictions, the infrared spectra of fairly simple molecules are complicated by the presence of overtone and combination bands.

Interpretation of an infrared spectrum is greatly facilitated by the concept of "group vibrations"; certain groups of atoms or types of bonds absorb radiation over a fairly narrow range of frequencies, irrespective of the



molecule which contains the group. However, the presence of overtone and combination bands introduces a limitation to the "group frequency" concept, since these effects may produce anomalous shifts of bands from their "expected" positions in certain molecules.

(i) The 5000 to 500  $\text{cm.}^{-1}$  region

It is in this region of the spectrum that most vibrations associated with organic molecules occur. When incorporated into a complex, many of the fundamental ligand vibrational modes are modified, and therefore the detection of shifts in ligand modes compared with those in the free ligand provides evidence of coordination. The most prominent modifications occur to those functional groups bonded directly to the metal atom. For example, a reduction in the  $\text{As}=\text{O}$  stretching frequency of  $\sim 30 \text{ cm.}^{-1}$  is observed on coordination,<sup>66</sup> and the C-O-C asymmetric and symmetric stretching frequencies in tetrahydrofuran shift by about  $50 \text{ cm.}^{-1}$  on complex formation.<sup>67</sup> The behaviour of the  $-\text{C}\equiv\text{N}$  stretching mode in alkyl cyanides is an exception to this general observation, as its frequency increases by about  $40 \text{ cm.}^{-1}$  on coordination.<sup>68</sup> The reason for this anomalous increase has been the subject of much speculation, but calculations<sup>69,70</sup> indicate that the C-N  $\sigma$  bond strength increases on donation of the nitrogen

lone pair, so causing an increase in the force constant of the  $C\equiv N$  bond, which, in turn, is responsible for the increase in frequency.

Changes in the internal deformation modes of ligands on coordination have been used as an effective diagnostic tool when the ligand exists, for example, as two conformers. Thus, 2,5-dithiahexane (DTH) is present as both the trans and gauche form, with bands due to  $-CH_2$  rocking modes, characteristic of both conformers, in the spectrum of the free ligand. Cotton et al.<sup>71</sup> were able to show that, whilst the spectrum of the complex  $[Re_2Cl_5(DTH)]_2$  contained only "gauche"  $CH_2$  rocking vibrations, DTH was present as its trans and gauche conformers in  $Re_3Cl_9(DTH)_{1.5}$ , consistent with its formulation as a polymeric compound with trans DTH bridging molecules.

Complications sometimes arise in assignment of spectra because modes which are only Raman active or completely inactive in the free ligand, often become excited on coordination as the site symmetry of the ligand changes.

(ii) The 500 - 200  $cm.^{-1}$  (Low Infrared) region<sup>72</sup>

In this region, direct metal-ligand vibrations are excited, and, in particular, a study of the position and number of metal-halogen vibrations is useful in the assignment of a possible stereochemistry to a complex

compound.

Table 2.1 shows the number and type of metal-halogen stretching vibrations in some commonly occurring six coordinate stereochemistries.

Table 2.1 Metal-halogen stretching vibrations for six coordinate complexes of the type  $\text{MX}_m\text{L}_n$ .

Type	Stereo-chemistry	Point Group	$\nu_{\text{M-X}}$	Infrared active species
$\text{MX}_4\text{L}_2$	<u>trans</u>	$D_{4h}$	$a_{1g} + b_{1g} + e_u$	$e_u$
$\text{MX}_4\text{L}_2$	<u>cis</u>	$C_{2v}$	$2a_1 + b_1 + b_2$	all
$\text{MX}_2\text{L}_4$	<u>trans</u>	$D_{4h}$	$a_{1g} + a_{2u}$	$a_{2u}$
$\text{MX}_2\text{L}_4$	<u>cis</u>	$C_{2v}$	$a_1 + b_1$	all
$\text{MX}_3\text{L}_3$	<u>trans</u>	$C_{2v}$	$2a_1 + b_1$	all
$\text{MX}_3\text{L}_3$	<u>cis</u>	$C_{3v}$	$a_1 + e$	all

It is thus possible, in principle at least, to distinguish between, say, cis and trans  $\text{MX}_3\text{L}_3$  complexes by examination of their low infrared spectra, which should show two and three peaks attributable to metal-halogen stretching vibrations respectively.

Factors affecting the position of metal-halogen stretching vibrations

(i) For a given complex, for example,  $\text{MX}_3\text{L}_3$ , the frequency of the metal-halogen bands on changing the halogen falls in the order  $\text{F} > \text{Cl} > \text{Br} > \text{I}$ .

(ii) For a given oxidation state, the frequency of the metal-halogen stretching mode decreases as the coordination number of the metal increases. This effect is illustrated in Table 2.2.

Table 2.2 The effect of Coordination Number of the Metal-Halogen Stretching Mode

Compound	Coordination No.	$\nu_{\text{M-Cl}}$ ( $\text{cm.}^{-1}$ )
$\text{VCl}_4$	4	482
$\text{VCl}_4, 2\text{L}$	6	$\sim 370$
$\text{VCl}_4, \text{otas}^+$	7	357
$\text{VCl}_4, 2\text{D}^*$	8	$\sim 317$

+ see ref. 22

\* D = o-phenylenebisdimethylarsine

The increase in the coordination number is reflected in an increase in the length of the metal-halogen bond, thus causing a lowering of its stretching frequency.

(iii) For a given stereochemistry, the metal-halogen

stretching frequency falls as the oxidation state of the metal is lowered. For example,  $\nu_{V-Cl}$  in  $VCl_4$  occurs at  $482\text{ cm.}^{-1}$ , but in  $VCl_4^-$ ,  $\nu_{V-Cl}$  appears at  $406\text{ cm.}^{-1}$ .

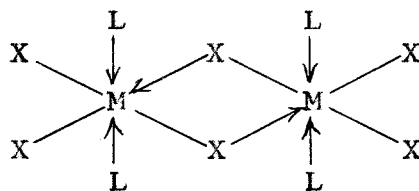
Problems encountered in the interpretation of spectra

(i) Solid State effects

The spectra of complexes are usually run as Nujol mulls. Unless a good mull is prepared, the metal-halogen bands will be invariably broad and poorly resolved, and their number may not be diagnostic of the stereochemistry of the complex. Another danger associated with solid state spectra is that degenerate (e and t) modes may be resolved due to low site symmetry of the metal atom in the crystal, given a misleading number of metal-halogen stretching bands in the spectrum.

(ii) Coupling with other modes

Metal-halogen stretching vibrations may couple with other normal modes of the same symmetry species, so that, in fact, pure metal-halogen stretching modes are never observed. The extent of coupling with other stretching vibrations is a problem of some complexity about which no generalisations may be made, but the coupling with metal-halogen deformation modes is unlikely, because the latter occur at much lower frequencies than the stretching modes. For example, in the bridged molecule:



the "terminal" M-X stretching modes may couple with the "bridging" M-X modes giving bands differing in position from those expected for a monomeric octahedral species  $\text{MX}_3\text{L}_3$ . The position of the bands when extensive coupling is present may not be diagnostic of a particular coordination number.

(iii) Metal-ligand stretching frequencies

Bands associated with metal-ligand vibrations may complicate the band structure of the metal-halogen stretching vibrations. Metal-ligand stretching modes have not been well characterised since they are unlikely to be "pure", but involve extensive coupling with internal ligand vibration and deformation modes.<sup>73,74</sup>

Interpretation of a low infrared spectrum is additionally complicated by the appearance of ligand vibrational modes which were either weak, Raman active or completely inactive in the free ligand, but which become excited on coordination. Examples of this type of problem are referred to in Chapter 3.

## II Visible and Ultraviolet Spectroscopy<sup>64,65,75</sup>

### (i) Energy Levels in Free ions and Complexes

The various forces acting on a multi-electron ion may be subdivided into the following:

- (a) central field forces
- (b) interelectronic repulsive forces
- (c) spin-orbit coupling forces

The central field forces are the largest and give rise to the various atomic energy levels 1s, 2s, 2p etc. In transition metal ions of the first row (b)  $\gg$  (c), and therefore the Russell-Saunders coupling approximation holds, with spin-orbit coupling as a small perturbation on the repulsive forces. Interelectronic repulsion splits the highly degenerate energy levels of the  $3d^2$  configuration of  $V^{3+}$  into a number of terms, namely, (in order of increasing energy):  ${}^3F < {}^1D < {}^3P < {}^1G < {}^1S$ . The term separation may be represented by combinations of Racah's parameters B and C; the energy separation between the  ${}^3P$  and  ${}^3F$  terms is  $15B$  ( $12,920 \text{ cm.}^{-1}$  in  $V^{3+}$ ). The triplet terms are further split into states by spin-orbit coupling. When an ion becomes incorporated into a complex, an additional perturbation, the ligand field, is introduced. The magnitude of the ligand field may be (a) less than the interelectronic repulsion - weak field

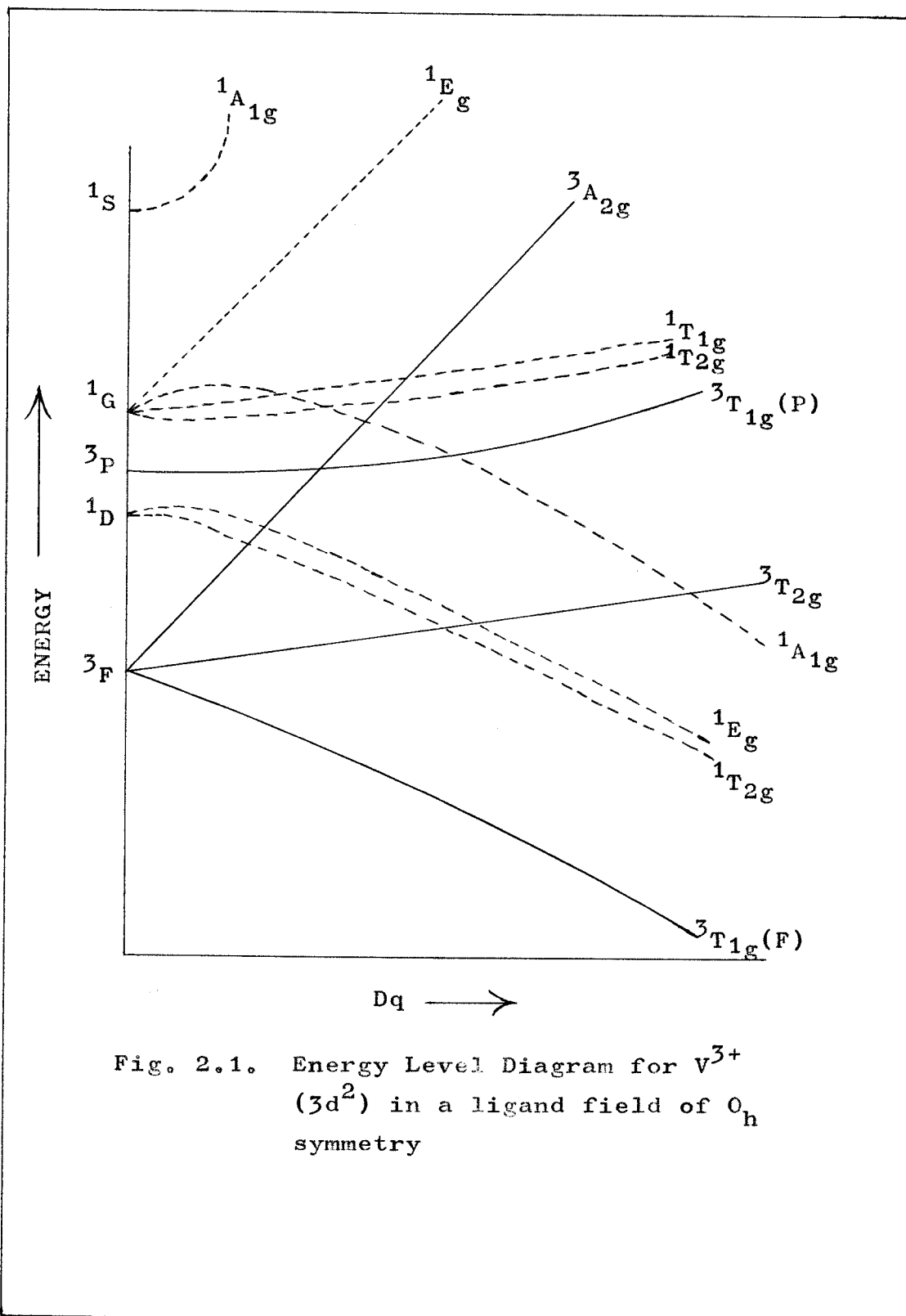


Fig. 2.1. Energy Level Diagram for  $V^{3+}$  ( $3d^2$ ) in a ligand field of  $O_h$  symmetry



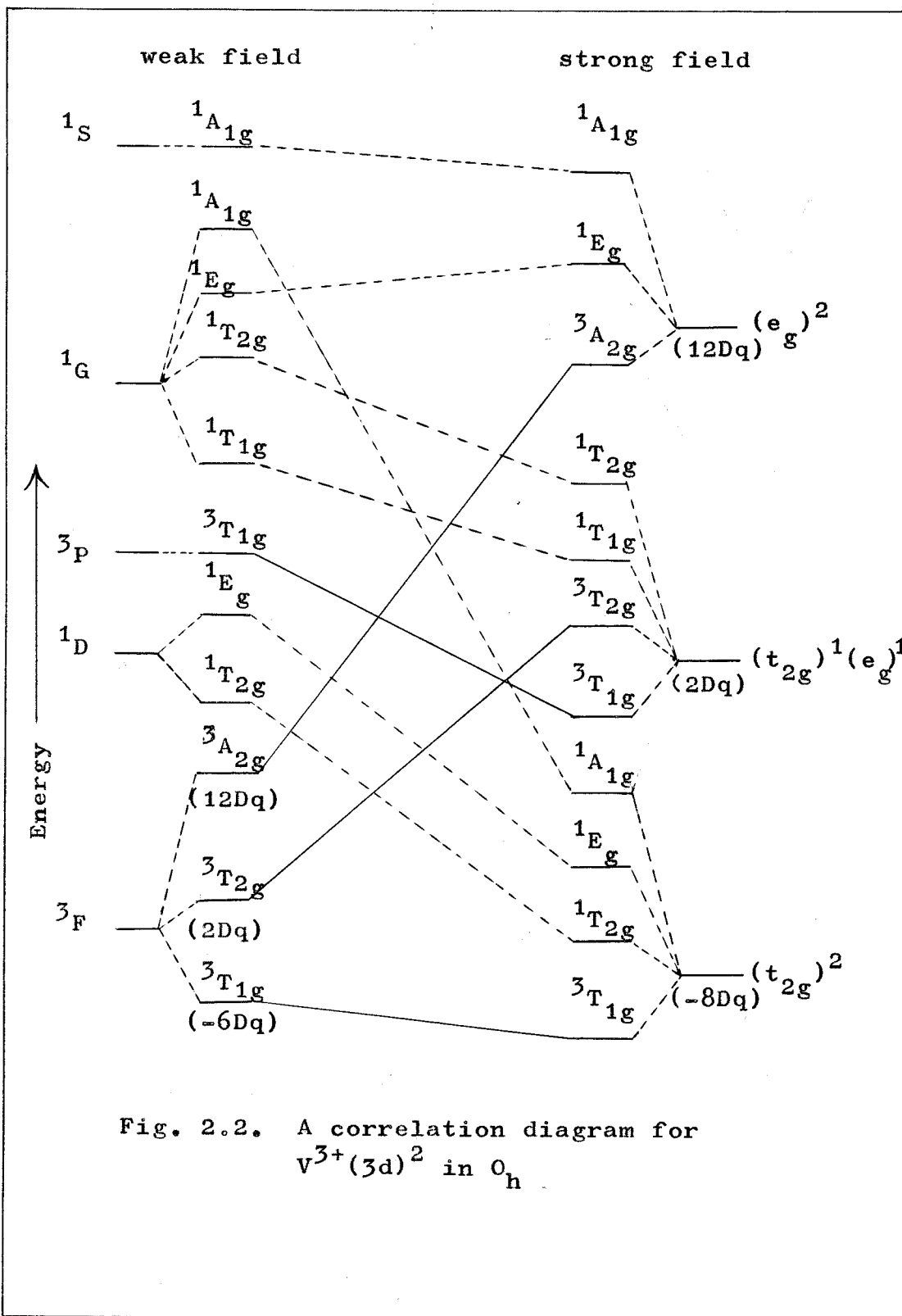
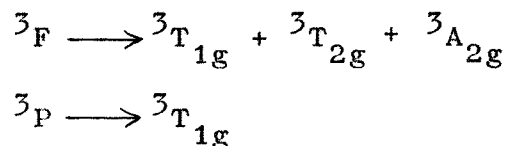


Fig. 2.2. A correlation diagram for  $V^{3+}(3d)^2$  in  $O_h$ .

(b) of the same order as the interelectronic repulsion - medium field.

(c) much greater than the interelectronic repulsion - strong field.

The orbital degeneracy of the Russell-Saunders terms is partially removed by the ligand field, and it may be shown that, in a field of cubic ( $O_h$ ) symmetry:



The increase in these splittings as the magnitude of the ligand field increases may be displayed on an energy level (Orgel) diagram (Fig. 2.1) and the transition from weak to strong ligand fields is illustrated on a correlation diagram (Fig. 2.2). The parameter  $Dq$  is used to represent the magnitude of the term splittings by the ligand field, and is correlated with the nature of the ligand which produces the perturbation, (see later). For first row transition elements, the splitting of the ligand field terms by spin-orbit coupling is small compared with the magnitude of the ligand field, but it becomes important when considering magnetic properties and spectral band widths.

There is a further second order effect, namely the configuration interaction (see Fig. 2.3) between the two

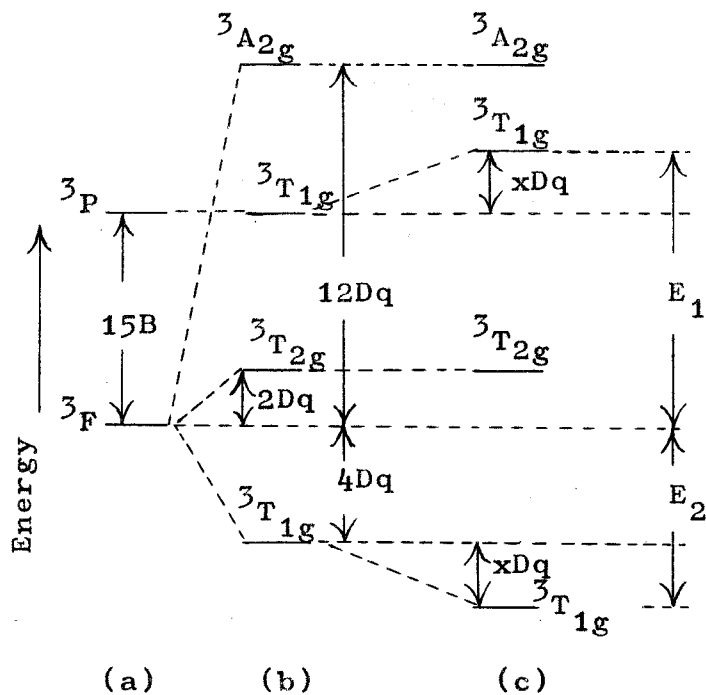


Fig. 2.3. Triplet terms arising from  $(3d)^2$  configuration  
 (a) Free ion  
 (b) " " in Ligand field of  $O_h$  symmetry  
 (c) Configuration interaction included

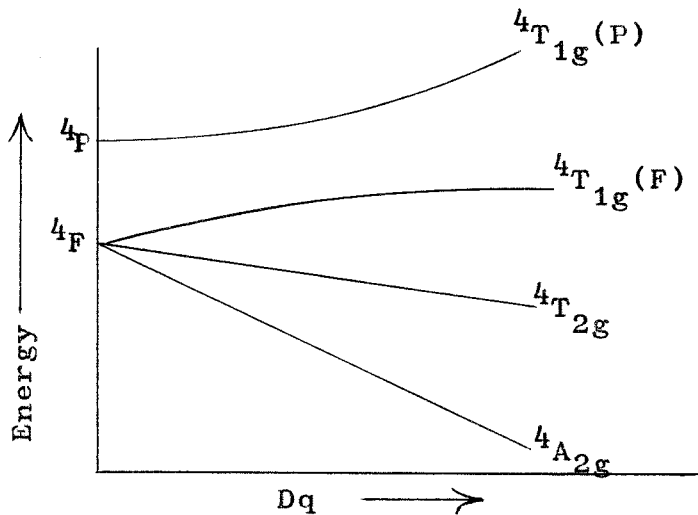


Fig. 2.4. Energy Level Diagram for a  $(d)^3$  ion in an Octahedral field (quartet terms only)

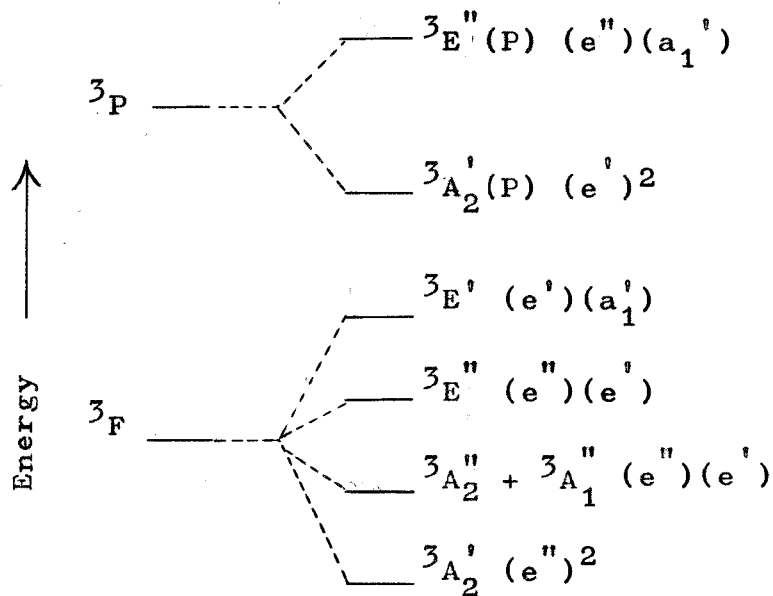


Fig. 2.5. Splitting of the Triplet terms of  $3d^2$  configuration by a Ligand field of  $D_{3h}$  symmetry.

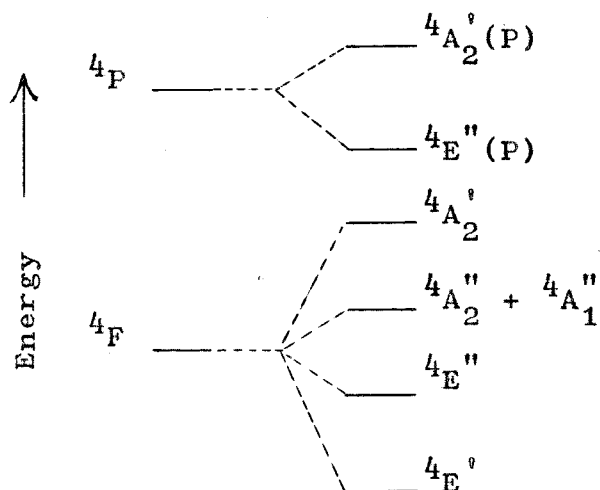


Fig. 2.6. Splitting of the Quartet terms of a  $3d^3$  configuration by a ligand field of  $D_{3h}$  symmetry.

${}^3T_{1g}$  terms arising from the  ${}^3P$  and  ${}^3F$  terms, because they have the same symmetry. The magnitude of the interaction is given by the determinant:<sup>76</sup>

$$\begin{vmatrix} -6Dq-E & 4Dq \\ 4Dq & 15B-E \end{vmatrix} = 0$$

The energy level diagram for chromium(III) is given in Fig. 2.4). Again, there is configuration interaction between the two  ${}^4T_{1g}$  terms, the magnitude of which is given by the determinant:<sup>76</sup>

$$\begin{vmatrix} 6Dq-E & 4Dq \\ 4Dq & 15B-E \end{vmatrix} = 0$$

Energy level diagrams may also be constructed for ions in ligand fields of symmetry less than  $O_h$ , but the calculation of the energies of the ligand-field terms is a problem of some complexity. These calculations<sup>77</sup> have recently been performed for  $d^2$  and  $d^3$  configurations in a ligand field of  $D_{3h}$  symmetry and the resulting energy levels are shown in Figs. 2.5 and 2.6.

### (ii) Electronic Spectra

Absorption of electromagnetic radiation in the region  $10,000 \text{ cm.}^{-1}$  to  $50,000 \text{ cm.}^{-1}$  causes electronic excitation within the complex compound. Two distinct types of transition may be recognised according to their intensities:

(a) those with  $\epsilon_{\text{max}} < 200$

(b) those with  $\epsilon_{\text{max}} > 1000$

Bands typified by (a) are known as "d-d" or ligand field

transitions, whilst bands typified by (b) include charge-transfer bands and internal ligand transitions (e.g.  $\pi \rightarrow \pi^*$  bands in pyridine). Internal ligand transitions are generally little affected by coordination and are not discussed further. Although arbitrary, this classification of spectral bands by intensity works fairly well in practice, especially with first row elements, but at the end of this section some "d-d" transitions with very high intensities will be discussed.

#### Selection rules

Two selection rules are operative.

(i) There must be no spin multiplicity change involved in the transition, i.e.  $\Delta S=0$ . Transitions for which  $\Delta S \neq 0$  are said to be "spin-forbidden".

(ii) The Laporte rule forbids transitions of the type  $g \leftrightarrow g, u \leftrightarrow u$  in systems with an inversion centre. Thus all "d-d" transitions are Laporte forbidden. The Laporte rule is a special case of a more general orbital selection rule which forbids transitions between certain orbitals. The distribution of these orbitally forbidden transitions may be evaluated in specific molecules of known symmetry by application of group theory.

#### (a) "d-d" transitions

These transitions are usually induced by absorption of radiation in the visible region of the spectrum; they

are fairly weak bands because they are all Laporte forbidden. The fact that both Laporte - and spin-forbidden bands are observed indicates that the selection rules are violated. Small departures from strict  $O_h$  symmetry and vibronic coupling cause relaxation of the Laporte rule, whilst the operation of spin-orbit coupling causes the spin selection rule to break down. Vibronic coupling occurs when suitable vibrational modes with "u" symmetry involving motion of the ligands, couple with the ground and excited electronic levels on the metal ion, endowing them with partial "u" character. The electronic transition then becomes partially allowed. Transitions in tetrahedral complexes become partially allowed because of "d-p" mixing, as p orbitals have inherent "u" properties.

#### Factors affecting the band widths of ligand field transitions

It is apparent from the appearance of "d-d" spectra that the bands, as well as being fairly weak, are also noticeably broad.

##### (1) Vibrational broadening

Bands are broadened by the vibronic coupling mechanism. The energy differences between the ground and excited levels is a function of  $Dq$ , which is very sensitive to the metal-ligand distance. Slight variations in this distance caused by vibrations will lead to an ill-defined energy gap,

with the consequent broadening of the band associated with the spectral transition.

(2) Spin-orbit coupling

Although spin-orbit coupling constants in the first transition series are small, T ground and excited terms may be split by spin-orbit coupling by amounts ranging from  $100 \text{ cm.}^{-1}$  to  $1000 \text{ cm.}^{-1}$ , causing a broadening of bands arising from transitions involving these terms.

(3) Departure from cubic symmetry

(i) The Jahn-Teller Theorem

This theorem may be stated by saying that, if a molecule initially has a degenerate ground term e.g.  ${}^3T_{1g}$  term of  $V^{3+}$  in a field of  $O_h$  symmetry, then the molecule will distort itself in some way to remove this degeneracy.

The consequence of this theorem is that there can, in principle, be no regular octahedral complexes of vanadium(III). Excited terms may also suffer Jahn-Teller distortions; for example, the spectrum of the complex  $VCl_6^{2-}$  shows a broad asymmetric band at  $\sim 15,000 \text{ cm.}^{-1}$  assigned to the  ${}^2E_g \leftarrow {}^2T_{2g}$  transition, the asymmetry of which has been ascribed to the Jahn-Teller distortion of the  ${}^2E_g$  term.<sup>30</sup>

(ii) Ligand Inequivalences

Complexes with formal  $O_h$  symmetry have not been encountered in this work, but have been of the type  $VX_3L_3$



in which the ligand field may have  $C_{3v}$  or  $C_{2v}$  symmetry. E and T terms are split by these lower symmetry ligand fields. The components arising from the cubic field terms in fields of lower symmetry are given in Table 2.3 below.

Table 2.3 Correlation table for the Group  $O_h$

$O_h$	$D_{4h}$	$C_{3v}$	$C_{2v}$
$A_{1g}$	$A_{1g}$	$A_1$	$A_1$
$A_{2g}$	$B_{1g}$	$A_2$	$A_2$
$E_g$	$A_{1g} + B_{1g}$	$E$	$A_1 + A_2$
$T_{1g}$	$A_{2g} + E_g$	$A_2 + E$	$A_2 + B_1 + B_2$
$T_{2g}$	$B_{2g} + E_g$	$A_1 + E$	$A_1 + B_1 + B_2$

The splittings produced are usually fairly small in vanadium(III) complexes and result in broadening of the "d-d" transitions. It is usual to consider distortions arising from ligand inequivalences and Jahn-Teller effects as perturbations of the main cubic field, retaining the  $O_h$  term designations when the spectra of mixed ligand systems are assigned.

#### (4) Solid state distortions

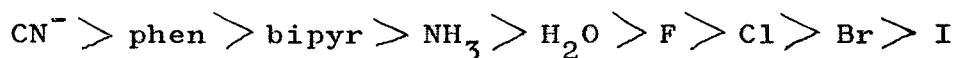
When the spectra of finely ground solids are measured

by diffuse reflectance, additional broadening or splitting of the spectral bands may be observed, because of distortions to the ligand field imposed by crystal-packing requirements.

Information obtained from visible spectra

(i) The parameter Dq

It is found that, amongst others, the factors contributing to Dq include electrostatic perturbations, the strength of the metal-ligand  $\sigma$  bond and the strength of metal-ligand  $\pi$  bonding;  $\pi$ -donor ligands tend to decrease Dq whilst  $\pi$  acceptors cause an increase in Dq. For a given metal in a given oxidation state, the magnitude of Dq is found to vary with the nature of the ligand; the following order (Dq decreasing), known as the spectrochemical series, is observed:



(ii) Evidence for metal electron delocalisation

When Dq and 15B are evaluated from visible spectral data, it is found that 15B is reduced to some 70% of its free ion value ( $12,920 \text{ cm.}^{-1}$  for  $\text{V}^{3+}$ ,  $15,450 \text{ cm.}^{-1}$  for  $\text{Cr}^{3+}$ ); the magnitude varies with the nature of the ligand in the order:  $\text{I} > \text{Br} > \text{Cl} > \text{en} > \text{NH}_3 > \text{H}_2\text{O} > \text{F}$  (I causes the greatest reduction), known as the nephelauxetic series.<sup>78</sup> The reduction in the P - F term separation from the free ion value arises from a decrease in electron repulsion

caused by partial delocalisation of the metal electrons on to the ligand, via the formation of a covalent bond. A further factor indicating the covalent nature of the metal-ligand bond is that in some cases the intensities of ligand-field transitions are much greater than expected, even allowing for breakdown in the selection rules. For example, in some low spin, five coordinate nickel(II) complexes with polydentate sulphur, selenium and arsenic ligands, the intensities of the strongest ligand field band were found to be very large, decreasing in the order:  $\text{As}(\epsilon \sim 4000) > \text{Se}(\epsilon \sim 1700) > \text{S}(\epsilon \sim 1100)$ .<sup>79</sup> The increased intensities were attributed to extensive covalent bonding, imparting ligand "character" to the metal orbitals.

#### (b) Charge Transfer Spectra

The appearance of intense, broad bands, usually in the ultraviolet spectral region is due to the presence of charge-transfer bands. As the name suggests, these transitions involve a re-distribution of electronic charge within the molecule and are usually strongly Laporte allowed, being from ligand to metal orbitals or vice versa. The charge-transfer spectra of vanadium(III) complexes are discussed in chapter 4.

(D) Magnetic Properties<sup>14,75</sup>

The types of magnetic behaviour encountered are summarised in table 2.4

Table 2.4 Types of Magnetic Behaviour

Type of magnetic susceptibility	Approximate magnitude of $\chi$ cgsu	Dependence on the applied field
Diamagnetism	$1 \times 10^{-6}$	Independent
Paramagnetism	$0 - 10^{-4}$	Independent
Ferromagnetism	$10^{-2} - 10^4$	Dependent
Anti-ferromagnetism	$0 - 10^{-4}$	may depend

(i) Diamagnetism

Diamagnetism, an inherent property of all substances, arises out of the motion of electrons, treated as charged particles, in a magnetic field. As the induced force is opposed to the applied field, the resulting susceptibilities are negative. It is usual, when estimating paramagnetism, to correct empirically for the diamagnetic contribution to the molecule, since it is likely to be substantial if a large number of diamagnetic atoms is present. The diamagnetic susceptibility per gram atom, which is temperature independent, is additive, and so the

total correction for a molecule may be estimated by the summation of the individual atomic susceptibilities (Pascal's constants).

(ii) Paramagnetism

Paramagnetism arises from the orbital and spin motion of one or more unpaired electrons, which in the case of the first transition series, constitute the partially filled 3d shell. In a complex there is usually a sufficient number of diamagnetic atoms in the form of ligands to prevent interactions between neighbouring atomic dipoles; such systems are said to be "magnetically dilute". However, when the diamagnetic "screening" is inefficient or nonexistent, dipolar exchange results. If the dipoles couple up so that they are parallel to the applied field, ferromagnetism results, if they couple up antiparallel to the field, the phenomenon is known as antiferromagnetism.

Magnetically dilute systems

Only a small excess of magnetic dipoles align themselves with the applied magnetic field, because the tendency of dipoles to align is opposed by the randomising effect of thermal energy. It may be shown that the excess of aligned dipoles gives rise to a susceptibility:

$$\chi = \frac{C}{T} \quad \text{where} \quad \begin{array}{l} C = \text{Curie constant} \\ T = \text{absolute temperature} \end{array}$$

This is known as Curie's law. If the molar suscepti-

bility is defined as  $\chi_m = \chi \times \text{Mol. wt.}$  and the total susceptibility of the paramagnetic ion or atom, corrected for the diamagnetic contribution of the ligand atoms, as  $\chi'_m$ , then the magnetic moment  $\mu_{\text{eff}}$  is given by the expression:

$$\mu_{\text{eff}} = \left( \frac{3k}{N\beta^2} \right)^{1/2} (\chi'_m T)^{1/2}$$

$$= 2.828 (\chi'_m T)^{1/2}$$

where  $k =$  Boltzmann's Constant

$N =$  Avogadro Number

$\beta =$  Bohr Magnetron

In practice, few systems obey the Curie law exactly, but many obey a modification known as the Curie-Weiss law:  $\chi'_m = C[T+\theta]^{-1}$ .  $\theta$  is best regarded as an empirical constant which has little fundamental significance, except perhaps in magnetically concentrated systems.

#### The magnetic properties of free ions

The perturbations acting on a free ion with a  $3d^2$  configuration were described on page 26. The splitting of the free ion terms into states specified by the quantum number  $J$  by spin-orbit coupling, and the subsequent removal of the  $(2J+1)$  spin degeneracy of these states by application of a magnetic field is illustrated in Fig.2.7. The separation of each microstate, specified by the quantum number  $M_J$ , is  $g\beta H$  where  $g =$  Lande splitting factor

$H =$  applied magnetic field

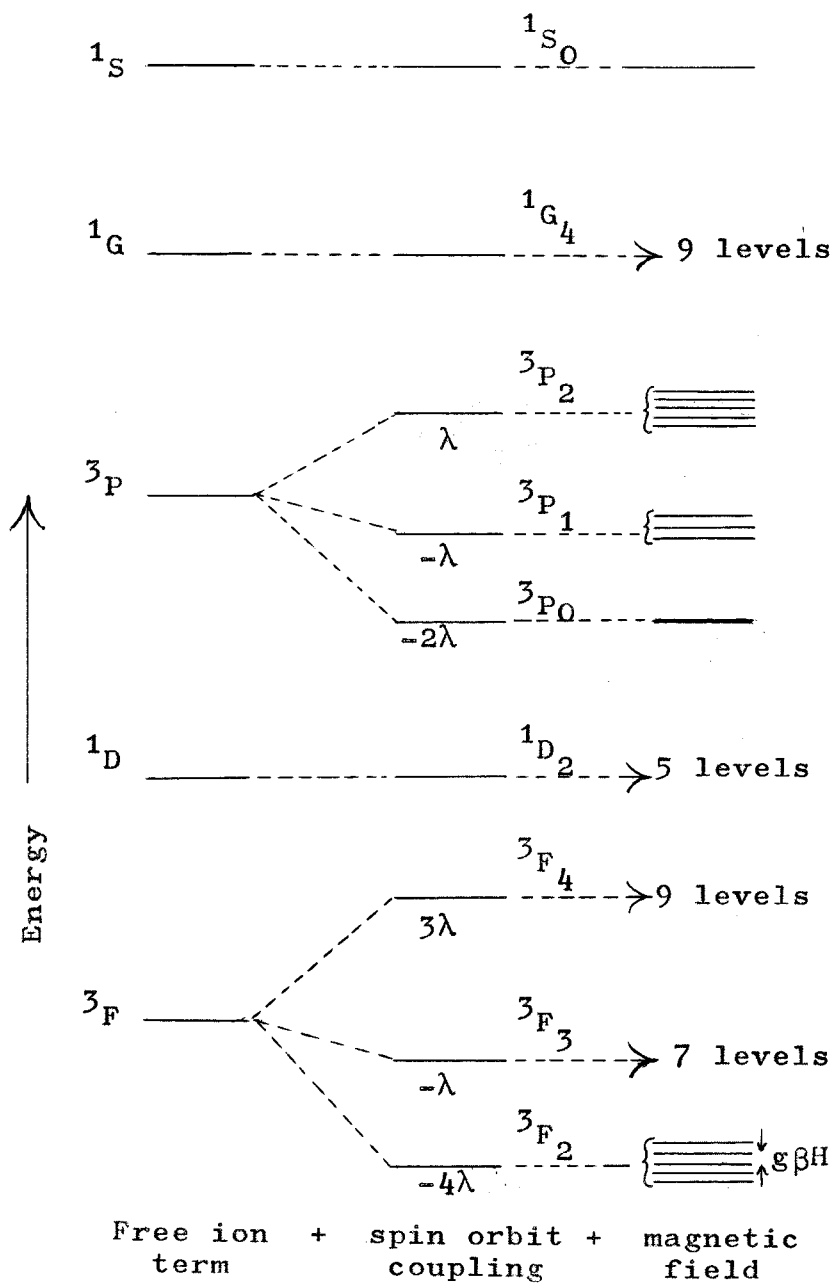


Fig. 2.7. Splitting of terms of a  $(3d)^2$  configuration by spin-orbit coupling and a magnetic field

$g\beta H$  has a value  $\sim 1 \text{ cm.}^{-1}$  with a magnetic field of  $\sim 10,000$  gauss, compared with the value of  $kT$  at room temperature of about  $200 \text{ cm.}^{-1}$ . The removal of the spin degeneracy of the states by a magnetic field is known as the "first order" Zeeman effect.

If spin-orbit coupling is so great that thermal population of  $J$  states other than the ground state is impossible at room temperature, the magnetic moment of the ion is given by :  $\mu_{\text{eff}} = g[J(J+1)]$  . This is a good approximation for Lanthanide ions where spin-orbit coupling is large and the resulting states are thermally inaccessible.  $g$  depends on the orbital and spin angular momentum of the state, and is given by the expression:  

$$g = 1 + [S(S+1) - L(L+1) + J(J+1)] / 2J(J+1)$$
.

In ions with no orbital angular momentum,  $L = 0$ ,  $J = S$  and  $g = 2$  so that  $\mu_{\text{eff}} = 2[S(S+1)]$  . If the number of unpaired electrons is  $n$ , then  $S = \frac{n}{2}$  and  

$$\mu_{\text{eff}} = [n(n+2)]$$
 .

This is the well-known "spin-only" formula.

If the states produced by spin-orbit coupling have energy separations from the ground state comparable in magnitude to  $kT$ , then thermal population of these levels becomes possible and the magnetic properties of the ion are expected to be complicated. This situation prevails in the first transition series. If there is virtually no



spin-orbit coupling, (a hypothetical situation), then the magnetic moment of the ground term is given by  $\mu_{\text{eff}} = [4S(S+1) + L(L+1)]$ . This formula has been used to estimate the amount of orbital contribution to a magnetic moment, but its use for this purpose is unjustified in view of the assumption from which it is derived. If  $L = 0$ , the "spin-only" formula is obtained.

The effect of a ligand field on the magnetic properties of ions

The ensuing discussion will be concerned with ligand fields of cubic symmetry.

That orbital angular momentum is lost when an ion becomes complexed is apparent by consideration of the following physical representation of orbital motion. Orbital angular momentum about an axis is associated with the ability to rotate an orbital about an axis to give an identical, degenerate orbital. For example, rotation of the  $d_{xz}$  orbital by  $90^\circ$  about the  $z$  axis gives the  $d_{yz}$  orbital, and the  $d_{xy}$  orbital may be rotated about the same axis to give the  $d_{x^2-y^2}$  orbital. In the presence of a cubic ligand field, the  $d_{xy}$  and  $d_{x^2-y^2}$  orbitals are no longer degenerate, and hence no orbital angular momentum arises between them. No orbital angular momentum is associated with the  $e_g$  set because the  $d_{x^2-y^2}$  and  $d_z^2$  orbitals differ in shape and may not be converted into

one another by rotation. Orbital angular momentum remains with the  $t_{2g}$  set since the  $d_{xy}$ ,  $d_{xz}$  and  $d_{yz}$  orbitals may be interconverted by rotation about the appropriate Cartesian axes. Another restriction is that there must not be an electron in the second orbital with the same spin as in the commencing orbital. Using these rules, it may be shown that orbital angular momentum is completely quenched in A and E ground terms, but when T ground terms arise some orbital angular momentum remains.

The magnetic properties of  $A_{2g}$  and  $E_g$  ground terms

As orbital angular momentum is quenched for  $A_{2g}$  and  $E_g$  ground terms, neither of which may be split by spin-orbit coupling, a spin-only moment, independent of temperature is expected. Spin-only moments are sometimes not observed because orbital angular momentum may be partially restored by two "second-order" effects:

(a) An excited term possessing orbital angular momentum may be "mixed-in" to the ground term via spin-orbit coupling. For example,  $Cr^{3+}$  has a  ${}^4A_{2g}$  ground term, with the  ${}^4T_{2g}$  excited term situated  $10Dq$  above it. The magnetic moment becomes  $\mu_{\text{eff}} = \mu_o \times \left[ 1 - \frac{4\lambda}{10Dq} \right]$  where  $\mu_o$  is the spin-only moment, and  $\lambda$  is the spin-orbit coupling constant.

(b) Excited terms possessing orbital angular momentum may be "mixed-in" to the ground term by a mechanism known as the "second-order" Zeeman effect. If the energy

of the excited term above the ground term is  $\gg kT$ , the resulting susceptibility is temperature independent. The contribution to the total susceptibility is fairly small,  $\sim 100 \times 10^{-6}$  cgsu in  $\text{Cr}^{3+}$ .

The magnetic properties of T Ground Terms (e.g.  ${}^3T_{1g}$  in  $V^{3+}$ )

T terms are split by spin-orbit coupling giving states of comparable energy with  $kT$ . This causes a thermal distribution to occur between the states and the magnetic moment is expected to be strongly temperature dependent. The magnetic properties of the  ${}^3T_{1g}$  term are further complicated by configuration interaction with the excited  ${}^3T_{1g}(P)$  term, the extent of the interaction being dependent upon the strength of the ligand field. Figgis<sup>80</sup> has calculated that the magnetic moment of  $V^{3+}$  in a cubic ligand field should be 2.7 B.M.

Two other effects, namely electron delocalisation and low symmetry ligand fields tend to produce spin-only moments in complexes. Delocalisation of the metal 'd' electrons on to the ligand causes loss of orbital angular momentum, so that moments approach the spin-only value. Low symmetry ligand fields arising from Jahn-Teller distortions or ligand inequivalences will split T ground terms, but the effect on the magnetic moment depends on the magnitude of the splitting. As the distortion of the term

increases relative to  $kT$ , the moment tends towards the spin-only value, and becomes less temperature dependent.

The success of the "spin-only" formula accounting for the magnetic properties of many (but not all) first row transition element complexes is now apparent. Because of the quenching effect of ligand fields, electron delocalisation and low symmetry ligand-field components, orbital contribution to the magnetic moment is almost entirely removed and the "spin-only" formula becomes a good approximation.

#### Illustrative Examples

(a) Chromium(III) has a  $d^3$  configuration giving rise to a  ${}^4A_{2g}$  ground term. The "spin-only" moment of 3.87 B.M. is expected to be only slightly modified by the  $\left[1 - \frac{4\lambda}{10Dq}\right]$  term, as  $\lambda$  is small for  $Cr^{3+}$ .  $CrCl_3 \cdot py_3$  is typical of many chromium complexes, with a room temperature moment of 3.80 B.M., independent of temperature.<sup>14</sup>

(b) The magnetic properties of several octahedral  $V^{3+}$  complexes have been extensively studied.<sup>34</sup> Contrary to expectation, they have spin-only moments  $\sim 2.8$  B.M. which are independent of temperature. These results have been explained by assuming the presence of a large ( $\sim 2000 \text{ cm.}^{-1}$ ) component of a low symmetry ligand field superimposed on the octahedral field, and by making an allowance for electron delocalisation on to the ligands.

The magnetic properties of five-coordinate complexes

The electronic configurations  $d^1$ ,  $d^2$ ,  $d^3$  give rise to  ${}^2E''$ ,  ${}^3A_2'$ ,  ${}^4E'$  ground terms respectively in a ligand field of  $D_{3h}$  symmetry. The magnetic properties of these terms, although complicated, have now been evaluated.<sup>77</sup> For the two E terms, an orbital contribution to the moment is expected, as well as the "second-order" contributions mentioned earlier. E terms may be split by spin-orbit coupling in  $D_{3h}$  symmetry, giving rise to temperature-dependent magnetic moments. The moments are expected to become less temperature-dependent and approach the spin-only value if the effects of low-symmetry ligand fields and electron delocalisation are significant. The orbital contribution to the  ${}^3A_2'$  ground term is completely quenched. A temperature-independent spin-only moment, modified by "second-order" contributions (as for A terms in  $O_h$  symmetry) is therefore predicted. The moment is expected to become temperature-dependent at low temperatures because of the fairly large zero field ("second-order" spin-orbit) splitting of the  ${}^3A_2'$  term by  $\sim 10 \text{ cm.}^{-1}$ .

(E) Crystal Structure Analysis Using X-rays<sup>81,82</sup>

The theory of diffraction of X-rays by crystalline materials (either as powders or single crystals) has been omitted from this section, since it may be found in many

standard texts.

An X-ray beam is diffracted when it interacts with the electron clouds surrounding atoms in a crystal. When the conditions for coherent scattering are fulfilled, the beam is diffracted only in specified directions which depend on the size of the unit cell, and the intensity of the beam diffracted from a particular crystal plane depends on the positions of the atoms in the unit cell.

The corrected intensity of a beam of X-rays diffracted from the crystal plane  $hkl$  is proportional to the quantity  $(F_{hkl})^2$ , where  $F_{hkl}$  is known as the structure amplitude.

$$\text{Now, } F_{hkl} = \sum f_i \exp[2\pi i(hx_i + ky_i + lz_i)]$$

where  $f_i$  is the atomic scattering factor of the  $i$ th atom and  $x_i, y_i, z_i$  are the coordinates (in fractions of the unit cell lengths) of the  $i$ th atom.

The atoms in an infinite array of unit cells (i.e. a crystal) give rise to a distribution of electron density,  $\rho$ , which is a continuous, periodic function and may be represented by a Fourier series in three dimensions.

The electron density at a point  $x, y, z$  (fractional coordinates) is given by the following summation:

$$\rho(x, y, z) = \frac{1}{V} \sum_h \sum_k \sum_{l=-\infty}^{+\infty} F(hkl) \exp[-2\pi i(hx+ky+lz)]$$

where  $V$  is the volume of the unit cell.

F is generally a complex quantity and may be represented as

$$F = A + iB$$

thus  $|F| = (A^2 + B^2)^{1/2}$  and the phase angle,  $\alpha = \tan^{-1} \frac{B}{A}$

For centrosymmetric crystals  $F = \pm A$ ,  $B = 0$  and  $\alpha = 0$  or  $\pi$  and the expression for the electron density  $\rho$  becomes:

$$\rho(x, y, z) = \frac{1}{V} \sum_h \sum_k \sum_l \begin{matrix} +\infty \\ -\infty \end{matrix} F_{hkl} [\cos 2\pi(hx + ky + lz)]$$

Other elements of symmetry will lead to further simplifications of this expression.

The general problem in determining atomic positions is that only  $|F|$  may be measured directly, and hence the phase angle remains unknown. This difficulty is known as the Phase Problem. In crystals containing Transition elements, the most important method used to overcome the Phase Problem, is to utilize the presence in the molecule of 'heavy atoms', (such as the metal and halogens) which will dominate the scattering power of the lighter atoms.

The Patterson function, defined in its general form as  $P(u, v, w) = \frac{1}{V} \sum_h \sum_k \sum_l |F_{hkl}|^2 \exp[-2\pi i(hu + kv + lw)]$  may now be computed using the corrected measured intensities, since these are proportional to  $|F|^2$ . The Patterson function, when plotted out as a "map" gives the interatomic vectors for every pair of atoms in the unit cell. Although Patterson maps are fairly complicated,

it is usually possible to obtain from them the positions of the heavy atoms, which may then be used to compute a Fourier synthesis. If the deduced positions of the heavy atoms are correct, some, if not all, of the lighter atoms may be located on the electron density map. A Fourier synthesis is now computed using all the atoms so far located and a search of the electron density map is made to find the remaining atoms. This procedure is repeated until all the atoms in the unit cell have been located.

$$\text{The residual is defined as } R = \frac{\sum (|F_o| - |F_c|)}{\sum |F_o|}$$

and is usually taken as the measure of agreement between the observed and calculated structure factors.

The atomic coordinates are now refined by a least-squares procedure which will be considered further in Chapter 6.



CHAPTER THREE

COMPLEXES OF VANADIUM(III) HALIDES  
WITH  
TERTIARY HETEROCYCLIC NITROGEN DONORS

## Introduction

Complexes of transition elements with the heterocyclic bases, pyridine, 2,2'-bipyridyl and 1,10-phenanthroline are well known,<sup>83,84</sup> although few have been reported until fairly recently for elements in the early part of the series. Thus, complexes with all three ligands have now been prepared from titanium(III) and (IV)<sup>85,86,87</sup> and zirconium(III)<sup>85,88</sup> and (IV) halides and vanadium(IV) chloride.<sup>86</sup> A brief report on some 1,10-phenanthroline adducts of vanadium(III) chloride has appeared<sup>83</sup> but no analytical or physical data were given; in these laboratories, Lanigan<sup>89</sup> prepared complexes of the type  $VCl_3 \cdot 2B$  where B = bipy or phen, showing that they contained cationic vanadium(III) with the probable structure  $[VCl_2 \cdot B_2]Cl$ . Pyridine complexes of vanadium(III) halides were unknown until Duckworth<sup>90</sup> reported a vanadium(III) chloride/pyridine adduct as the reduction product of the reaction of vanadium(IV) chloride with pyridine. He obtained a similar product by the direct reaction of vanadium(III) chloride with pyridine, but in neither case was a complex isolated which contained a stoichiometric quantity of pyridine.

As no complex with any of the ligands with vanadium(III) bromide has been reported, and in view of the paucity of data on the vanadium(III) chloride systems, it was decided

to investigate the reactions of vanadium(III) halides (or their derivatives) with pyridine, 2,2'-bipyridyl and 1,10-phenanthroline. During the course of this work, some anionic complexes of the type  $[\text{VCl}_4\text{L}_2]^-$  (L = pyridine,  $\frac{1}{2}$ bipyr.,  $\frac{1}{2}$ phen.) were reported.<sup>49</sup>

I Reaction of vanadium(III) chloride and bromide with pyridine

Duckworth<sup>90</sup> found that direct reaction of pyridine with vanadium(III) chloride gave inhomogeneous products, and therefore, displacement reactions were attempted using a dilute solution of pyridine in benzene, and the trimethylamine adducts,  $\text{VX}_3 \cdot 2\text{NMe}_3$  (X = Cl, Br).

The chloro complex gave a green crystalline solid and purple solution. The former was collected, washed free of excess pyridine with fresh benzene and pumped overnight.

Found: C, 45.6; H, 4.0; Cl, 27.2; N, 10.4; V, 13.1%.

Calc. for  $\text{VCl}_3 \cdot 3\text{C}_5\text{H}_5\text{N}$ : C, 45.6; H, 3.8; Cl, 27.0; N, 10.6;  
V, 12.9%.

The analogous reaction of pyridine with tribromobis-(trimethylamino) vanadium(III) in benzene yielded a brown solid, which was washed free of pyridine as above.

Found: C, 33.9; H, 3.0; Br, 43.8; N, 7.9; V, 9.7%.

$\mu_{\text{eff}}$ : 2.73 B.M. at 20°C.

Calc. for  $\text{VBr}_3 \cdot 3\text{C}_5\text{H}_5\text{N}$ : C, 34.1; H, 2.9; Br, 45.4; N, 8.0; V, 9.6%.

The chloro-product was insoluble in benzene but dissolved slightly in chloroform and appreciably in pyridine to give a red-purple solution. The bromo-complex was slightly soluble in benzene and chloroform, but a molecular weight determination in benzene was unsuccessful as the complex was not soluble enough. Both complexes were fairly stable to hydrolysis.

The conductivities of the complexes measured in pyridine are shown in table 3.1.

Table 3.1 Conductivities of Complexes in Pyridine

Compound	conc. $\times 10^3 M.$	conductivity $\text{ohm}^{-1} \text{cm}^2$	ref.
$(C_2H_5)_4NBr$	0.28	134	91
$VCl_3, 3py$	1.57	2.2	this work
$VBr_3, 3py$	0.98	24.9	this work
$TiCl_3, 3py$	1.79	8	91
$TiBr_3, 3py$	1.71	27	92

### Discussion

Trimethylamine is readily displaced by pyridine diluted with benzene from the adducts  $VX_3, 2NMe_3$  ( $X = Cl, Br$ ) to form stoichiometric complexes of the type  $VX_3, 3py$ . Both complexes dissolve in pyridine to give solutions of

low conductance, (cf. table 3.1); the chloro complex is clearly a non-electrolyte whilst the conductivity of the bromide is well below that expected for a 1:1 electrolyte in pyridine. A similar trend is noted for the analogous titanium complexes, the increase in conductivity on passing from chloride to bromide being due to a weakening of the metal-halogen bond. The complexes are tentatively formulated as non-ionic monomers containing six coordinate vanadium.

The infrared spectra of the complexes recorded in the  $4000\text{ cm.}^{-1}$  to  $650\text{ cm.}^{-1}$  are similar to other compounds containing coordinated pyridine;<sup>93,94</sup> in particular, the out-of-plane C-H deformation bands (at  $747\text{ cm.}^{-1}$  and  $700\text{ cm.}^{-1}$ ) in free pyridine are shifted in the complexes. In  $\text{VBr}_3, 3\text{py}$ , there are strong, sharp peaks at  $765\text{ cm.}^{-1}$  and  $692\text{ cm.}^{-1}$ , but in  $\text{VCl}_3, 3\text{py}$ , these bands occur at  $783, 760\text{ cm.}^{-1}$  (split band) and  $698\text{ cm.}^{-1}$  (broad). There are other changes in the skeletal vibrational modes of the ring (in the region  $1400\text{-}1600\text{ cm.}^{-1}$  in free pyridine) which show a general increase in frequency of  $10\text{-}20\text{ cm.}^{-1}$  on complex formation. Gill et al.<sup>93</sup> have explained these changes in terms of an increase in charge on the heterocyclic ring in the complexes, due to the back-donation of charge from the metal ion. However, a recent paper by Durig et al.<sup>94</sup> suggests that the changes

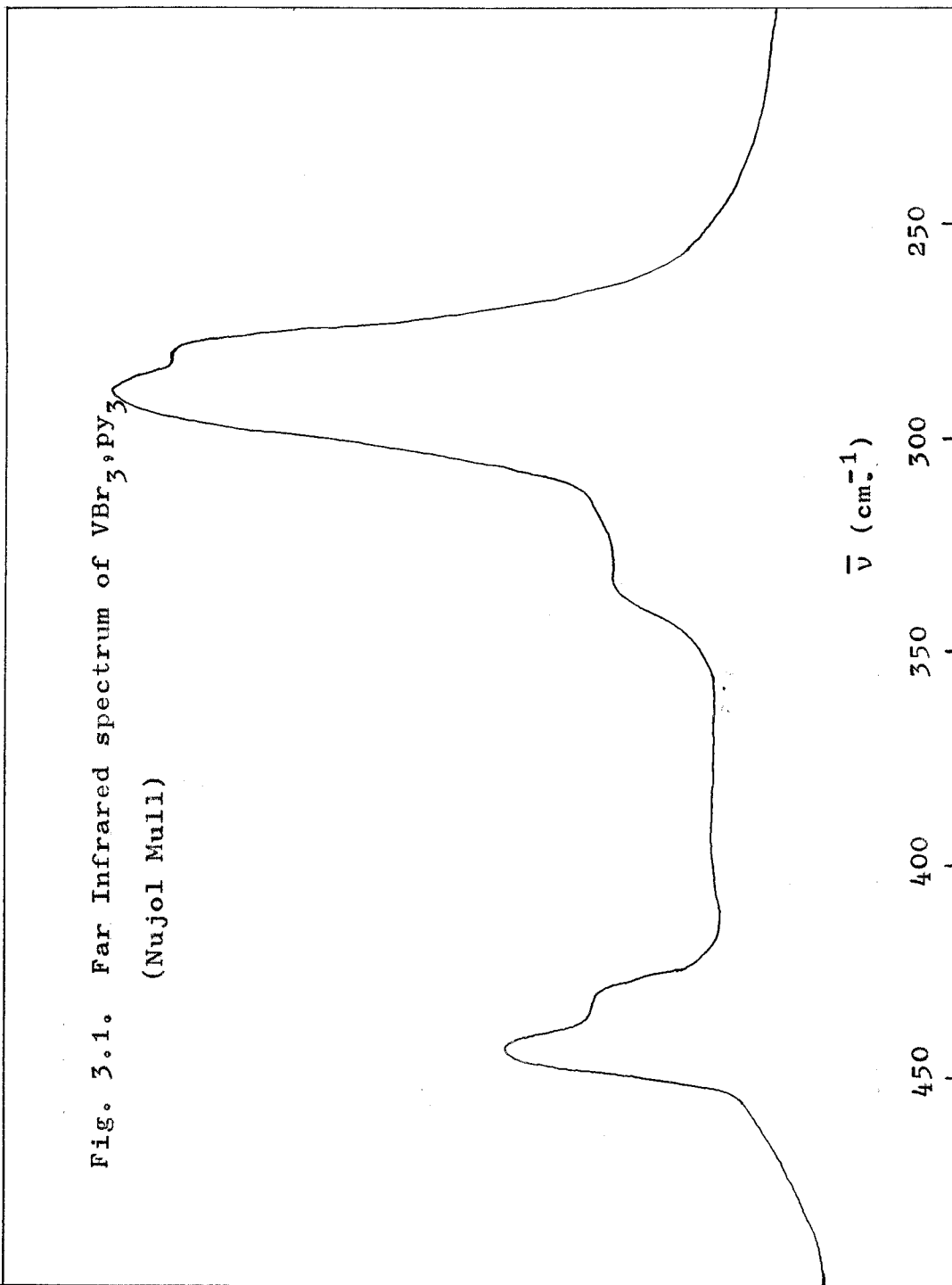
are caused by a redistribution of ring electron density, due to the donation of the nitrogen lone pair, since similar shifts in ring frequencies occur in boron derivatives where no back-donation to pyridine is possible.<sup>95</sup>

The far infrared spectra of the complexes have been measured in an attempt to establish the molecular symmetry. Thus, three metal-halogen stretching vibrations of symmetry ( $2a_1 + b_1$ ) are expected for  $\text{MX}_3 \cdot 3\text{L}$  complexes with  $\text{C}_{2v}$  symmetry (trans), and two of symmetry ( $a_1 + e$ ) are predicted to occur in  $\text{MX}_3 \cdot 3\text{L}$  complexes with  $\text{C}_{3v}$  symmetry (cis). The results are noted in table 3.2 and a spectrum of  $\text{VBr}_3 \cdot 3\text{py}$  is reproduced in fig. 3.1.

Table 3.2 Low infrared spectra of the pyridine complexes in Nujol mulls

Compound	pyridine bands $\text{cm}^{-1}$	M-X stretching frequencies $\text{cm}^{-1}$	unassigned $\text{cm}^{-1}$
pyridine	405		
$\text{VCl}_3 \cdot 3\text{py}$	439	352sh 312s,br 283s	395sh
$\text{VBr}_3 \cdot 3\text{py}$	444 431sh	289s 280sh	330w

Fig. 3.1. Far Infrared spectrum of  $VBr_3 \cdot py_3$   
(Nujol Mull)



On the basis of this data trans and cis configurations are assigned to the chloro and bromo complexes respectively. Vanadium-nitrogen stretching frequencies are not expected above  $300 \text{ cm.}^{-1}$  and they are likely to be weak; in trans  $\text{CrCl}_3 \cdot 3\text{py}$  for example, a chromium-nitrogen stretching vibration has been tentatively assigned to a peak observed at  $221 \text{ cm.}^{-1}$  <sup>96</sup> It is interesting to note that the analogous acetonitrile complexes,  $\text{VX}_3 \cdot 3\text{MeCN}$ , have been assigned a cis configuration, <sup>72</sup> with the vanadium-halogen stretching bands occurring at  $354 \text{ cm.}^{-1}(\text{s})$ ,  $332 \text{ cm.}^{-1}(\text{sh})$  and  $312 \text{ cm.}^{-1}(\text{s})$  and  $293 \text{ cm.}^{-1}(\text{s})$  for the chloride and bromide derivatives respectively.

The band occurring at  $440 \text{ cm.}^{-1}$  in the complexes is due to an internal ligand out-of-plane bending mode which Clark assigns to the modified vibration 16b, occurring at  $405 \text{ cm.}^{-1}$  in free pyridine. <sup>96</sup> In the cis bromide complex this band is split, and since the vibration is nondegenerate, this may reflect some interaction between different pyridine molecules, either coordinated to the same metal atom, or as near neighbours in the crystal lattice.

The visible and near ultraviolet spectra shown in table 3.3 have one striking feature, namely that while the bromide complex has the same spectrum in the solid



as in solution (pyridine or benzene), the spectrum of the chloride complex changes significantly when dissolved in pyridine.

Table 3.3 Electronic Spectra of  $VX_3, 3py$

Compound	State	Peak Positions ( $cm^{-1}$ )
$VCl_3, 3py$	Solid	14,490      22,220
	py soln.	14,000(sh) 18,320    21,000(sh) 27,900(sh)
$VBr_3, 3py$	Solid	13,500(sh) 17,700(sh) 21,300(sh) 24,700(sh)
	py soln.	13,700(sh) 17,900(sh) 21,300 24,500 28,800(sh) 30,500(sh)
	benzene soln.	13,300(sh) 17,300(sh) 21,050 24,900 28,900(sh)
$Et_4N[VCl_4, py_2]^*$	Solid	13,100    21,200

\* ref. 49.

The lowest energy band in each complex is assigned unambiguously to the transition  ${}^3T_{2g} \leftarrow {}^3T_{1g}(F)$ , the red shift on passing from chloride to bromide being consistent with the ligand-field strength order  $Cl > Br$ .<sup>78</sup> The first band in the chloro complex is seen to be at a slightly higher frequency than observed in  $[VCl_4, py_2]^-$ ,

since, in the latter, the environment of the vanadium is four chlorines and two pyridines, and chlorine lies lower than pyridine in the spectrochemical series. The assignment of the remaining bands is much more difficult, for, although a second "d-d" band is expected in the chloro complex in the 21,000 to 22,000  $\text{cm.}^{-1}$  region, it is possible that the peak actually observed there is a charge-transfer band which shifts to around 18,000  $\text{cm.}^{-1}$  upon dissolution of the complex in pyridine. The appearance of this peak, giving the intense purple colour in solution could be associated with a change in stereochemistry from trans to cis, since a band is found in a similar position in the bromo complex. A tentative suggestion is that these bands around 18,000  $\text{cm.}^{-1}$  are of the type  $\text{pyridine}(\pi^*) \leftarrow \text{V}(d)$ , i.e. the transfer of an electron from the metal to the  $\pi^*$  antibonding orbitals of pyridine; the position of such a transition could depend on the arrangement of the ligands round the metal. The peaks observed around 28,000  $\text{cm.}^{-1}$  in  $\text{VCl}_3 \cdot 3\text{py}$  and around 21,000  $\text{cm.}^{-1}$  and 25,000  $\text{cm.}^{-1}$  in  $\text{VBr}_3 \cdot 3\text{py}$  are typical of transitions observed in other vanadium(III) chloro and bromo complexes (see Chapter 4) and have been tentatively assigned as charge-transfer bands of the type  $\text{V}(d) \leftarrow \text{Halogen}(\pi)$ .

II Reaction of vanadium(III) halides (or their derivatives) with 2,2'-bipyridyl and 1,10-phenanthroline

The stoichiometry of the products obtained from these reactions varied with the nature of the starting materials and the experimental conditions.

(i) Reaction of 2,2-bipyridyl with trichlorotriscetonitrile vanadium(III)

(a) When equimolar quantities of the reactants were refluxed together under benzene for 24 hr., a brown solid was produced. This compound was collected, washed with benzene and dried in vacuo, where it became yellow-brown in colour.

Found: C, 37.8; H, 2.9; Cl, 33.0; N, 8.75; V, 16.2%.

Calc. for  $VCl_3, C_{10}H_8N_2$ : C, 38.3; H, 2.6; Cl, 33.9; N, 8.9;  
V, 16.2%.

The complex was insoluble in benzene.

(b) When a two-fold excess of bipyridyl was used with either acetonitrile or benzene as a solvent, a golden brown product resulted:

Found: Cl, 26.2; V, 12.8%.

Calc. for  $VCl_3, 1.5C_{10}H_8N_2$ : Cl, 27.2; V, 13.0%.

(ii) Reaction of vanadium(III) chloride with 2,2'-bipyridyl

2,2'-bipyridyl (10.2 m.mole) and vanadium(III) chloride (4.2 m.mole) reacted in acetonitrile under reflux to give

a golden-brown solid, which was collected and washed free of excess ligand with acetonitrile.

Found: C, 46.2; H, 3.1; Cl, 27.3; N, 10.6; V, 12.9%.

Calc. for  $VCl_3, 1.5C_{10}H_8N_2$ : C, 46.0; H, 3.1; Cl, 27.2; N, 10.7;  
V, 13.0%.

The compound was insoluble in benzene and chloroform, but dissolved slightly in acetonitrile and nitromethane.

When the reaction was carried out with equimolar quantities of reactants, a light-green solid was formed.

Found: C, 40.3; H, 3.4; Cl, 30.1; N, 12.1; V, 14.4%.

Calc. for  $VCl_3, C_{10}H_8N_2, CH_3CN$ : C, 40.7; H, 3.1; Cl, 30.0;  
N, 11.9; V, 14.4%.

This complex was also obtained by dissolving  $VCl_3, C_{10}H_8N_2$  in acetonitrile, followed by the removal of excess solvent by evaporation.

Found: Cl, 29.6; V, 14.5%.

Calc. for  $VCl_3, C_{10}H_8N_2, CH_3CN$ : Cl, 30.0; V, 14.4%.

The compound was insoluble in benzene and chloroform.

Its infrared spectrum showed a peak at  $2300\text{ cm.}^{-1}$ , characteristic of coordinated acetonitrile.<sup>97</sup>

As  $VCl_3, C_{10}H_8N_2, CH_3CN$  was exceptionally stable to hydrolysis and oxidation, a thermogravimetric analysis of the complex was attempted using a Stanton Thermogravimetric balance. No weight change of the complex was noted until the temperature reached  $\sim 150^\circ\text{C.}$ , at which point weight was steadily lost until the temperature

reached  $210^{\circ}\text{C}$ , when the weight loss ceased and the remaining complex held a constant weight until the experiment was terminated at  $240^{\circ}$ .

Found: Molecular weight of remaining solid: 299.

Calc. for  $\text{VOCl}_2, \text{C}_{10}\text{H}_8\text{N}_2$  : M.W. = 294.

For the gaseous species evolved:

Found: Mol. wt. of species lost was 56

Calc: for loss of 1 mole of acetonitrile + 1 gm. atom of chlorine + gain of 1 gm. atom of oxygen : 61.

(iii) Reaction of vanadium(III) chloride with 1,10-phenanthroline

Equimolar quantities of the two reactants were refluxed in acetonitrile producing a green solid which was collected and washed with acetonitrile in the usual way.

Found: C, 45.6; H, 3.6; Cl, 25.6; N, 13.5; V, 12.6%

Calc. for  $\text{VCl}_3, \text{C}_{12}\text{H}_8\text{N}_2, 2\text{CH}_3\text{CN}$ : C, 45.8; H, 3.4; Cl, 25.4;  
N, 13.4; V, 12.1%.

This complex was insoluble in benzene but soluble in acetonitrile. Its infrared spectrum showed two peaks at  $2260 \text{ cm.}^{-1}$  and  $2300 \text{ cm.}^{-1}$  indicating the presence of both coordinated and uncoordinated acetonitrile molecules.

(iv) Reaction of 1,10-phenanthroline with trichlorobis(trimethylamino)vanadium(III)

When excess of the ligand was allowed to react with  $\text{VCl}_3, 2\text{NMe}_3$  in benzene in a molar ratio of 2.4:1, a buff-coloured solid was produced. The solid was filtered off, washed with benzene to remove excess ligand and pumped free of benzene.

Found: C, 54.9; H, 2.7; Cl, 20.5; N, 10.4; V, 9.6%.

Calc. for  $\text{VCl}_3, 2\text{C}_{12}\text{H}_8\text{N}_2$ : C, 55.7; H, 3.1; Cl, 20.5; N, 10.8; V, 9.8%

Lanigan's<sup>89</sup> previous preparation of this complex was thus confirmed.

(v) Reaction of 2,2'-bipyridyl with vanadium(III) bromide

2,2'-bipyridyl (10.2 m.mole) and vanadium(III) bromide (4.9 m.mole) were refluxed together in acetonitrile to yield a green solid, slightly soluble in acetonitrile but insoluble in benzene.

Found: C, 41.4; H, 3.3; Br, 37.4; N, 10.9; V, 7.9%.

Calc. for  $\text{VBr}_3, 2\text{C}_{10}\text{H}_8\text{N}_2, \text{CH}_3\text{CN}$ : C, 41.0; H, 3.0; Br, 37.2; N, 10.9; V, 7.9%.

The compound remained unchanged on heating in vacuo to 100°C for 3 hr. and its infrared spectrum in each case had a peak at 2260  $\text{cm}^{-1}$ , indicative of uncoordinated acetonitrile. When the complex was treated with chloroform, another green solid was produced.

Found: Br, 32.3; V, 7.0%.

Calc. for  $VBr_3, 2C_{10}H_8N_2, CHCl_3$ : Br, 33.2; V, 7.05%.

The infrared spectrum of the solid showed no peak in the  $2250\text{ cm.}^{-1}$  to  $2350\text{ cm.}^{-1}$  region, but it contained a band due to a C-Cl stretching vibration at  $760\text{ cm.}^{-1}$ .

This compound was stable in vacuo up to  $120^\circ\text{C}$ , but on further heating to  $190^\circ$ , a golden-brown product was produced.

Found: C, 39.1; H, 3.2; Br, 40.0; N, 9.1; V, 8.75%.

Calc. for  $VBr_3, 2C_{10}H_8N_2$ : C, 39.8; H, 2.8; Br, 39.8; N, 9.3;  
V, 8.5%.

It dissolved in acetonitrile to give a green solution and gave a green solid on addition of chloroform.

(vi) Reaction of 1,10-phenanthroline with vanadium(III) bromide

The reaction of vanadium(III) bromide (1.8 m.mole) with 1,10-phenanthroline (3.9 m.mole) under reflux in acetonitrile yielded a green solid which turned brown when isolated and pumped under vacuum at room temperature.

Found: C, 44.0; H, 2.5; Br, 37.1; N, 8.4; V, 7.7%.

Calc. for  $VBr_3, 2C_{12}H_8N_2$ : C, 44.3; H, 2.5; Br, 36.8; N, 8.6;  
V, 7.8%.

The complex was insoluble in benzene but dissolved in acetonitrile to give a green solution.

All the complexes formed were fairly stable to oxidation and hydrolysis, but were hydrolysed on standing

Table 3.4 2,2-bipyridyl and 1,10-phenanthroline Complexes of Vanadium(III)

Halides

	Compound	Colour	Magnetic Moment B.M.	Probable Structure
I	$VCl_3, 2phen$	mustard-yellow	2.84*	$[VCl_2, (phen)_2]Cl$
II	$VBr_3, 2bipy$	golden-brown		$[VBr_2, (bipy)_2]Br$
III	$VBr_3, 2phen$	brown	2.73	$[VBr_2, (phen)_2]Br$
IV	$VBr_3, 2bipy, CH_3CN$	green		$[VBr_2, (bipy)_2]Br, CH_3CN$
V	$VBr_3, 2bipy, CHCl_3$	green	2.76	$[VBr_2, (bipy)_2]Br, CHCl_3$
VI	$VCl_3, bipy$	yellow-brown	2.73	$[VCl_3, bipy]_2$
VII	$VCl_3, bipy, CH_3CN$	light-green	2.78	$VCl_3, bipy, CH_3CN$
VIII	$VCl_3, phen, 2CH_3CN$	green	2.75	$[VCl_3, phen, CH_3CN], CH_3CN$
IX	$2VCl_3, 3bipy$	golden-brown	2.81	$[VCl_2, (bipy)_2][VCl_4, (bipy)]$

\* ref. 89



in water or sulphuric acid to give purple solutions, initially, which gradually became green.

### Discussion

A variety of complexes, both cationic and neutral are formed by reaction of vanadium(III) halides (or their derivatives) with 2,2'-bipyridyl and 1,10-phenanthroline. Table 3.4 lists the compounds formed together with their magnetic moments and probably structures.

The presence of trivalent vanadium in the adducts has been confirmed in every case by measurement of the magnetic susceptibility, the room temperature magnetic moments falling in the range 2.73 to 2.81 B.M. The infrared spectra ( $400-650 \text{ cm.}^{-1}$ ) taken in Nujol mulls are typical of complexes containing coordinated bipyridyl or phenanthroline.<sup>94,98,99</sup> The most significant modifications on coordination occur in the positions of the C-C and C-N ring stretching vibrations ( $\sim 1400$  to  $\sim 1600 \text{ cm.}^{-1}$  in the free ligand), and the strong out-of-plane C-H deformation bands ( $750-780 \text{ cm.}^{-1}$  in the free ligand), which all show a general increase in frequency of around  $10-20 \text{ cm.}^{-1}$ . The frequency of the C-H deformation band at  $742 \text{ cm.}^{-1}$  in free bipyridyl and  $730 \text{ cm.}^{-1}$  in free phenanthroline is lowered on coordination by some  $10 \text{ cm.}^{-1}$

Table 3.5 Conductivities of the bipyridyl and phenanthroline Complexes

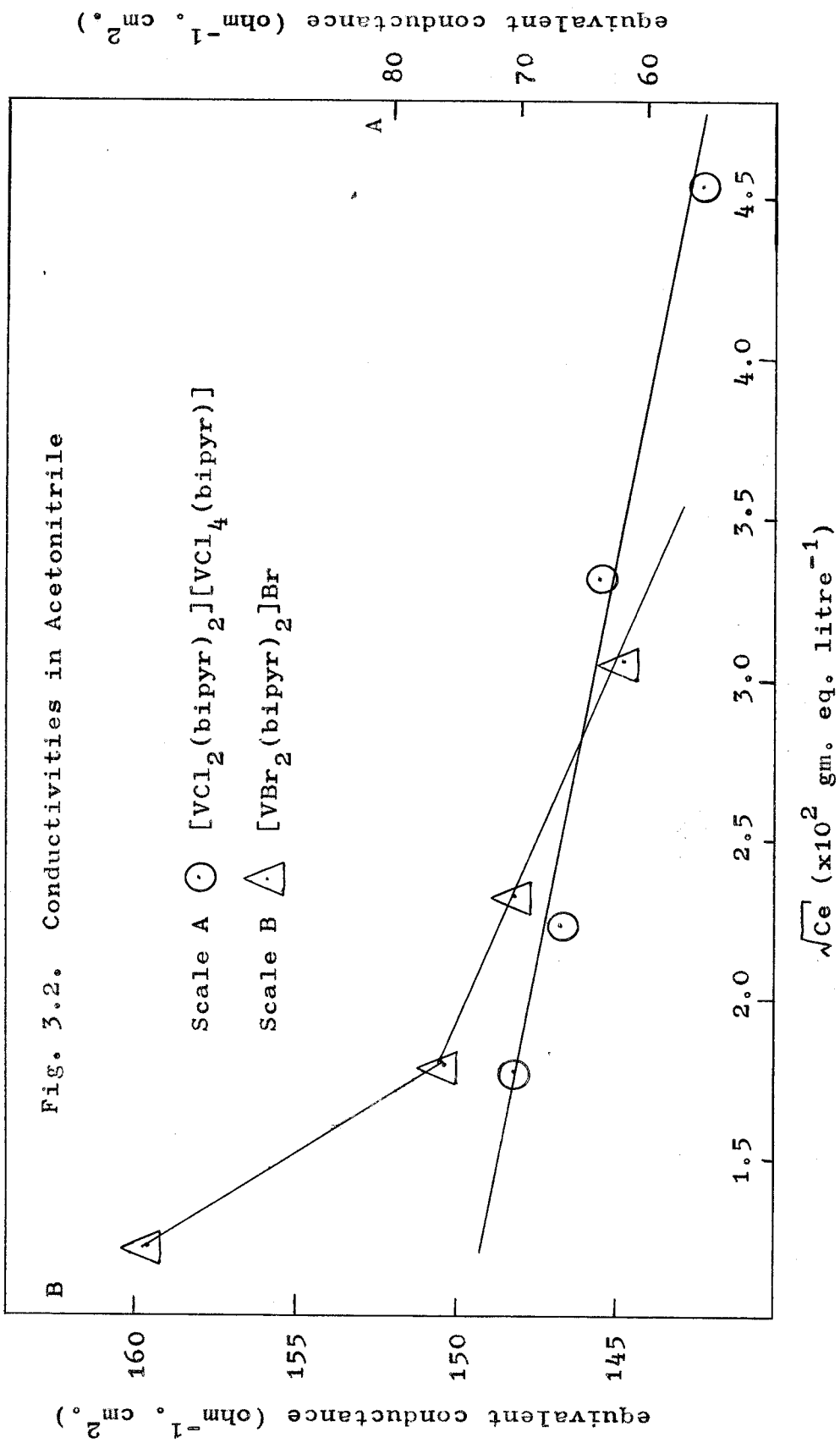
Compound	Nitromethane soln.		Acetonitrile soln.	
	Conc. <sup>o</sup> (x10 <sup>3</sup> M)	Molar Conductance ohm <sup>-1</sup> cm <sup>2</sup> mol <sup>-1</sup>	Conc. <sup>o</sup> (x10 <sup>3</sup> M)	Molar Conductance ohm <sup>-1</sup> cm <sup>2</sup> mol <sup>-1</sup>
(C <sub>2</sub> H <sub>5</sub> ) <sub>4</sub> NBr			1.0	159*
(C <sub>2</sub> H <sub>5</sub> ) <sub>4</sub> NI	0.5	97 <sup>b</sup>	—	—
VCl <sub>3</sub> , 2bipyr	1.7	59 <sup>+</sup>	—	—
VCl <sub>3</sub> , 2phen	1.6	63 <sup>+</sup>	—	—
2VCl <sub>3</sub> , 3bipyr	0.7	64.5	0.55	127 <sup>a</sup>
VCl <sub>3</sub> , bipyr, MeCN	—	—	1.0	3.9
VCl <sub>3</sub> , phen, 2MeCN	—	—	2.6	43.7
VBr <sub>3</sub> , 2phen	—	—	0.96	139
VBr <sub>3</sub> , 2bipyr, MeCN	—	—	0.54	148 <sup>a</sup>

+ ref. 89

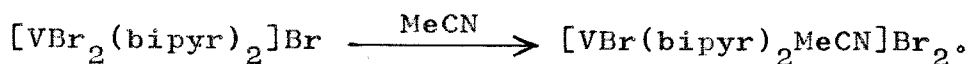
\* ref. 91

a see fig. 2 for conc. plot

b ref. 100



The conductivities of the complexes were measured in acetonitrile or nitromethane and the results obtained are tabulated in table 3.5. Of the 1:2 complexes prepared,  $VCl_3 \cdot 2phen$  has previously been reported by Lanigan,<sup>89</sup> who showed that it, and its bipyridyl analogue, were 1:1 electrolytes in nitromethane. The analogous bromide adducts, III and IV are 1:1 electrolytes in acetonitrile; values of the conductivities at  $10^{-3}M$  are in the expected range for 1:1 electrolytes in this solvent, and over a concentration range  $3 \times 10^{-4}M$  to  $\sim 10^{-3}M$ , the conductance of IV obeys the Onsager law (cf. fig. 3.2). The slope of the straight line is 440 and may be compared with the value of 460 obtained<sup>61</sup> for tetraethylammonium bromide in the same solvent. The conductance rises more rapidly than expected in more dilute solutions, possibly indicating ionisation of the type:



Conductivity measurements on the analogous titanium(III) bromide systems show marked deviations from the behaviour expected by the Onsager Law.<sup>101</sup> Extensive ion pairing is thought to be responsible for this phenomenon, although it is not clear why the titanium(III) and vanadium(III) systems behave differently.

Complex IV contains a molecule of uncoordinated acetonitrile, which may be replaced by chloroform; the

presence of the latter molecule is clearly shown by the appearance of a C-Cl stretching mode at  $760\text{ cm.}^{-1}$  in the infrared spectrum. These species show remarkable thermal stability and may be heated to  $100^{\circ}\text{C}$  in vacuo without change in composition. However, if the temperature is raised above  $120^{\circ}$ , loss of solvate occurs, accompanied by a colour change from green to brown (the charge-transfer band at  $25,000\text{ cm.}^{-1}$  moves to  $\sim 23,000\text{ cm.}^{-1}$ ). This change was reversible on addition of chloroform or acetonitrile. The phenanthroline complex III did not form a stable solvate at room temperature, although, in the presence of acetonitrile or chloroform, its colour was green and this changed to brown on removal of the solvents at the pump.  $\text{TiBr}_3 \cdot 2\text{bipy}$  behaves similarly, but its thermal stability is less than its vanadium(III) counterpart, as heating above  $170^{\circ}\text{C}$  results in the loss of some bipyridyl as well as solvate.

Recently, crystal structures of several complexes containing chloroform of crystallisation have been published,<sup>102,103</sup> and these have shown that chloroform does not contribute to the first coordination sphere of the metal. In the complex  $[\text{TiCl}(\text{acac})_2]_2 \cdot \text{O} \cdot \text{CHCl}_3$ ,<sup>103</sup> it has been suggested that the solvate molecule is held by hydrogen bonding to the oxygen molecules of the acetylacetonone group. Chloroform or acetonitrile may be

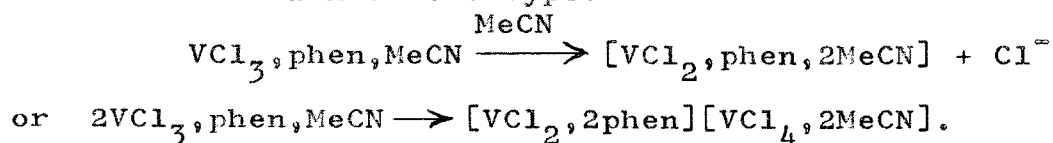
similarly bound to the bromine atoms in the vanadium complexes, but it is difficult to rationalise their thermal stabilities with this postulate since strong bonds between hydrogen and bromine would not be anticipated. A more plausible explanation of this stability would seem to be that the solvate molecule is trapped in a "cage" like structure in the crystal lattice, since more energy would be needed to disrupt the "cage" than hydrogen bonds. The change in position of the charge-transfer band, assigned (see later) to a  $V(d) \leftarrow Br(\pi)$  transition, to lower energy on removal of the solvate may suggest some participation of the bromine  $\pi$  electrons in hydrogen bonding with the solvate.

2,2'-bipyridyl displaces acetonitrile from  $VCl_3 \cdot 3MeCN$  to give a solvate-free complex  $VCl_3 \cdot bipyr(VI)$ , which is given a dimeric structure in which a six-coordinate environment round the vanadium is achieved by chlorine bridging. This compound dissolves in acetonitrile yielding a non-conducting solution from which  $VCl_3 \cdot bipyr \cdot MeCN(VII)$  could be isolated. The infrared spectrum of the compound showed that the acetonitrile was coordinated to the vanadium, and therefore, a six-coordinate, monomeric structure, obtained by the degradation of the chlorine-bridged dimer(VI), is proposed for (VII).

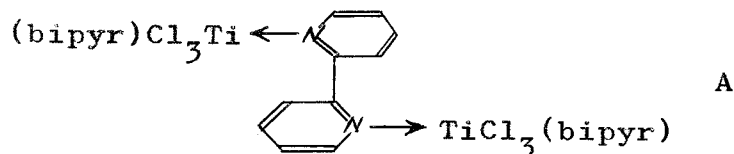
A thermogravimetric analysis showed that acetonitrile

was not lost from the complex(VII) until it had been heated to above 150°C. This stability is in marked contrast to other acetonitrile complexes of vanadium(III); for example,  $\text{VCl}_3, 3\text{MeCN}$ <sup>68</sup> begins to lose ligand above 40°C when heated in vacuo, and  $[\text{VCl}_4, 2\text{MeCN}]^-$  loses all its coordinated acetonitrile when heated to 80°C in vacuo, producing  $[\text{VCl}_4]^-$ .<sup>49</sup>

The analogous phenanthroline complex,  $\text{VCl}_3, \text{phen}$ (VIII) crystallizes from solution with two molecules of acetonitrile, and its infrared spectrum shows that one molecule is coordinated to the vanadium atom and the other not. The conductivity of this complex is appreciably higher than that of the bipyridyl analogue and this may be due to ionization of the type:



Compound IX has the unusual stiochiometry  $2\text{VCl}_3, 3\text{bipyr}$ ; complexes of similar composition with bipyridyl have been reported for  $\text{TiCl}_3$ ,<sup>87</sup>  $\text{TiBr}_3$ ,<sup>92, 101</sup>  $\text{MoX}_3$ ,<sup>104</sup> and  $\text{ZrCl}_3$ .<sup>88</sup> On the basis of conductance measurements,  $2\text{TiCl}_3, 3\text{bipyr}$  was assigned the neutral structure (A)



but additional conductivity studies by Lester have shown that it and the  $\text{TiBr}_3$  analogue are 1:1 electrolytes in acetonitrile,<sup>101</sup> and the ionic structure  $[\text{TiCl}_2(\text{bipyr})_2][\text{TiCl}_4\text{bipyr}]$  has been suggested. A similar proposal has been made for the molybdenum analogues, but Willey<sup>88</sup> has found that the zirconium complex  $2\text{ZrCl}_2,3\text{bipyr}$  is definitely non-conducting in acetonitrile and has accordingly suggested the bridged structure A for this complex. The vanadium complex has a conductivity in acetonitrile less than the value expected for a 1:1 electrolyte in this solvent, but the slope of the equivalent conductance vs (equivalent concentration)<sup>1/2</sup> graph (see fig. 3.2) is 490, thus indicating the probable presence of a 1:1 electrolyte. The conductance of the complex in nitromethane is just below that expected for a 1:1 electrolyte and therefore, the ionic formulation  $[\text{VCl}_2,(\text{bipyr})_2][\text{VCl}_4,\text{bipyr}]$  is proposed.

The far infrared spectra of the complexes have been measured and the results have been recorded in table 3.6. Examples of some of the spectra obtained are reproduced in Fig. 3.3. The spectra of the vanadium(III) bromide complexes were kindly measured by Dr. W.R. McWhinnie.

Complexes of the type  $[\text{VX}_2\text{B}_2]\text{X}$  (where X = Cl, Br,



Fig. 3.3. Far Infrared Spectra

—  $\text{VCl}_3$ , bipyr, MeCN

-----  $[\text{VCl}_2(\text{bipyr})_2][\text{VCl}_4(\text{bipyr})]$

-----  $[\text{VCl}_2(\text{phen})_2]\text{Cl}$

(Nujol Mulls)

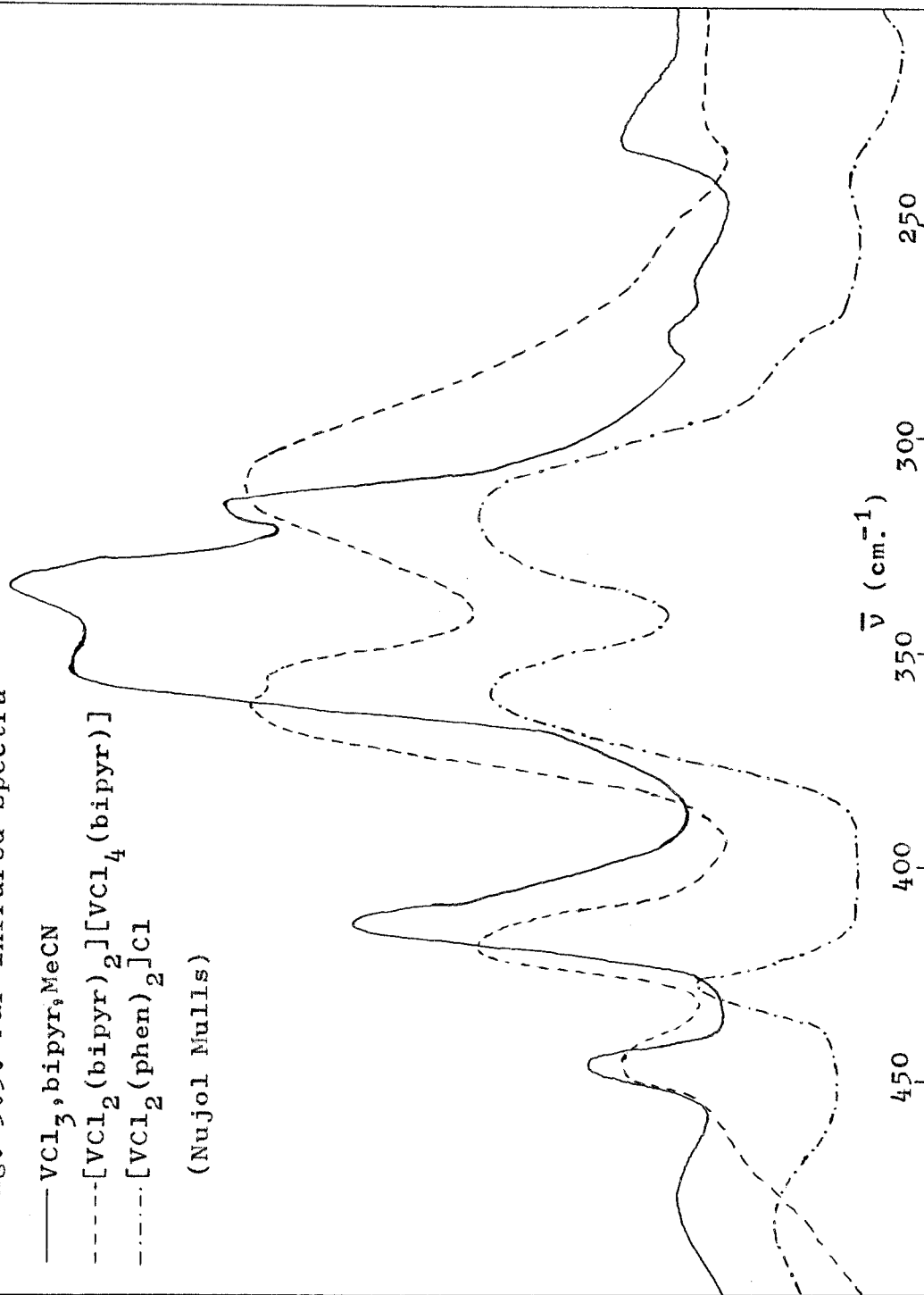


Table 3.6 Far Infrared Spectra of the Bipyridyl  
and Phenanthroline Complexes.

Compound	Peaks $\text{cm.}^{-1}$				
2,2'-bipyridyl	430w	405m.	<sup>86</sup>		
1,10-phenanthroline	411m. <sup>86</sup>				
$\text{VCl}_3, 2\text{phen}$	428m	361s	321s		
$\text{VCl}_3, \text{bipyr}$	437w	418m	363s	310s	277sh
$\text{VCl}_3, \text{bipyr}, \text{CH}_3\text{CN}$	446w	413m	354s	334s	316m 232w
$2\text{VCl}_3, 3\text{bipyr}$	447w	418m	363s	356sh	309br, s
$\text{VBr}_3, 2\text{phen}$	427m	317br, s 301m 282m			
$\text{VBr}_3, 2\text{bipyr}$	437w	415m	362m	323s	304s 282w 254w
$\text{VBr}_3, 2\text{bipyr}, \text{CH}_3\text{CN}$	440w	414m	365m	327s	321s 302m 282w
$\text{VBr}_3, 2\text{bipyr}, \text{CHCl}_3$	439w	419m	362m	325br, s	304m 282w 254w
$\text{TiBr}_3, 2\text{bipyr}$ <sup>101</sup>	412m	358s	320s		272m

and B = bipyr or phen.) may be either trans ( $D_{2h}$ ) or cis ( $C_2$ ), in which case either one or two infrared active vanadium halogen stretching modes of symmetry  $b_{1u}$  and  $a + b$  respectively are expected.

In systems of this type, involving the possibility of cis or trans bipyridyl or phenanthroline rings, it has been suggested<sup>105, 106</sup> that the cis conformation will be preferred, because when the rings are trans there appear to be strong interactions between hydrogen atoms on the

6,6' positions of one bipyridyl ring (2-9 positions in phenanthroline) with those in similar positions on the opposing ring.

The bromide complexes all show two bands around  $320 \text{ cm.}^{-1}$  and  $304 \text{ cm.}^{-1}$  assigned to vanadium-bromine stretching modes; a cis configuration is thus proposed for these complexes. The positions of the bands are at significantly higher frequencies than those usually observed for six-coordinate vanadium(III) bromide complexes ( $\sim 300 \text{ cm.}^{-1}$ ); this increase in frequency is tentatively accounted for by the presence of a positive charge on the metal. The highest frequency V-Br stretching band of the complexes (IV and V) containing solvate molecules is broadened and split. As this mode is non-degenerate, the splitting is probably caused by sets of bromine atoms on different metal atoms being in differing environments in the crystal lattice, due to the presence of the solvate.

The internal bipyridyl and phenanthroline bands around  $410 \text{ cm.}^{-1}$  in the free ligand are due to ring deformation modes,<sup>86</sup> and are shifted to slightly higher frequencies on coordination. The bromo complexes with bipyridyl show an additional band at about  $360 \text{ cm.}^{-1}$ , which has been assigned to an internal ligand vibration, too weak to be observed in the free ligand, but gaining

intensity on coordination.<sup>107,108</sup> This bipyridyl mode complicates the assignment of the spectra of the chloro complexes since V-Cl stretching vibrations are expected in this region. However, in  $VCl_3 \cdot 2phen$ , this complication does not arise, so that the appearance of two strong bands (see. fig. 3.3) at  $361\text{ cm}^{-1}$  and  $321\text{ cm}^{-1}$  is good evidence for the molecule's possessing  $C_2$  (cis) symmetry.  $VCl_3 \cdot bipyr \cdot MeCN$  has no elements of symmetry (except the identity operation) and, therefore, three V-Cl stretching bands are expected, and indeed observed (cf fig. 3.3). In this case, the  $\sim 360\text{ cm}^{-1}$  bipyridyl band must be submerged by the strong V-Cl stretching mode at  $354\text{ cm}^{-1}$ .

The spectra of  $2VCl_3 \cdot 3bipyr$  and  $2[VCl_3 \cdot bipyr]$  are inconclusive, showing only two broad bands in the  $360\text{ cm}^{-1}$  and  $310\text{ cm}^{-1}$  regions. These peaks are probably the envelopes of a more complicated system of bands expected for these binuclear species.

In the range  $220\text{-}280\text{ cm}^{-1}$ , the spectra of all the complexes exhibit weak bands which have been the subject of much discussion recently. Several workers<sup>94,109,110</sup> have assigned these bands to "metal-nitrogen" stretching frequencies; for example, in  $Sc(bipyr)_2Cl_3$  and  $Sc(phen)_2Cl_3$ , they are found at  $287\text{ cm}^{-1}$  and  $275\text{-}283\text{ cm}^{-1}$  respectively.<sup>110</sup> Clark,<sup>86</sup> however, finds no evidence for the existence of such bands in the spectra of  $MCl_4 \cdot B$

(where M = Ti, V and B = bipyridyl, phenanthroline), and concludes from recent studies on complexes such as  $M(\text{bipyridyl})_3^{2+}$  (M = Fe, Co, Ni) which are uncomplicated by the presence of metal-halogen stretching frequencies, that bands appearing in this region are due to weak internal ligand vibrations which gain intensity on coordination.<sup>108</sup>

The visible and ultraviolet spectra of the adducts are presented in table 3.7. The chloro complexes generally show two peaks around  $14,000 \text{ cm.}^{-1}$  and  $20,000 \text{ cm.}^{-1}$  of fairly low intensity assigned to the transitions  ${}^3T_{2g} \leftarrow {}^3T_{1g}(F)$  and  ${}^3T_{1g}(P) \leftarrow {}^3T_{1g}(F)$  respectively. The lowest energy bands in some of the complexes,  $VCl_3, \text{bipyridyl, MeCN}$ , for example, were asymmetric and partially resolved into two peaks, presumably because the molecular symmetry is very much lower than  $O_h$ . The positions of the "d-d" bands in the bromo analogues are uncertain; the low energy shoulder observed in some of the complexes around  $12,000 \text{ cm.}^{-1}$  is probably the first expected transition  ${}^3T_{2g} \leftarrow {}^3T_{1g}(F)$ . In bromo complexes with other ligands (see Chapter 4), the second "d-d" transition is always submerged by the  $V(d) \leftarrow Br(\pi)$  charge-transfer bands at  $\sim 23,000 \text{ cm.}^{-1}$ , and so the band observed at  $\sim 17,000 \text{ cm.}^{-1}$  in these complexes is probably charge-transfer in origin.

Table 3.7 Electronic Spectra of Bipyridyl and Phenanthroline Complexes

Complex	State	Peak positions in $\text{cm.}^{-1}$ ( $\epsilon_{\text{max}}$ in parentheses) <sup>+</sup>
$\text{VCl}_3, \text{bipy}, \text{MeCN}$	Solid MeCN soln.	15,200 $\sim$ 22,200(sh) $\sim$ 25,500(sh) $\sim$ 27,900(br) 15,400 $\sim$ 16,800(sh) 22,400 $\sim$ 25,000(sh) 31,200(sh)
$\text{VCl}_3, \text{phen}, 2\text{MeCN}$	Solid MeCN soln.	11,600(sh) 14,500(sh) $\sim$ 17,200(br) $\sim$ 23,800(br, sh) 14,500 15,000(sh) 23,500(br, sh) $\sim$ 28,600(sh) 31,200(sh)
$(\text{VCl}_3, \text{bipy})_2$	Solid	13,200 20,600(sh) $\sim$ 23,000(sh) $\sim$ 24,400(sh)
$[\text{VCl}_2(\text{bipy})_2]^-$ $[\text{VCl}_4(\text{bipy})]$	Solid	13,100 20,500(sh) $\sim$ 22,600(sh) $\sim$ 25,300(sh)
	$\text{MeNO}_2$ soln	13,400(35) 20,600(sh $\sim$ 200) $\sim$ 23,000( $\sim$ 700) 24,100(sh $\sim$ 900)
	MeCN soln.	15,040(55) 20,400(sh $\sim$ 90) $\sim$ 22,700(sh)
$[\text{VCl}_2(\text{phen})_2]\text{Cl}$	Solid MeCN soln*	13,600 $\sim$ 20,600(sh) $\sim$ 23,000(sh) 14,500(40) $\sim$ 23,000(sh $\sim$ 190) 25,400(1460) 34,200(10,500)
$[\text{VBr}_2(\text{bipy})_2]\text{Br}$	Solid MeCN soln.	$\sim$ 12,300(sh) 17,100(sh) 23,800(br, sh) $\sim$ 12,100(sh) 17,100(sh) 25,300(sh) 26,300
$[\text{VBr}_2(\text{phen})_2]\text{Br}$	Solid MeCN soln.	$\sim$ 16,700(sh) 22,000 16,700 24,700(sh) 27,900

/cont'd.

Table 3.7 cont'd.. Electronic Spectra of Bipyridyl and Phenanthroline Complexes

Complex	State	Peak positions in $\text{cm.}^{-1}$ ( $\epsilon_{\text{max}}$ in parentheses) <sup>†</sup>
$[\text{VBr}_2(\text{bipyridyl})_2]^-$ Br, MeCN	Solid	10,900(w) 16,800 ~22,200(sh) 25,000br
$[\text{VBr}_2(\text{bipyridyl})_2]^-$ Br, $\text{CHCl}_3$	Solid	16,800 26,000

<sup>†</sup> Internal bipyridyl and phenanthroline transitions omitted.

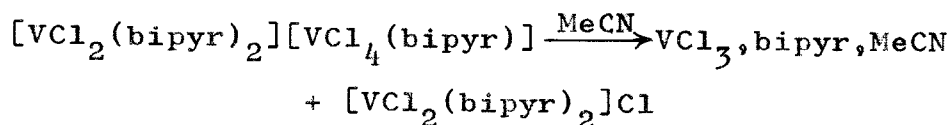
\* ref. 89

The structures proposed for the complexes are generally supported by their visible spectra. Thus  $2[\text{VCl}_3, \text{bipyr}]$  has a very similar spectrum to  $[\text{VCl}_4, 2\text{py}]^-$ , which would be expected if the former were dimeric with chlorine bridging, so giving the vanadium atom an environment of four chlorine and two nitrogen donor atoms.  $2\text{VCl}_3, 3\text{bipyr}$  has a similar spectrum to the above complexes, which is to be expected if it contains the  $[\text{VCl}_4, \text{bipyr}]^-$  entity, inherent in the proposed ionic structure  $[\text{VCl}_2(\text{bipyr})_2][\text{VCl}_4, \text{bipyr}]$ . Unfortunately, peaks due to the cationic species  $[\text{VCl}_2, (\text{bipyr})_2]^+$  probably occur in a similar region of the spectrum, (since the complex  $[\text{VCl}_2, (\text{phen})_2]^+\text{Cl}^-$  shows peaks at  $13,600 \text{ cm.}^{-1}$  and  $\approx 20,600 \text{ cm.}^{-1}$  (sh) in its reflectance spectrum), and hence the structure of this unusual compound cannot be unambiguously inferred from its visible spectrum. However, the fact that the reflectance spectrum of  $2\text{VCl}_3, 3\text{bipyr}$  and its solution spectrum in nitromethane (in which it is also a 1:1 electrolyte) are virtually identical strongly supports the ionic rather than the dimeric structure (A) involving a bridging bipyridyl molecule.

When  $2\text{VCl}_3, 3\text{bipyr}$  dissolves in acetonitrile it still behaves as a 1:1 electrolyte, but a significant



spectral change occurs, the first band undergoing a blue shift so that the pattern of peaks is similar to that found in the spectrum of  $VCl_3, \text{bipyr}, \text{MeCN}$ . This suggests that the following reaction may be occurring upon dissolution in acetonitrile:



The presence of complex species such as  $[V(\text{bipyr})_3][VCl_6]$  is eliminated since the anion  $[VCl_6]^{3-}$  has two transitions at  $11,400 \text{ cm.}^{-1}$  and  $18,000 \text{ cm.}^{-1}$ .<sup>44</sup>

Bipyridyl and phenanthroline complexes generally give complicated ultraviolet spectra, with strong electron transfer bands dominating the region;<sup>111</sup> it is therefore difficult to make a detailed assignment of the bands observed in the spectra of these complexes. Peaks found in the region of  $29,000 \text{ cm.}^{-1}$  and  $25,000 \text{ cm.}^{-1}$  for the chloro and bromo complexes respectively are probably  $V(d) \leftarrow \text{halogen}(\pi)$  (see Chapter 4). Peaks at lower energies ( $\sim 23,000 \text{ cm.}^{-1}$  for the chloro and  $\sim 17,000 \text{ cm.}^{-1}$  for the bromo complexes) probably involve transitions of the type  $\text{bipyr}(\text{phen})\pi^* \leftarrow V(d)$ , by analogy with the proposals made earlier for the pyridine complexes.

The internal  $\pi \rightarrow \pi^*$  transitions of phenanthroline are little influenced by coordination, but the lowest energy band of bipyridyl occurring at  $35,500 \text{ cm.}^{-1}$  in the

free ligand is shifted to  $\sim 33,000 \text{ cm.}^{-1}$  on coordination. This change has been attributed to the bipyridyl's adopting a cis conformation on complex formation, whereas in the solid or solution in organic solvents, the molecule possesses trans stereochemistry.<sup>112</sup>

CHAPTER FOUR

COMPLEXES OF VANADIUM(III) HALIDES

WITH

ETHER DONOR MOLECULES

## Introduction

Complexes of vanadium(III) halides with ether donor ligands have received little attention, although compounds formed by reaction of cyclic and bidentate ethers with vanadium(IV) chloride are well known,<sup>113</sup> and the analogous titanium(III) halide systems have been extensively studied.<sup>114,115</sup>

A 1:3 adduct of vanadium(III) chloride with tetrahydrofuran (THF) is well established<sup>67,116</sup> but the analogous bromo complex has been only briefly studied.<sup>117</sup> No complex of either halide with a bidentate ether ligand has been prepared.

The vanadium(III) halide/tetrahydrofuran systems have been re-investigated, together with the previously reported compound trichlorotris(tetrahydrofuran)chromium(III),<sup>118</sup> to extend their range of known physical properties, and to compare their ultraviolet spectra with those of some titanium(III) halide complexes. The reactions of vanadium(III) halides with the bidentate ether 1,2-dimethoxyethane ( $C_4H_{10}O_2$ ) have been studied, and compounds of the type  $VX_3 \cdot C_4H_{10}O_2$  and  $VX_3 \cdot 1.5C_4H_{10}O_2$  have been isolated.

## Preparation of the Complexes

The complexes were prepared by refluxing approximately

1 gm. of the appropriate halide with excess of the ligand (20 ml.) for approximately 24 hr. in a sealed ampoule. Crystalline products, slightly soluble in the ligand were obtained and isolated by filtration on the vacuum line. Trichlorotris(tetrahydrofuran)chromium(III) was prepared<sup>118</sup> by extracting a mixture of anhydrous chromium(III) chloride and zinc dust with dry tetrahydrofuran in a Soxhlet apparatus attached to the vacuum line. The adducts  $VX_3 \cdot C_4H_{10}O_2$  were prepared by heating  $VX_3 \cdot 1.5C_4H_{10}O_2$  to  $106^\circ$  under vacuum for 2.5 hr.

The analytical and magnetic susceptibility data are summarised in table 4.1.

The complexes were all soluble in their respective parent ethers, but dissolution in acetonitrile resulted in irreversible replacement of the coordinated ligands. For example,  $VCl_3 \cdot 1.5C_4H_{10}O_2$  gave a green solution (conductivity  $1.94 \text{ohm}^{-1} \text{cm}^2$  at  $3.0 \times 10^{-3} \text{gm. mol. litre}^{-1}$ ) on addition of acetonitrile. Evaporation of the liquid phase left a green solid whose infrared spectrum contained a peak at  $2,300 \text{ cm.}^{-1}$ , characteristic of coordinated acetonitrile, but no peaks attributable to coordinated 1,2-dimethoxyethane. When  $VCl_3 \cdot C_4H_{10}O_2$  was dissolved in 1,2-dimethoxyethane and excess ligand removed by evaporation, the remaining product was  $VCl_3 \cdot 1.5C_4H_{10}O_2$ .

Table 4.1 Analytical and Magnetic Data for the Vanadium(III) Halide Ether Complexes

Compound	Colour	$\mu$ (B.M.)	Analysis % +			
			C	H	M	X
$\text{VCl}_3 \cdot 3\text{C}_4\text{H}_8\text{O}$	Pink	2.80*	-	-	13.5 (13.6)	28.3 (28.5)
$\text{VBr}_3 \cdot 3\text{C}_4\text{H}_8\text{O}$	Red- brown	2.78	27.2 (28.4)	4.6 (4.8)	10.1 (10.1)	48.5 (47.3)
$\text{VCl}_3 \cdot 1.5\text{C}_4\text{H}_{10}\text{O}_2$	red- pink	2.82	24.3 (24.2)	5.4 (5.2)	17.4 (17.4)	36.0 (36.4)
$\text{VBr}_3 \cdot 1.5\text{C}_4\text{H}_{10}\text{O}_2$	brown	2.68	-	-	11.8 (12.0)	55.5 (56.3)
$\text{VCl}_3 \cdot \text{C}_4\text{H}_{10}\text{O}_2$	brick- red	2.85	18.8 (19.4)	4.3 (4.1)	20.8 (20.6)	42.4 (43.0)
$\text{VBr}_3 \cdot \text{C}_4\text{H}_{10}\text{O}_2$	brown	-	12.7 (12.6)	2.8 (2.7)	-	62.6 (63.0)
$\text{CrCl}_3 \cdot 3\text{C}_4\text{H}_8\text{O}$	magenta	3.88	-	-	13.9 (13.9)	28.4 (28.4)

+ Calculated values in parentheses

\* ref. 67

Found: V, 17.4%. Calc. for  $VCl_3 \cdot 1.5C_4H_{10}O_2$ : V, 17.4%.  
None of the complexes was soluble in benzene.

Attempts to isolate 1,4-dioxan adducts by displacement of trimethylamine from  $VX_3 \cdot 2NMe_3$  with 1,4-dioxan diluted with benzene were unsuccessful, as little trimethylamine was replaced. Reaction of 1,4-dioxan with trichlorotris(acetonitrile)vanadium(III) resulted in the isolation of a pink product whose infrared spectrum indicated that some ether had coordinated but there was also a strong band at  $2,300 \text{ cm.}^{-1}$  due to coordinated acetonitrile. The vanadium(III) halide/1,4-dioxan system was not studied further.

### Results and Discussion

Owing to the insolubility of the complexes in solvents (other than the parent ligand) with which they do not react, collection of conductivity and molecular weight data was not possible. However, the properties of the compounds are shown to be consistent with the presence of simple six-coordinate vanadium(III) species.

The room temperature magnetic moments of the adducts are in the range 2.68 - 2.85 B.M., thus confirming the presence of tervalent vanadium. The chromium(III) complex has the expected moment for three unpaired electrons, namely 3.88 B.M.

Table 4.2 Infrared Spectra (1300  $\text{cm.}^{-1}$  to 700  $\text{cm.}^{-1}$ ) of the  
1,2-dimethoxyethane Complexes

1,2-dimethoxyethane	$\text{VCl}_3$ , $1.5\text{C}_4\text{H}_{10}\text{O}_2$	$\text{VCl}_3$ , $\text{C}_4\text{H}_{10}\text{O}_2$	$\text{VBr}_3$ , $1.5\text{C}_4\text{H}_{10}\text{O}_2$	$\text{VBr}_3$ , $\text{C}_4\text{H}_{10}\text{O}_2$
1248w	1272s	1278s	1280m	1280w
1195m	1230m	1237s 1208w	1235m 1202w	1235m
1111s, br	1178m 1152w 1102vw	1183m 1152w 1105w, sh	1182m 1160w, sh 1108w	1185m 1102w, sh
1028m	1068 } vs 1040 } br 1015 }	1072s 1025s	1065s } 1010s } br 980s }	1065s 1010s
982w-m				
937w				
924sh	865 } s, 850 } br	863s 825sh	858s 840s	910m 857s 839s
853m-s				
821sh	815sh 805sh	805sh	805sh 780sh	805sh



The most prominent feature of the spectrum of tetrahydrofuran itself is the presence of two strong bands at  $1068\text{ cm.}^{-1}$  and  $908\text{ cm.}^{-1}$  assigned to the asymmetric and symmetric C-O-C stretching vibrations respectively.<sup>119</sup> On coordination, these bands disappear and are replaced by new peaks at around  $1040$  and  $1010\text{ cm.}^{-1}$ , and  $\sim 850\text{ cm.}^{-1}$ . The assignment of the infrared spectra of the 1,2-dimethoxyethane complexes (table 4.2) is not unambiguous since the interpretation of the spectrum of the free ligand is subject to some doubt. There are two strong bands in the spectrum of 1,2-dimethoxyethane at  $1111\text{ cm.}^{-1}$  and  $853\text{ cm.}^{-1}$  which have been attributed to the asymmetric and symmetric C-O stretching frequencies respectively,<sup>120</sup> by comparison with the spectrum of tetrahydrofuran. However, whilst the  $1111\text{ cm.}^{-1}$  peak splits and shows the expected fall in frequency on coordination, the  $853\text{ cm.}^{-1}$  band splits and moves to a slightly higher frequency. 1,2-dimethoxyethane may exist as the trans, cis or gauche conformers, but in the liquid phase of the free ligand the trans and gauche forms are thought to be present.<sup>121</sup> On coordination, however, the ligand must adopt either the cis or the gauche form if it is to function as a bidentate ligand. In principle, it is possible to distinguish between these different forms on the basis of infrared spectra and, accordingly, the

bands at  $937\text{ cm.}^{-1}$  and  $924\text{ cm.}^{-1}$  in free 1,2-dimethoxyethane have been assigned to  $\text{CH}_2$  rocking modes due to the presence of the gauche form,<sup>121</sup> and the  $853\text{ cm.}^{-1}$  band as a  $\text{CH}_2$  rocking mode associated with the trans form. Other workers<sup>122</sup> disagree with this proposal, pointing out that the  $853\text{ cm.}^{-1}$  band persists in the complex  $\text{TiBr}_4 \cdot \text{C}_4\text{H}_{10}\text{O}_2$ , which molecular weight and NMR measurements have shown to be monomeric with the ligand acting as a bidentate donor. Simple calculations have shown that the gauche rather than the cis conformer of the ligand will be favoured when the ligand is present as a bidentate donor.<sup>122</sup>

It is tentatively suggested that the  $853\text{ cm.}^{-1}$  band is a  $\text{CH}_2$  rocking mode associated with the gauche conformer rather than the symmetric C-O stretching vibration. The bands appearing at  $937$  and  $924\text{ cm.}^{-1}$  in the free ligand may now be assigned to  $\text{CH}_2$  rocking modes arising from the presence of the trans conformer. As the  $937$  and  $924\text{ cm.}^{-1}$  peaks are absent from the spectra of the complexes it may be concluded that only the gauche form of the ligand is present.

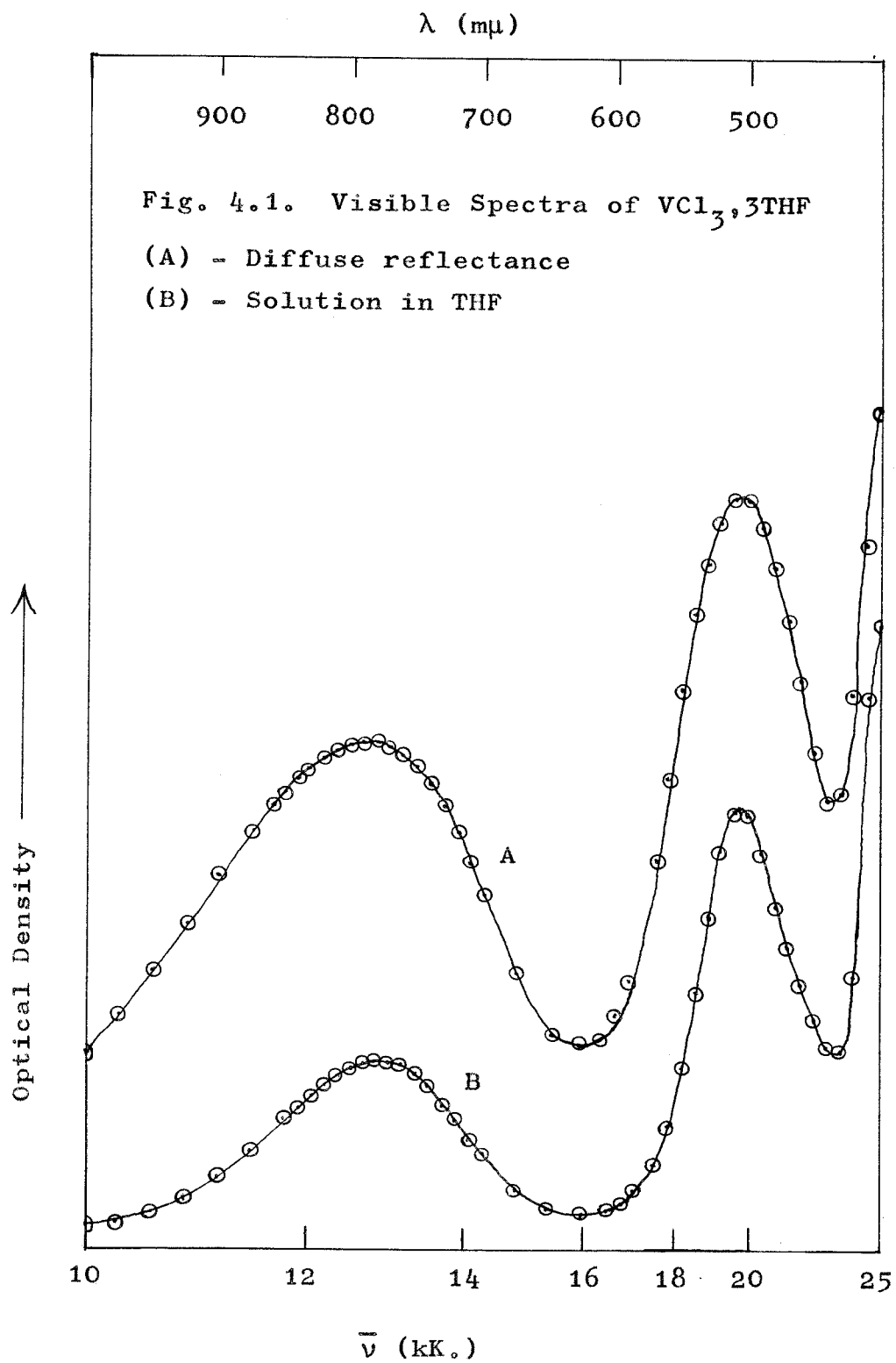
The low infrared spectra of the complexes have been measured in the region  $500\text{ cm.}^{-1}$  to  $200\text{ cm.}^{-1}$  and the results are recorded in table 4.3. The tetrahydrofuran complexes,  $\text{VCl}_3 \cdot 3\text{THF}$  and  $\text{CrCl}_3 \cdot 3\text{THF}$  show three bands in

Table 4.3 Low Infrared Spectra (500  $\text{cm.}^{-1}$  - 200  $\text{cm.}^{-1}$ )

Complex	State	$\nu_{\text{M-X}} \text{ cm.}^{-1}$	unassigned $\text{cm.}^{-1}$
$\text{CrCl}_3, 3\text{THF}$	N.M.* THF soln.	366s 344s 308m 360s	470w 275m 395sh 282s, br
$\text{VCl}_3, 3\text{THF}$	N.M. THF soln.	366s 327s 300m 354s	423w 266m 418w 280s, br
$\text{VBr}_3, 3\text{THF}$	THF soln.	282s, br	356w
$\text{VCl}_3, 1.5\text{C}_4\text{H}_{10}\text{O}_2$	N.M.	362s 333m 303s	437m 414m
$\text{VCl}_3, 1\text{C}_4\text{H}_{10}\text{O}_2$	N.M.	364sh 348s 302s	426m

\* N.M. = Nujol Mull

the metal-chlorine stretching region, and thus a trans ( $C_{2v}$ ) configuration may be assigned to them; a similar structure has been proposed by Clarke for the analogous  $TiCl_3 \cdot 3THF$  on the basis of low infrared evidence.<sup>72</sup>  $VBr_3 \cdot 3THF$  would not mull satisfactorily and so its spectrum was recorded in tetrahydrofuran, which has no observable peaks in the  $500-200\text{ cm.}^{-1}$  region. A broad band appeared at  $282\text{ cm.}^{-1}$  in the position expected for V-Br stretching frequencies. When the spectra of  $VCl_3 \cdot 3THF$  and  $CrCl_3 \cdot 3THF$  were measured in tetrahydrofuran, a marked change occurred. The triplet structure of the metal-chlorine bands disappeared and was replaced by a single, strong band at around  $360\text{ cm.}^{-1}$ ; in addition a broad absorption appeared at around  $280\text{ cm.}^{-1}$ . The reason for this change is not clear. The collapse of the triplet structure into a single band may indicate that  $VCl_3 \cdot 3THF$  and  $CrCl_3 \cdot 3THF$  possess a cis rather than a trans configuration, and in the solid, the two bands (of symmetry  $a_1 + e$ ) expected for the cis complex are resolved into three peaks. It is unlikely that the band at  $\sim 280\text{ cm.}^{-1}$  is a metal-chlorine stretching mode, however, but it may be one involving "metal-oxygen" ligand stretching. The spectra of  $VCl_3 \cdot C_4H_{10}O_2$  and  $VCl_3 \cdot 1.5C_4H_{10}O_2$  exhibit three peaks in the  $360-300\text{ cm.}^{-1}$  region attributable to V-Cl stretching modes, indicating that the site symmetry of



the vanadium atom is low.

Bands not observed in the free ligands are found in the far infrared spectra of all the complexes at around 414-470  $\text{cm.}^{-1}$ . These bands may possibly be "metal-oxygen" stretching in origin, or they may be weak ligand deformation modes which have gained intensity on coordination.

Measurement of the visible spectra of the complexes, recorded in table 4.4, are consistent with the presence of six-coordinate vanadium(III) species both in the solid and solution of the free ligand. The two expected "d-d" transitions in  $\text{VCl}_3, 3\text{THF}$  are in almost identical positions both in the solid and in solution in tetrahydrofuran, (see fig. 4.1), and in good agreement with the values reported by Duckworth for the same complex.<sup>90</sup> Only the lowest energy transition, namely  ${}^3\text{T}_{2g} \leftarrow {}^3\text{T}_{1g}(\text{F})$  is observed in the bromo analogue, as the  ${}^3\text{T}_{1g}(\text{P}) \leftarrow {}^3\text{T}_{1g}(\text{F})$  band is masked by the more intense charge transfer band at about 22,000  $\text{cm.}^{-1}$ . The spectrum of the chromium complex contains all three expected "d-d" bands, namely (in order of increasing energy)  ${}^4\text{T}_{2g} \leftarrow {}^4\text{A}_{2g}$ ,  ${}^4\text{T}_{1g}(\text{F}) \leftarrow {}^4\text{A}_{2g}$  and  ${}^4\text{T}_{1g}(\text{P}) \leftarrow {}^4\text{A}_{2g}$ . The first two peaks are broad in the reflectance spectrum, and split in solution. Calculation of 10Dq and 15B for  $\text{VCl}_3, 3\text{THF}$  and  $\text{CrCl}_3, 3\text{THF}$  based on the positions of the first two ligand field

Table 4.4 Visible Spectra

Complex	State	Peak positions ( $\text{cm.}^{-1}$ ) +	10Dq ( $\text{cm.}^{-1}$ )	15B ( $\text{cm.}^{-1}$ )
$\text{VCl}_3, 3\text{THF}$	Solid THF soln.	12,700 19,800 12,800(12) 19,800(28)	13,800	8,200
$\text{VBr}_3, 3\text{THF}$	Solid THF soln.	12,500 12,400(31)		
$\text{VCl}_3, 1.5\text{C}_4\text{H}_{10}\text{O}_2$	Solid	12,300, $\sim$ 13,000 sh $\sim$ 13,800sh 19,800		
	$\text{C}_4\text{H}_{10}\text{O}_2$ soln.	13,200 20,600		
	MeCN soln.	14,700 21,300 sh		
$\text{VCl}_3, 3\text{MeCN}^*$	MeCN soln.	14,800 21,400	15,500	8,100
$\text{VCl}_3, \text{C}_4\text{H}_{10}\text{O}_2$	Solid	12,400 19,050 23,300 sh		
$\text{VBr}_3, 1.5\text{C}_4\text{H}_{10}\text{O}_2$	Solid	11,600 $\sim$ 12,300 sh $\sim$ 13,300sh $\sim$ 17,900sh		
	$\text{C}_4\text{H}_{10}\text{O}_2$ soln.	12,500		
$\text{VBr}_3, \text{C}_4\text{H}_{10}\text{O}_2$	Solid	$\sim$ 12,100sh 14,200br		
$\text{CrCl}_3, 3\text{THF}$	Solid	13,800br 19,700br 30,500	13,800	9,070
	THF soln.	13,700(21) 14,400(21) 17,400 sh 19,800(41) 31,700 sh		

 +  $\epsilon_{\text{max}}$  in parentheses

\* ref. 115

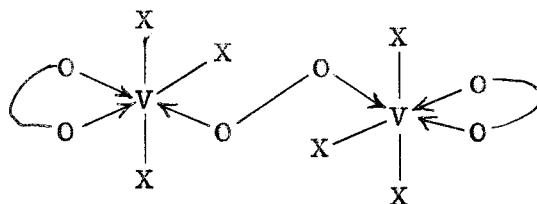
bands gives the parameters recorded in table 4.4. The value of  $15B$  shows the expected reduction from the free ion values of  $12,920 \text{ cm.}^{-1}$  and  $15,450 \text{ cm.}^{-1}$  for  $V^{3+}$  and  $Cr^{3+}$  respectively. The parameter  $10Dq$  is similar in magnitude for the vanadium and chromium complexes, but less than the value of  $14,700 \text{ cm.}^{-1}$  found for  $TiCl_3 \cdot 3THF$ ,<sup>91</sup> in agreement with the ligand field order  $Ti^{III} > V^{III} > Cr^{III}$ .<sup>78</sup>  $10Dq$  should be less for chromium(III) than vanadium(III); the reason for the discrepancy is probably that the calculation of  $10Dq$  is based on the assumption that the complexes have  $O_h$ , rather than  $C_{3v}$  or  $C_{2v}$  symmetry. From a calculation based on the positions of the first two bands in the reflectance spectrum of  $CrCl_3 \cdot 3THF$ , the third transition,  ${}^4T_{1g}(P) \leftarrow {}^4A_{2g}$  is predicted to occur at  $30,800 \text{ cm.}^{-1}$  and is observed experimentally at  $30,500 \text{ cm.}^{-1}$ .

The spectra of the  $VX_3 \cdot 1.5C_4H_{10}O_2$  adducts are similar to the simple, six-coordinate  $VX_3 \cdot 3THF$  compounds, but the lowest energy band in their reflectance spectra is resolved into a triplet, presumably because of a low site symmetry for the vanadium. The spectrum of  $VCl_3 \cdot 1.5C_4H_{10}O_2$  in acetonitrile is identical with that of trichlorotris-(acetonitrile)vanadium(III) in the same solvent, demonstrating conclusively that 1,2-dimethoxyethane has been replaced by the acetonitrile.

Probable structures for these complexes include an



ionic formulation such as  $[\text{VX}_2(\text{C}_4\text{H}_{10}\text{O}_2)_2][\text{VX}_4\text{C}_4\text{H}_{10}\text{O}_2]$  as suggested earlier for  $2\text{VCl}_3, 3\text{bipy}$  on the basis of conductivity data, or a neutral, dimeric structure with bridging ether molecules, as illustrated schematically below:



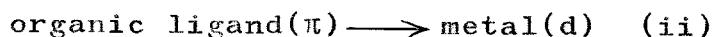
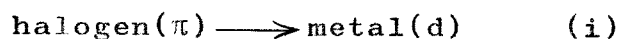
If the assignments of the  $\text{CH}_2$  rocking modes in the infrared are correct, the ionic structure is favoured since this contains only gauche 1,2-dimethoxyethane. A complete X-ray structure analysis of  $\text{TiBr}_3, 1.5\text{C}_4\text{H}_{10}\text{O}_2$  is in progress;<sup>101</sup> in view of this, and the lack of conductivity or molecular weight data, further speculation concerning the nature of the  $\text{VX}_3, 1.5\text{C}_4\text{H}_{10}\text{O}_2$  complexes seems unjustified.

On heating,  $\text{VX}_3, 1.5\text{C}_4\text{H}_{10}\text{O}_2$  complexes lose 1,2-dimethoxyethane yielding the 1:1 adducts  $\text{VX}_3, \text{C}_4\text{H}_{10}\text{O}_2$ . The visible spectra again suggest the presence of six-coordinate vanadium(III), the spectral bands suffering small red shifts compared with those in the spectra of the  $\text{VX}_3, 1.5\text{C}_4\text{H}_{10}\text{O}_2$  adducts. By analogy with  $\text{VCl}_3, \text{bipy}$ , the vanadium atom probably achieves six-coordination

through dimerisation with chlorine bridges.

It is convenient at this point to discuss the charge-transfer spectra of six-coordinate vanadium(III) complexes as a whole, in addition to those compounds reported in this chapter. No assignments of the spectra can profitably be attempted since the molecular symmetry of the adducts is generally lower than  $O_h$ , but several trends may be noted, and comparisons made with the analogous titanium(III) systems.

In mixed organic ligand/halogen adducts of the type  $MX_3L_3$ , three types of charge-transfer transition may be anticipated:



Type (iii) transitions may only occur if the metal possesses unpaired electrons, and the ligand,  $\pi^*$  antibonding orbitals of suitable energy. Recent studies on a wide range of hexahalogenotitanates(IV) and titanium(IV) halide complexes of the type  $TiX_4 \cdot 2L$  have shown that, taking into account internal ligand  $\pi \rightarrow \pi^*$  transitions, the remainder of the charge-transfer spectra observed depends only on the nature of the halogen, and is independent of the nature of the ligands.<sup>123</sup> Furthermore, it has been

Table 4.5 Ultraviolet Spectra

Compound	State	Peak positions (cm. <sup>-1</sup> )
CrCl <sub>3</sub> , 3THF	Solid	36,000 45,600
	THF soln.	36,600 41,700
VC1 <sub>3</sub> , 3THF	THF soln.	28,600 32,500 38,900(sh) 42,600
VC1 <sub>3</sub> , 1.5C <sub>4</sub> H <sub>10</sub> O <sub>2</sub>	C <sub>4</sub> H <sub>10</sub> O <sub>2</sub> soln.	28,900 32,700 43,100
VC1 <sub>3</sub> , 3MeCN <sup>a</sup>	MeCN soln.	30,850 41,800
TiCl <sub>3</sub> , 3dioxan <sup>b</sup>	dioxan soln.	31,200 36,600 44,800
TiCl <sub>3</sub> , 3MeCN <sup>b</sup>	MeCN soln.	31,000(sh) 35,100 43,500
[Et <sub>2</sub> NH <sub>2</sub> ] <sub>2</sub> VC1 <sub>6</sub> <sup>c</sup>	Solid	19,400(sh) 22,600 28,200 36,400 45,400
VBr <sub>3</sub> , 3THF	Solid	20,400(sh) 23,300
		21,500 25,600 32,300 37,000sh 41,800
	Solid	21,700(sh) 24,400(br)
		22,300 26,000 32,800 42,400
VBr <sub>3</sub> , C <sub>4</sub> H <sub>10</sub> O <sub>2</sub>	Solid	21,700(sh) 24,700(br)
VBr <sub>3</sub> , 3MeCN <sup>a</sup>	MeCN soln.	21,000 24,200 36,400(br) 42,000
TiBr <sub>3</sub> , 3dioxan <sup>b</sup>	dioxan soln.	29,900 34,400 40,500
TiBr <sub>3</sub> , 3MeCN <sup>b</sup>	MeCN soln.	29,000 33,000 38,100

a ref. 68

b ref. 101

c ref. 123

concluded that the transitions are all of type (i). Measurements of the ultraviolet spectra of a number of titanium(III) halide complexes have led to the same conclusion, namely that the nature of the charge-transfer spectra is governed by the halogen,<sup>101</sup> except where the ligand has low lying  $\pi^*$  levels e.g. pyridine.

The results obtained for some six-coordinate vanadium(III) compounds are given in table 4.5, together with the spectra of some related titanium(III) species. In the light of the evidence quoted above it is probable that the transitions observed in the vanadium complexes are all of type (i), that is to say halogen( $\pi$ )  $\rightarrow$  vanadium(d).

The first transition in the bromo complexes occurs at  $\sim 22,000 \text{ cm.}^{-1}$ , some  $7000 \text{ cm.}^{-1}$  lower than the first transitions in the chloro complexes. It is the presence of this strong band which is responsible for masking the second "ligand-field" band,  ${}^3T_{1g}(P) \leftarrow {}^3T_{1g}(F)$  in vanadium(III) bromo complexes. The band shift on passing from Cl to Br is due to the decrease in electronegativity of the halogens in the order:  $F > Cl > Br > I$  (i.e. an increase in their electron-releasing, or reducing powers). The first transitions in the analogous titanium(III) systems are found at slightly higher frequencies in agreement with the fact that it is harder to reduce Ti(III) than V(III). If the spectrum of  $VCl_6^{2-}$  (where vanadium is formally in

oxidation state 4) is considered, the lowest energy charge-transfer band has suffered a red shift to around  $22,000 \text{ cm.}^{-1}$ ,<sup>123</sup> an observation expected on chemical grounds, since it is easier to reduce V(IV) than V(III). The first band in  $\text{CrCl}_3 \cdot 3\text{THF}$  is at a higher frequency than in  $\text{VCl}_3 \cdot 3\text{THF}$ . This is unexpected since the reduction of Cr(III) is more feasible than V(III); however, this difficulty may be resolved if the blue shift of the first allowed band is attributed to the additional spin-pairing energy involved in the transition to the half-filled level,  $(t_{2g})^3$ .

Transitions of type (iii) have been postulated to account for strong bands observed in the region  $17,000 - 24,000 \text{ cm.}^{-1}$  in the spectra of vanadium(III) adducts with pyridine, 2,2'-bipyridyl and 1,10-phenanthroline (see preceding chapter), since it is known that these ligands have the energetically available  $\pi^*$  orbitals necessary to participate in these transitions.<sup>78</sup>

CHAPTER FIVE

FIVE COORDINATE COMPLEXES

## Introduction

Few five coordinate complexes of first row transition metal halides with monodentate ligands have been reported for early members of the series.  $\text{TiCl}_4 \cdot \text{NMe}_3$  was found to be monomeric and hence five coordinate in benzene,<sup>60</sup> and its far infrared spectrum recorded both in solid and in benzene solution is consistent with this monomeric formulation.<sup>124</sup> Several complexes of the type  $\text{MX}_3 \cdot \text{L}_2$  have been reported. The titanium complexes  $\text{TiX}_3 \cdot 2\text{NMe}_3$  ( $\text{X} = \text{Cl}, \text{Br}$ ) were first thought to be dimeric, achieving six coordination through halogen bridging,<sup>125</sup> but a recent single crystal X-ray study of  $\text{TiBr}_3 \cdot 2\text{NMe}_3$  has shown that the complex possesses an essentially trans trigonal bipyramidal structure.<sup>126</sup> Five coordination has been inferred, in solution at least, for some trialkylphosphine and trialkylphosphineoxide complexes of vanadium(III) chloride on the basis of molecular weight and conductivity data.<sup>127</sup> Preliminary reports<sup>128, 129</sup> of molecular weight, conductance, infrared spectra and dipole moment measurements on solutions of  $\text{VCl}_3 \cdot 2\text{NMe}_3$ ,  $\text{VBr}_3 \cdot 2\text{NMe}_3$ ,  $\text{VCl}_3 \cdot 2\text{SMe}_2$  and  $\text{VCl}_3 \cdot 2\text{SEt}_2$  showed that the complexes were monomeric with probable  $\text{D}_{3h}$  symmetry.

The previously reported work<sup>128, 129</sup> has now been extended to include measurements of ultraviolet and visible spectra, and magnetic susceptibility over a

temperature range. The existing range of complexes has been augmented by the preparation of  $VBr_3 \cdot 2SMe_2$ , adducts with tetrahydrothiophen,  $VX_3 \cdot 2C_4H_8S$  ( $X = Cl, Br$ ), and the chromium compound,  $CrCl_3 \cdot 2NMe_3$ .

### Experimental

#### (1) Reaction of Vanadium(III) chloride and Vanadium(III) bromide with Dimethylsulphide

(a)  $VCl_3$  (0.735gm) dissolved on shaking with  $(CH_3)_2S$  ( $\sim 20$ ml.) in an ampoule for three days, giving a deep red solution which yielded a pink solid when the excess liquid phase was removed by evaporation.

Found: Cl, 37.2; V, 18.1%

Calc. for  $VCl_3 \cdot 2S(CH_3)_2$ : Cl, 37.8; V, 18.1%.

(b)  $VBr_3$  (0.94gm) and  $(CH_3)_2S$  (1.5ml.) were mixed in an ampoule with benzene (20ml.) as diluent; overnight reflux resulted in the formation of a brown solution and a small quantity of brown solid. The solid was filtered off leaving a brown filtrate, which gave a brown solid on evaporation of the liquid phase. This solid dissolved in benzene to give a purple solution, and was very susceptible to hydrolysis.

Found: C, 11.2; Br, 58.1; S, 15.8; V, 12.4%. M, 481  
(0.56% in  $C_6H_6$ )

Calc. for  $VBr_3 \cdot 2S(CH_3)_2$ : C, 11.6; Br, 57.8; S, 15.45; V, 12.3%;  
M, 415.



(2) Reaction of Vanadium(III) chloride and Vanadium(III) bromide with Tetrahydrothiophen ( $C_4H_8S$ )

(a)  $VCl_3$  (0.85gm) was refluxed with a 1:20  $C_4H_8S/C_6H_6$  mixture in an ampoule for 12 hours and formed a pink solution with a small quantity of pink solid. The pink solution was isolated by filtration, and evaporation of the volatiles left a pink solid.

Found: C, 29.1; H, 4.8; Cl, 31.8; S, 19.5; V, 14.8%. M, 391  
 $\mu$ , 2.60 B.M. (0.63% in  $C_6H_6$ )

Calc. for  $VCl_3, 2C_4H_8S$ : C, 28.8; H, 4.8; Cl, 31.9; S, 19.2;  
 V, 15.3%. M, 334.

(b)  $VBr_3$  (0.9gm) was treated with  $C_4H_8S$  (1ml.) in  $C_6H_6$  (20ml.) under reflux for 12 hours and an orange-brown solution together with a black solid was produced. Evaporation of the solution gave a brown solid which fumed in moist air and dissolved in dry benzene to give a purple solution.

Found: C, 19.6; H, 3.8; Br, 50.9; V, 10.8%;  $\mu$ , 2.55 B.M.  
 M, 504 (0.75% in  $C_6H_6$ )

Calc. for  $VBr_3, 2C_4H_8S$ : C, 20.6; H, 3.5; Br, 51.3; V, 10.9%.  
 M, 467.

(3) Reaction of Chromium(III) chloride with Trimethylamine

No reaction occurs unless zinc dust is present. Anhydrous  $CrCl_3$  (1.2gm) and Zn dust (0.02gm) were placed in a double-ampoule,  $(CH_3)_3N$  distilled in and the

ampoule system sealed. The reaction appeared to be complete after about 12 hours when a purple-blue solution had formed. Filtration and evaporation within the ampoule system gave a purple-blue solid which was recrystallised from benzene. The solid was insoluble in 'iso-octane'.

Found: C, 25.9; H, 6.6; Cl, 38.7; N, 9.5; Cr, 19.0%;  
M, 294 (0.56% in  $C_6H_6$ )

Calc. for  $CrCl_3, 2N(CH_3)_3$ : C, 26.1; H, 6.6; Cl, 38.5; N, 10.1;  
Cr, 18.8%; M, 277.

(4) The preparation and analytical data for  $VCl_3, 2NMe_3$  and  $VBr_3, 2NMe_3$  are given in appendix A.  $TiCl_3, 2NMe_3$  was supplied by T.E. Lester.

Magnetic Susceptibility Data(a)  $\text{VCl}_3, 2(\text{CH}_3)_2\text{S}$   $\theta = 72^\circ$ 

$T^\circ\text{K}$	$\chi'_m$ (c.g.s. $\times 10^6$ )	$\mu_{\text{eff}}$ (B.M.)
298.1	3027	2.69
290.7	3100	2.69
283.2	3151	2.67
273.2	3247	2.66
253.2	3446	2.64
233.2	3676	2.62
213.2	3946	2.59
193.2	4259	2.57
173.2	4617	2.53
153.2	4978	2.47
133.1	5489	2.42
113.1	6085	2.35
93.3	6799	2.25
83.2	7144	2.18

(b)  $\text{VBr}_3 \cdot 2(\text{CH}_3)_2\text{S}$   $\theta = 61^\circ$ 

$T^\circ\text{K}$	$\chi'_m$ (c.g.s. $\times 10^6$ )	$\mu_{\text{eff}}$ (B.M.)
298.2	2912	2.64
293.1	2947	2.63
283.2	3030	2.62
273.2	3127	2.61
253.2	3330	2.60
233.2	3563	2.58
213.2	3818	2.55
193.2	4119	2.52
173.2	4481	2.49
153.2	4896	2.45
133.0	5396	2.40
113.0	5982	2.33
93.0	6677	2.23

(c)  $\text{CrCl}_3 \cdot 2\text{NMe}_3$   $\theta = 7^\circ$ 

$T^\circ\text{K}$	$\chi'_m$ (c.g.s. $\times 10^6$ )	$\mu_{\text{eff}}$ (B.M.)
298.2	6305	3.88
291.9	6448	3.88
283.2	6646	3.88
273.2	6899	3.89
253.2	7424	3.88
233.2	8049	3.88
213.2	8794	3.88
193.2	9661	3.87
173.2	10,753	3.86
153.1	12,123	3.86
133.0	13,873	3.84
113.0	16,153	3.82
93.0	19,110	3.77

(d)  $\text{VBr}_3, 2\text{NMe}_3 \quad \theta = 12^\circ$ 

$T^\circ\text{K}$	$\chi'_m$ (c.g.s. $\times 10^6$ )	$\mu_{\text{eff}}$ (B.M.)
298.1	3198	2.76
288.2	3288	2.75
273.2	3450	2.75
253.2	3726	2.75
233.2	4008	2.73
213.2	4385	2.73
193.2	4819	2.73
173.2	5354	2.72
153.2	5965	2.70
133.1	6809	2.69
113.1	7889	2.67
83.0	10,407	2.63

(e)  $\text{TiCl}_3, 2\text{NMe}_3 \quad \theta = 41^\circ$ 

$T^\circ\text{K}$	$\chi'_m$ (c.g.s. $\times 10^6$ )	$\mu_{\text{eff}}$ (B.M.)
298.2	1195	1.69
288.2	1223	1.68
273.2	1279	1.67
253.2	1366	1.66
233.1	1459	1.65
213.1	1574	1.64
193.2	1709	1.63
173.2	1859	1.60
153.2	2055	1.59
133.0	2299	1.56
113.0	2606	1.53
84.9	3280	1.49

### Results and Discussion

The vanadium(III) chloride/dialkyl sulphide system was first investigated by Duckworth<sup>90</sup> who isolated the complexes  $VCl_3, 2S(CH_3)_2$  and  $VCl_3, 2S(C_2H_5)_2$ , which were found to be monomeric in benzene and non-conducting in nitrobenzene. These and the higher dialkyl sulphide adducts are thermally unstable compounds which readily lose dialkyl sulphide on heating. Bridgland et al. obtained reduction products when reacting the cyclic thioethers tetrahydrothiophen and pentamethylene sulphide (PMS) with vanadium(IV) chloride.<sup>113</sup> They isolated a complex  $VCl_3, 2PMS$ , but obtained no structural data for it. The two trimethylamine complexes,  $VX_3, 2NMe_3$ , (X = Cl, Br) reported previously<sup>128, 129</sup> are soluble in non-polar solvents, and the chloride derivative is non-conducting in nitrobenzene and monomeric in benzene in which it possesses a dipole moment of 0.4D.

The complexes prepared in this work of the type  $MX_3, L_2$  are all potential five coordinate species. They are very unstable to hydrolysis and are soluble in benzene in which they are all monomeric; bromo complexes are more unstable than chloro derivatives, and the solubilities in benzene decrease in the order

Table 5.1 The Infrared Spectrum (1300-400  $\text{cm.}^{-1}$ )  
of  $\text{CrCl}_3 \cdot 2\text{NMe}_3$

$\text{CrCl}_3 \cdot 2\text{NMe}_3$	$\text{NMe}_3$	Assignment*
1238m-w	1272	C-N str. (e)
1165w, br	1183	$\text{CH}_3$ rock ( $a_1$ )
1108m, s	1104	$\text{CH}_3$ rock (e)
1037vw		
983s	1043	$\text{CH}_3$ rock (e)
811s	826	C-N str. ( $a_1$ )
763w		} combination bands?
735w		
724w		
683m-w		
524m	425	C-N deformation (e)
442m	365	C-N deformation ( $a_1$ )

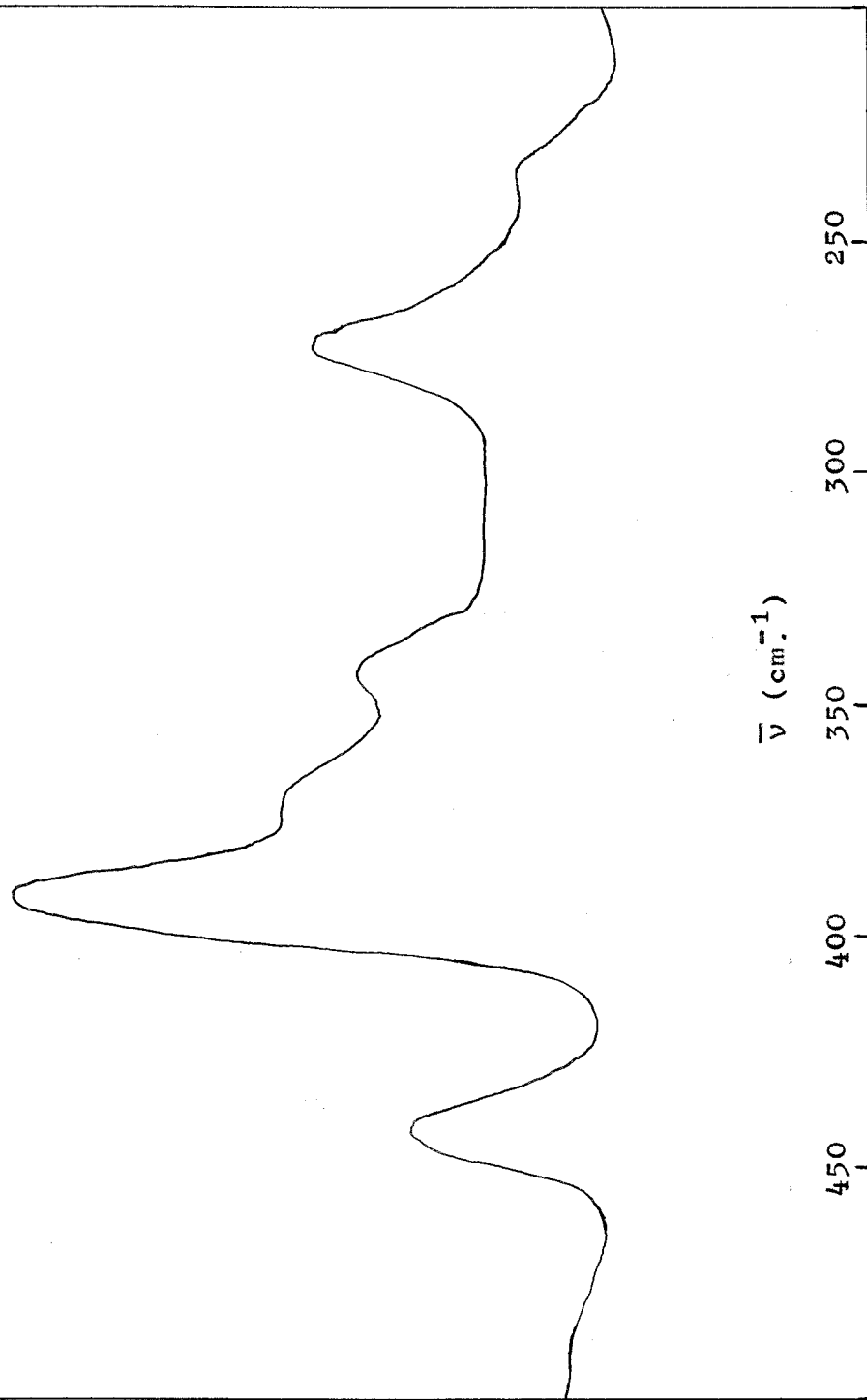
\* ref. 130

$VX_3, 2NMe_3, CrCl_3, 2NMe_3 > VX_3, 2SMe_2 > VX_3, 2C_4H_8S$ . The spectral properties of all the complexes dissolved in benzene are interpreted in terms of a trans trigonal bipyramidal model with essentially  $D_{3h}$  symmetry, whilst in the solid state, only the trimethylamine complexes appear to retain their five coordinate geometry.

The infrared spectra in the  $450-4000\text{ cm.}^{-1}$  region show bands expected for the coordinated ligand. Thus, in trimethylamine peaks observed at  $1272\text{ cm.}^{-1}$  and  $826\text{ cm.}^{-1}$ , attributed<sup>130</sup> to the asymmetric and symmetric C-N stretching modes, are lowered on coordination, appearing at  $1240\text{ cm.}^{-1}$  and  $810\text{ cm.}^{-1}$  in the spectrum of  $CrCl_3, 2NMe_3$  (see table 5.1). Similarly, the strong  $CH_3$  rocking mode at  $1043\text{ cm.}^{-1}$  shifts to  $983\text{ cm.}^{-1}$  on complex formation. The infrared spectra of the thioethers show little change on coordination. The  $CH_3$  rocking modes observed in free dimethyl sulphide at 1027, 972 and  $906\text{ cm.}^{-1}$ <sup>131</sup> are slightly increased in frequency ( $\sim 15\text{ cm.}^{-1}$ ) in the complexes. The C-S stretching modes are weak in organosulphur complexes,<sup>132</sup> and are not readily discernable. The asymmetric C-S stretching vibration observed as a weak band at  $742\text{ cm.}^{-1}$  in the free ligand<sup>131</sup> is not seen in the spectrum of  $VBr_3, 2SMe_2$ , whereas the symmetric C-S stretching frequency at  $692\text{ cm.}^{-1}$  suffers the expected lowering in frequency on



Fig. 5.1. Far Infrared spectrum of  $\text{CrCl}_3 \cdot 2\text{NMe}_3$  (Nujol Mull)



complex formation to  $683 \text{ cm.}^{-1}$ . Both C-S stretching frequencies are observed in the spectrum of free tetrahydrothiophen at  $819 \text{ cm.}^{-1}$  and  $685 \text{ cm.}^{-1}$ ,<sup>133</sup> and are modified on coordination, appearing  $\sim 810 \text{ cm.}^{-1}$  and  $\sim 670 \text{ cm.}^{-1}$  in the spectra of the complexes.

The far infrared spectra recorded in the region  $500\text{-}200 \text{ cm.}^{-1}$  provide the most direct evidence for the molecular symmetry of the complexes. The spectra are reported in table 5.2. For a complex  $\text{MX}_3\text{L}_2$  with trans trigonal bipyramidal geometry and  $\text{D}_{3h}$  symmetry, only one M-X stretching vibration of  $e'$  symmetry is expected. If the molecular symmetry is lowered to  $\text{C}_{2v}$ , three infrared active metal-halogen bands (of symmetry  $2a_1 + b_1$ ) are predicted. Thus, the spectra of the trimethylamine complexes,  $\text{VX}_3\text{,}2\text{NMe}_3$  exhibit only one band which may be ascribed to a metal-halogen stretching mode, at 410 and  $340 \text{ cm.}^{-1}$  for the chloride and bromide derivatives respectively.<sup>124</sup> As expected,<sup>72</sup> the frequencies of these bands are much higher than those observed in six-coordinate species such as  $\text{VX}_3\text{L}_3$  where M-X stretching modes are observed at about  $360 \text{ cm.}^{-1}$  for chloro- and  $\sim 300 \text{ cm.}^{-1}$  for bromo adducts. It was concluded therefore that these complexes possessed  $\text{D}_{3h}$  symmetry. The analogous  $\text{CrCl}_3\text{,}2\text{NMe}_3$  whose spectrum is shown in fig. 5.1 has only one strong band which may be ascribed to a

Table 5.2 Far infrared Spectra (450-200  $\text{cm.}^{-1}$ )

Compound	State <sup>+</sup>	Peak positions ( $\text{cm.}^{-1}$ )			
		M-X stretching modes	"M-L" str	*Ligand/solvent	unassigned
$\text{CrCl}_3, 2\text{NMe}_3$	N	392s	274m	441m 373sh,w	344sh,w 234w
$\text{VCl}_3, 2\text{NMe}_3^a$ $\text{VBr}_3, 2\text{NMe}_3^a$	$\text{C}_6\text{H}_6$ $\text{C}_6\text{H}_6$	409s 345vs		442m 439w	325w 298w 290w
$\text{VCl}_3, 2\text{SMe}_2$	$\text{C}_6\text{H}_6$ N	422s 420m 373s 342s	262w 259m	293w	373w
$\text{VBr}_3, 2\text{SMe}_2$	$\text{C}_6\text{H}_6$ N	340vs 351sh 340m 308s 280s	260w 261s	390w 294w	250sh,w
$\text{VCl}_3, 2\text{C}_4\text{H}_8\text{S}$	$\text{C}_6\text{H}_6$ N	418s 373s 344s	266m 266m	298w	$\sim$ 370sh,w
$\text{VBr}_3, 2\text{C}_4\text{H}_8\text{S}$	$\text{C}_6\text{H}_6$ N	336s 305s 276s	263m 262sh	395w 296m	350sh 227sh,w

<sup>+</sup> N = Nujol Mull  $\text{C}_6\text{H}_6$  = benzene soln.

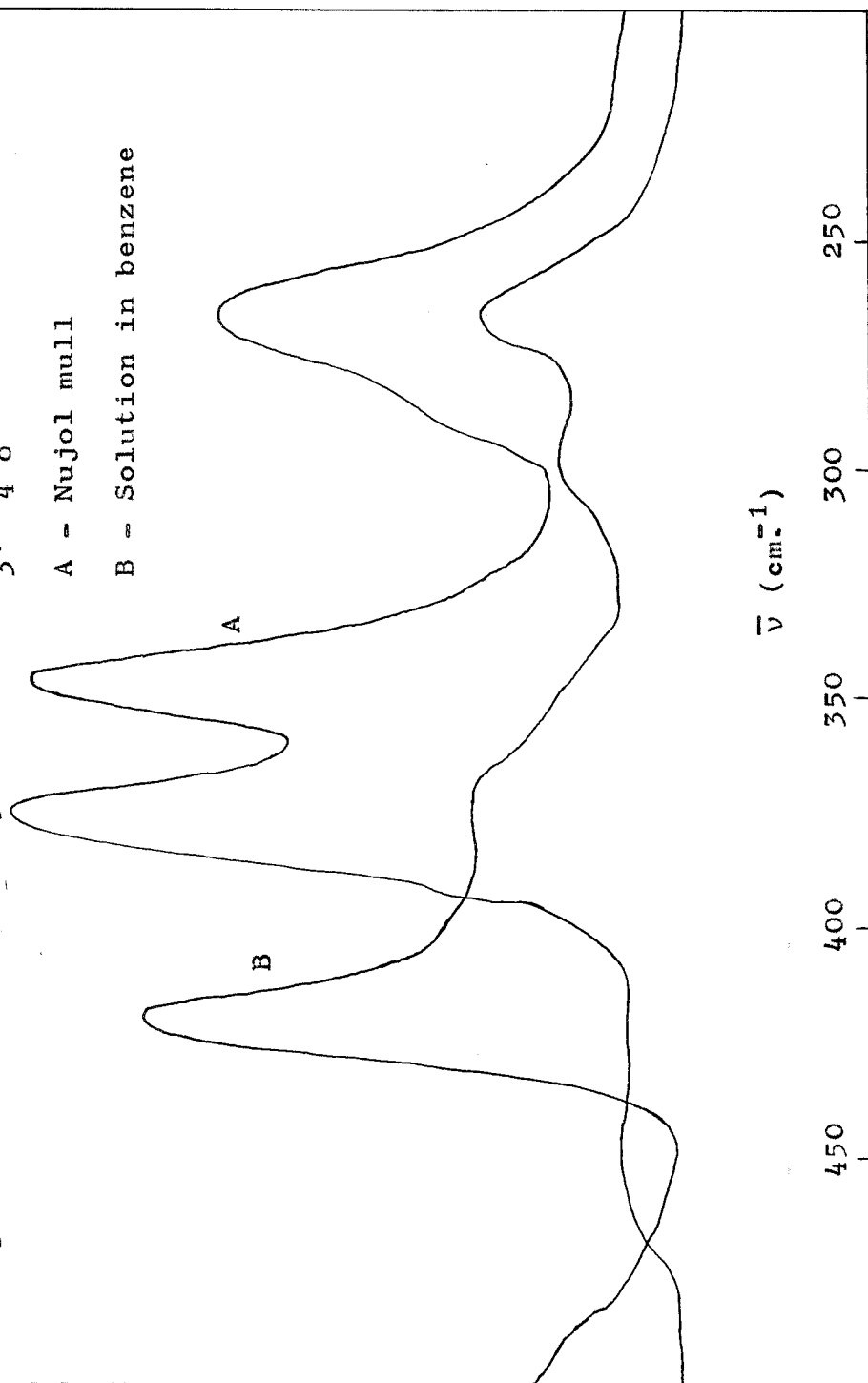
\* solvent and ligand absorptions: Benzene: 395w;  $\text{NMe}_3$ : 130 425, 365, 264;  
 $\text{Me}_2\text{S}$ : 131 282br,w;  $\text{C}_4\text{H}_8\text{S}$ : 133 280vw

<sup>a</sup> ref. 124

Fig. 5.2. Far Infrared spectra of  $VCl_3 \cdot 2C_4H_8S$

A - Nujol mull

B - Solution in benzene



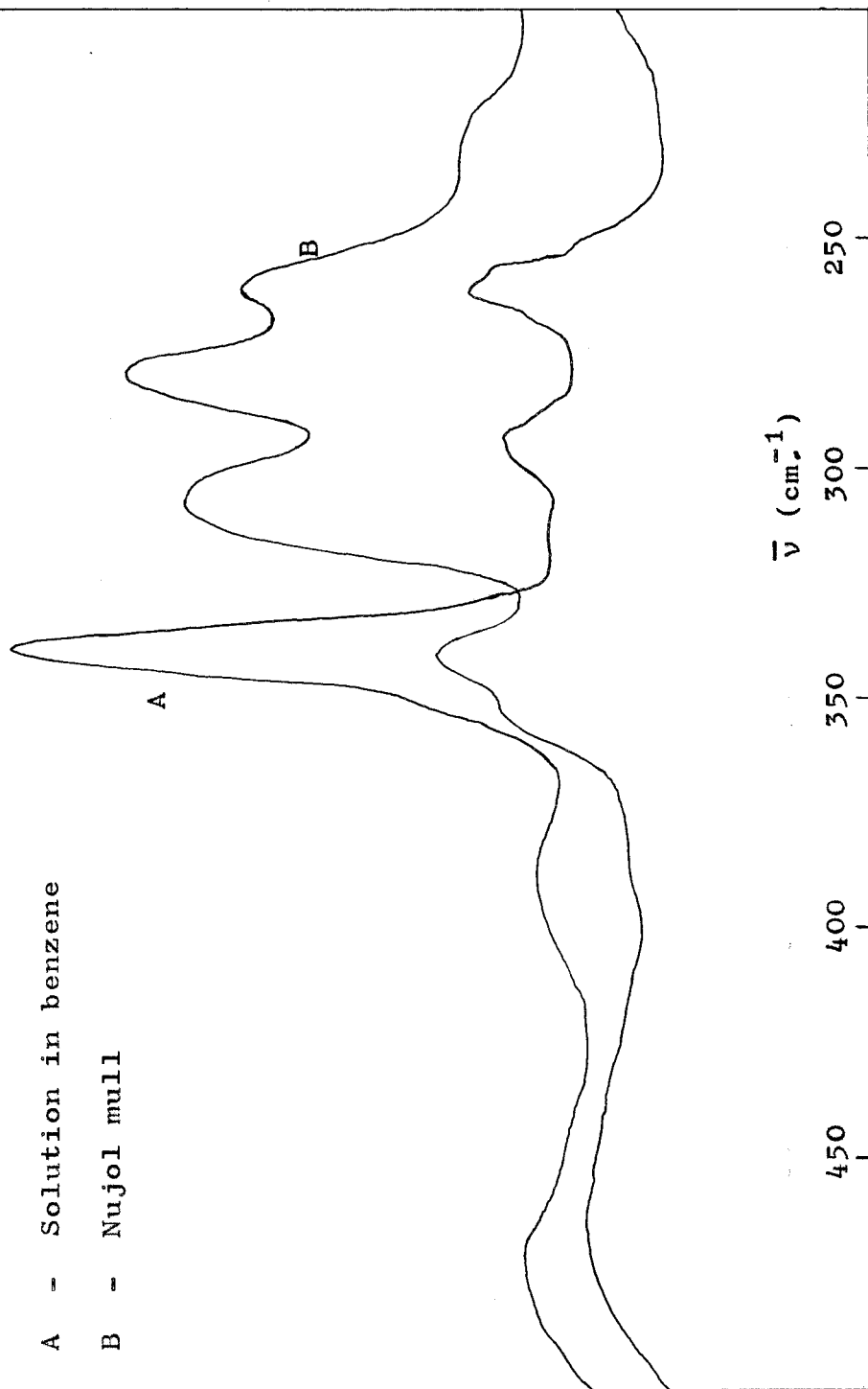
chromium-chlorine stretching mode, at  $392 \text{ cm.}^{-1}$ .  $D_{3h}$  symmetry is again indicated, although X-ray evidence (see chapter 6) has shown that the molecule only possesses  $C_{2v}$  symmetry in the solid state. The distortion is evidently insufficient to resolve the degeneracy of the  $e'$  Cr-Cl mode and to excite the Raman active  $a'_1$  symmetric stretching mode into infrared activity. The structures of the trimethylamine complexes will be discussed further in chapter 6.

Whereas the trimethylamine complexes of vanadium have the same spectra in the Nujol mulls as in benzene solution, it is apparent from table 5.2 that the mull and solution spectra of the thioether complexes are quite different. It is suggested that, although the thioether complexes are five coordinate in solution with  $D_{3h}$  symmetry, they become six-coordinate in the solid through some form of bridging. The spectra of  $VCl_3 \cdot 2C_4H_8S$  and  $VBr_3 \cdot 2SMe_2$  reproduced in figs. 5.2 and 5.3 clearly illustrate the modification of the vanadium-halogen stretching frequency which occurs when the complexes are dissolved in benzene. In the chloride complexes, for example, the V-Cl stretching frequency is shifted from the  $340\text{-}370 \text{ cm.}^{-1}$  region in the solid, to a single band  $\sim 418 \text{ cm.}^{-1}$  in benzene solution. The bands due to the five-coordinate species still persist,

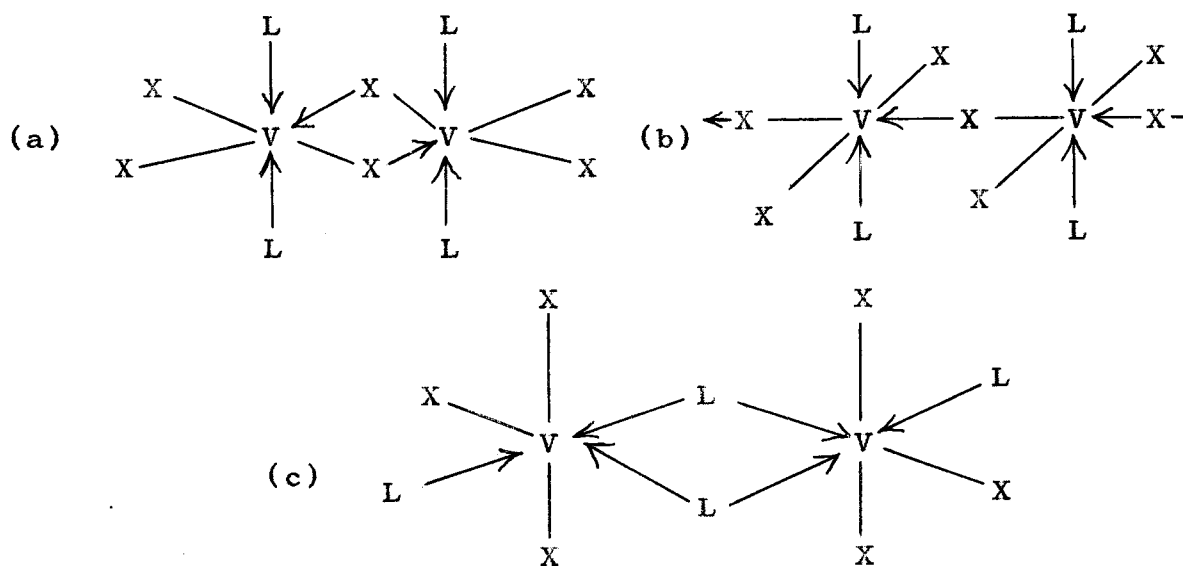
Fig. 5.3. Far Infrared Spectra of  $VBr_3 \cdot 2SMe_2$

A - Solution in benzene

B - Nujol mull



albeit at a much reduced intensity, in the mull spectra of the dimethylsulphide adducts (see fig. 5.3 for example). Five- and six-coordinate species must be present in the mull although the former may occur through partial dissolution of the complexes in Nujol. Possible structures for the thioether complexes in the solid include those show below:



Although the available physical and chemical evidence is insufficient to distinguish between the possibilities, structure (c) is less likely than (a) or (b) because of the unfavourable build-up of charge.

The spectra of all the thioether adducts have bands around  $260 \text{ cm.}^{-1}$  which may be tentatively assigned to vanadium-ligand vibrations, although it is clear that such modes must incorporate a considerable contribution

Table 5.3

## Visible Spectra

Complex	State*	Peak position (cm. <sup>-1</sup> ) ( $\epsilon_{\max}$ in parentheses)
VCl <sub>3</sub> , 2NMe <sub>3</sub>	iso-oct.	4700 7000br 11,400w 12,700w 16,500 19,650
	C <sub>6</sub> H <sub>12</sub> C <sub>6</sub> H <sub>6</sub> <sup>a</sup> R	4800 7000br 11,600w ~13,000w 16,600 19,800 13,100(7) 16,700(sh, 11) 20,000(59) 11,400sh 12,900br 16,300 20,000
VBr <sub>3</sub> , 2NMe <sub>3</sub>	iso-oct.	6000 12,500 14,700 18,300
	CCl <sub>4</sub> C <sub>6</sub> H <sub>6</sub> NMe <sub>3</sub> <sup>a</sup> R	~4200br 6000(12) 12,500(~8) 14,700(~8) 18,600(66) 6000(14) 12,600(5) 14,400(7) 18,400(50) 12,900 12,700 14,300 18,700
VCl <sub>3</sub> , 2SMe <sub>2</sub>	iso-oct. <sup>a</sup>	18,300(48)
	C <sub>6</sub> H <sub>6</sub> Me <sub>2</sub> S <sup>a</sup> R	5500(53) 7200(br, 18) 13,400(sh ~5) 18,500(51) 12,900 20,000(br) 12,050 18,100 20,500sh
VBr <sub>3</sub> , 2SMe <sub>2</sub>	C <sub>6</sub> H <sub>6</sub> Me <sub>2</sub> S R	4700(61) 6400(br, 15) 12,800sh, w 15,800sh 18,300(52) 12,000(21) 10,870
	C <sub>6</sub> H <sub>6</sub> C <sub>4</sub> H <sub>8</sub> S R	5400(37) 7050(br, 13) 12,200( ~5) 18,000(40) 12,500(16) 17,100sh 19,350(17) 12,050 18,100br

/cont'd...



Table 5.3. cont'd...

## Visible Spectra

Complex	State	Peak position (cm. <sup>-1</sup> ) ( $\epsilon_{\max}$ in parentheses)
VBr <sub>3</sub> , 2C <sub>4</sub> H <sub>8</sub> S	C <sub>6</sub> H <sub>6</sub>	4700(50) 6400(br, 20) ~12,300sh,w 18,100(60)
	C <sub>4</sub> H <sub>8</sub> S	12,100(21)
	R	10,930
CrCl <sub>3</sub> , 2NMe <sub>3</sub>	C <sub>6</sub> H <sub>6</sub>	10,100(23) 13,000w,sh 17,600(130) 23,200w,sh 30,200sh(~1000)
	R	~10,000 12,900sh 17,600(br) 23,000sh 30,000

\* R = reflectance;

others measured in solvent stated

iso-oct. = iso-octane

C<sub>6</sub>H<sub>12</sub> = cyclohexane

a ref. 90

from the internal ligand vibrations via coupling.<sup>73,74</sup> Similarly, the band at  $274 \text{ cm.}^{-1}$  in the spectrum of  $\text{CrCl}_3 \cdot 2\text{NMe}_3$ , may be a "Cr-N" stretching mode, or the modified  $\text{CH}_3$  "twisting" vibration which occurs at  $264 \text{ cm.}^{-1}$  for the free ligand.<sup>130</sup> The weak band  $\sim 295 \text{ cm.}^{-1}$  in the spectrum of the thioether compounds is tentatively assigned to a modified C-S-C deformation mode which is found at  $\sim 280 \text{ cm.}^{-1}$  in the free ligand.

The visible spectra are recorded in table 5.3.

Jørgensen has predicted that, in a ligand field of  $D_{3h}$  symmetry, vanadium(III) complexes should exhibit two electronic transitions in the near infrared region.<sup>134</sup> This prediction has been confirmed in more detailed calculations by Wood.<sup>77</sup> Two bands are found at  $\sim 5000 \text{ cm.}^{-1}$  and  $\sim 7000 \text{ cm.}^{-1}$  in the spectra of the compounds dissolved in benzene (and, in certain cases, other non-polar solvents - see table 5.3 for examples); these peaks disappear when the solvent medium used is the free ligand, and the spectra become typical of six-coordinate vanadium(III). These spectral changes are illustrated for  $\text{VCl}_3 \cdot 2\text{C}_4\text{H}_8\text{S}$  in fig. 5.4. The benzene solutions also show weaker bands or shoulders in the 11,000-13,000  $\text{cm.}^{-1}$  region, and these are tentatively assigned to spin-forbidden transitions. The assignments of the spectra of the five-coordinate species are typified by

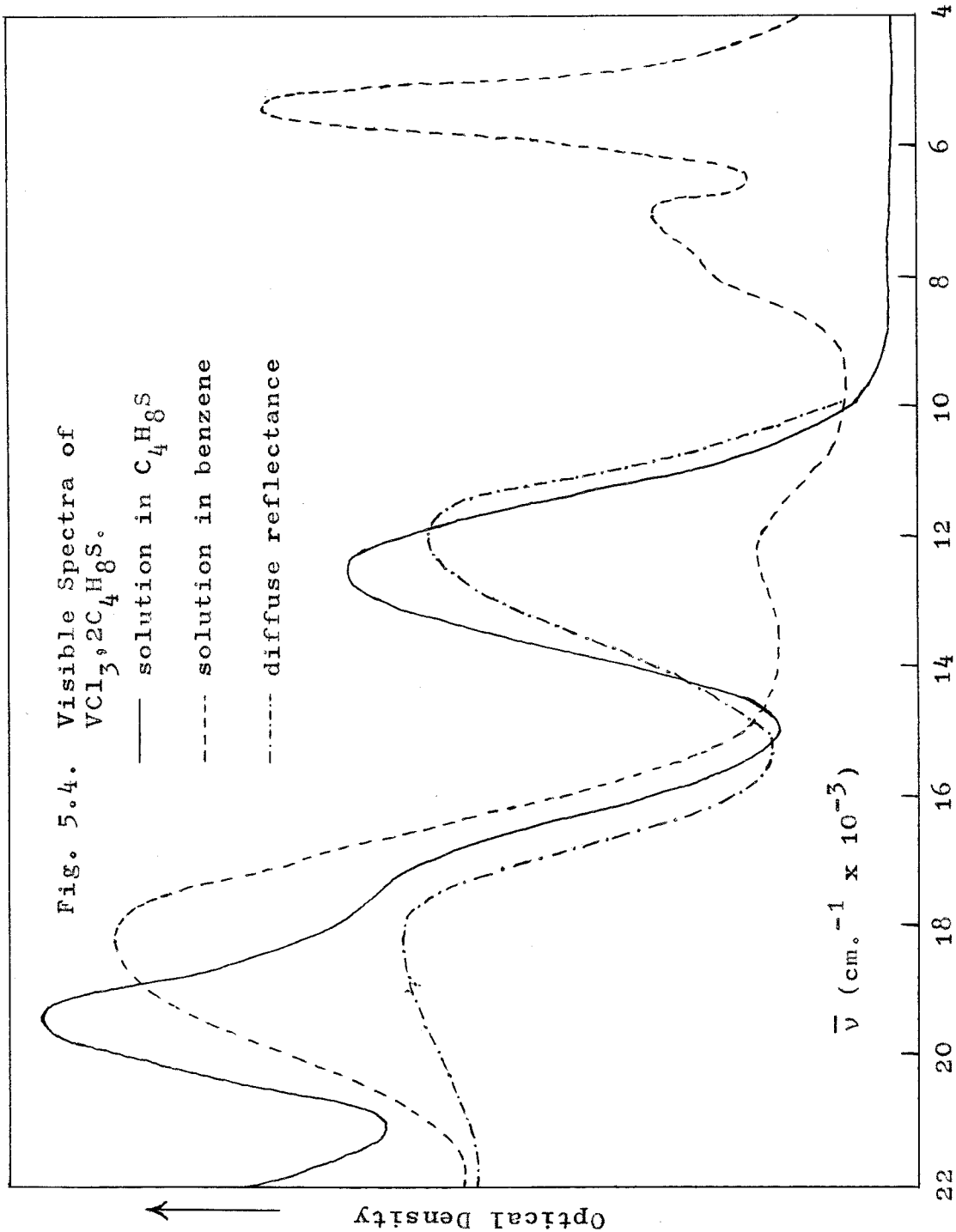


Table 5.4

## Assignments of Visible Spectra

Compound	Peak (cm. <sup>-1</sup> )	Assignment
VCl <sub>3</sub> , 2NMe <sub>3</sub>	4700	$\nu_1$ $3A_1'', 3A_2'' \leftarrow 3A_2'$
	7000	$\nu_2$ $3E''(F) \leftarrow 3A_2'$
	11,400	$1E'' \leftarrow 3A_2'$
	12,700	$1E' \leftarrow 3A_2'$
	16,500	$\nu_3$ $3E'(F) \leftarrow 3A_2'$
	19,650	$\nu_4$ $\left. \begin{array}{l} 3E''(P) \\ 3A_2'(P) \end{array} \right\} \leftarrow 3A_2'$
CrCl <sub>3</sub> , 2NMe <sub>3</sub>	10,100	$4E''(F) \leftarrow 4E'(F)$
	13,000sh,w	spin-forbidden
	17,600	$4A_2'; 4A_1'' + 4A_2'' \leftarrow 4E'(F)$
	23,200sh,w	spin-forbidden
	30,200sh	$\left. \begin{array}{l} 4E''(P) \\ 4A_2'(P) \end{array} \right\} \leftarrow 4E'(F)$

those for  $\text{VCl}_3 \cdot 2\text{NMe}_3$ , based on calculations by Wood,<sup>77</sup> and presented in table 5.4.

In  $\text{VBr}_3 \cdot 2\text{NMe}_3$ , all the bands show a red shift, whereas, in the thioether complexes  $\nu_3$  tends to coalesce with  $\nu_4$  and both peaks show a red shift, but  $\nu_1$  and  $\nu_2$  show slight blue shifts. Similar assignments may be made using the modified energy level diagrams constructed for  $d^7$  and  $d^8$  configurations by Ciampolini et al.<sup>135</sup> The interpretation of the spectrum of  $\text{CrCl}_3 \cdot 2\text{NMe}_3$  given in table 5.4 must remain very tentative since the observed spectrum could not be reproduced very well from calculations based on a  $D_{3h}$  model.<sup>77</sup>

The spectra of the trimethylamine complexes are virtually identical in both solid and solution, thus confirming the same coordination number in both states, as suggested by their far infrared spectra. The presence of six-coordinate vanadium(III) species inferred from the far infrared spectra of the thioether adducts is confirmed by their reflectance spectra, which show two peaks around 12,000 and 20,000  $\text{cm}^{-1}$  for the chloro adducts, and  $\sim$  10,900 and 22,000  $\text{cm}^{-1}$  for the bromo compounds. The lower energy band in each case is assigned to the  ${}^3T_{2g} \leftarrow {}^3T_{1g}(\text{F})$  transition, and the second band in the chloro complexes to the transition  ${}^3T_{1g}(\text{P}) \leftarrow {}^3T_{1g}(\text{F})$ ; the second "d-d" band is not observed

Table 5.5

## Ultraviolet Spectra

Complex	State <sup>+</sup>	Peak positions (cm. <sup>-1</sup> ) ( $\epsilon_{\max}$ in parentheses)
VCl <sub>3</sub> , 2NMe <sub>3</sub>	iso-oct. R	37,850 44,050 37,800 45,400
VBr <sub>3</sub> , 2NMe <sub>3</sub>	iso-oct. C <sub>6</sub> H <sub>6</sub> NMe <sub>3</sub> <sup>a</sup>	30,100 34,400 40,800 45,500 30,100(2700) 21,050br
VCl <sub>3</sub> , 2SMe <sub>2</sub>	iso-oct. <sup>a</sup> R	37,740(7000) 41,200(9800) 28,600 37,800sh 45,000
VBr <sub>3</sub> , 2SMe <sub>2</sub>	C <sub>6</sub> H <sub>6</sub> Me <sub>2</sub> S R	30,000(5,200) 33,800(8,900) 23,500(980) 22,700sh
VCl <sub>3</sub> , 2C <sub>4</sub> H <sub>8</sub> S	C <sub>6</sub> H <sub>6</sub> C <sub>4</sub> H <sub>8</sub> S R	29,000sh 27,900(br, 1400) 28,600 33,500sh 38,200 45,800
VBr <sub>3</sub> , 2C <sub>4</sub> H <sub>8</sub> S	C <sub>6</sub> H <sub>6</sub> C <sub>4</sub> H <sub>8</sub> S R	~22,000sh, w 29,400(sh ~ 5000) 23,200(br, 1500) 33,000(5,700) 21,900 30,000 37,100 45,400
CrCl <sub>3</sub> , 2NMe <sub>3</sub>	R	37,500 45,600
TiCl <sub>3</sub> , 2NMe <sub>3</sub>	R <sup>b</sup>	30,000 37,000 44,900
TiBr <sub>3</sub> , 2NMe <sub>3</sub>	R <sup>b</sup>	27,700 35,600 44,800

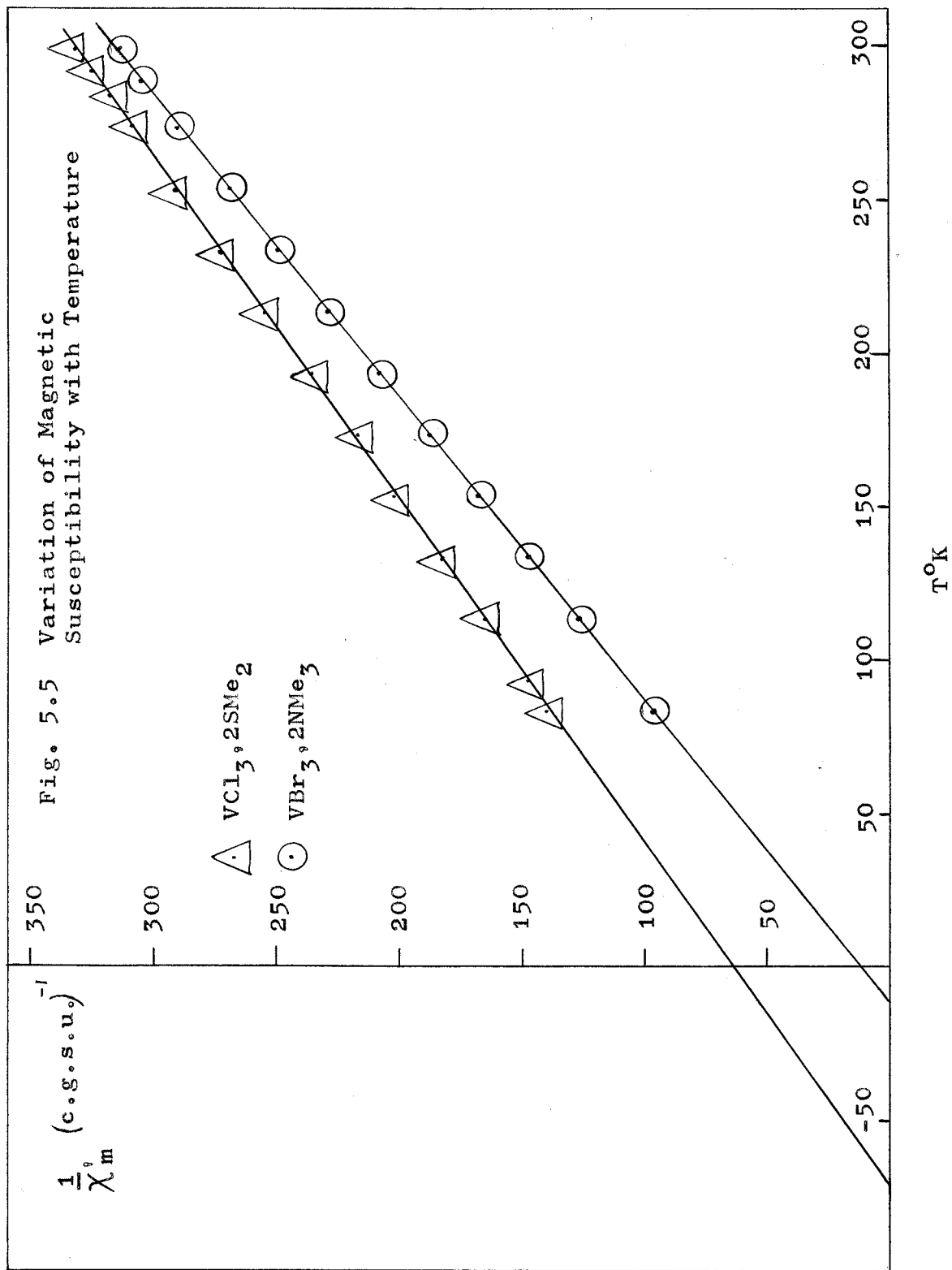
a ref. 90

b ref. 101

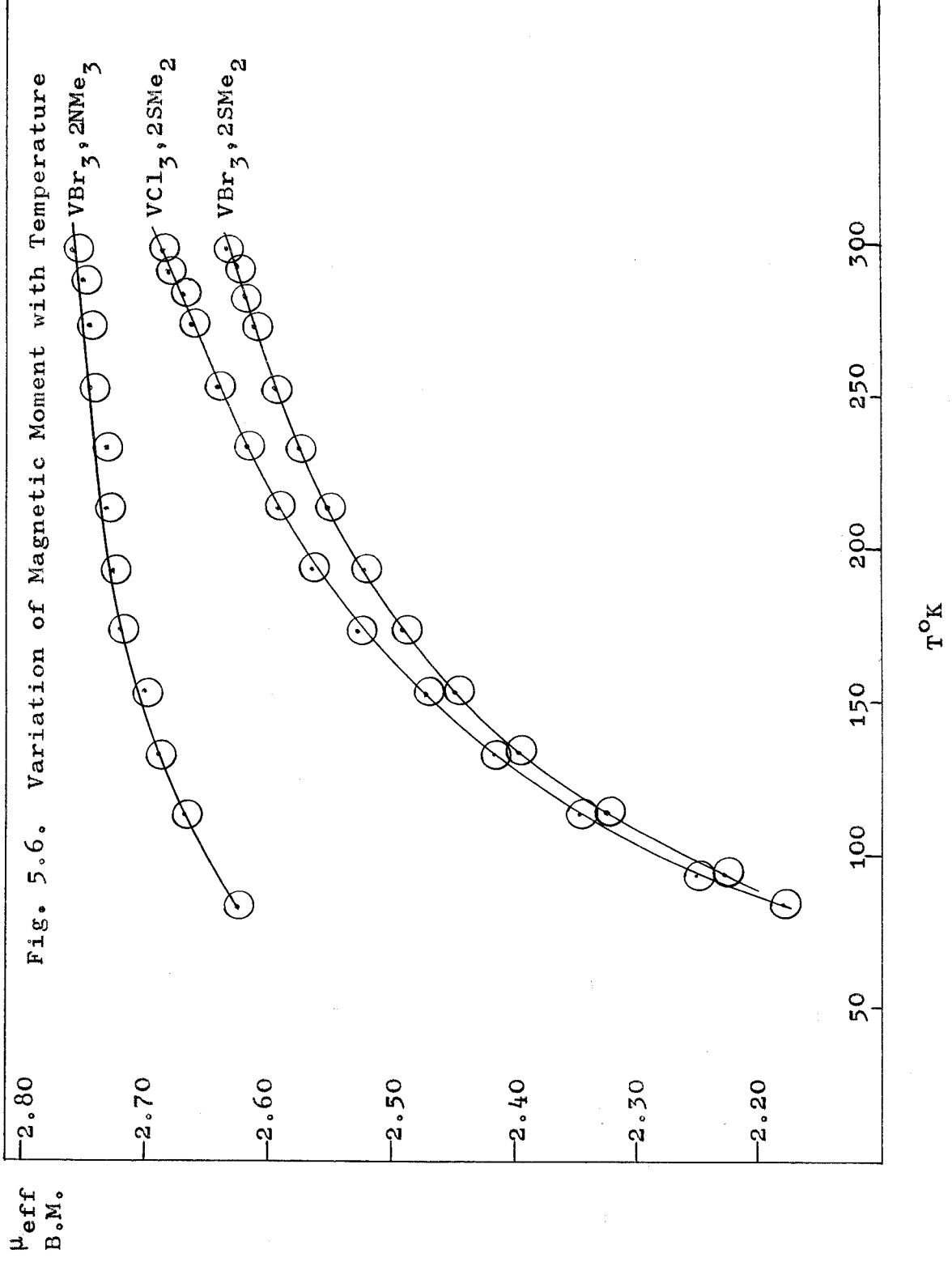
+ see table 5.3 for abbreviations

in the bromo complexes as it is obscured by the strong charge transfer band at  $\sim 22,000 \text{ cm.}^{-1}$ . Unfortunately, it was not possible to measure reflectance spectra below  $10,000 \text{ cm.}^{-1}$  to check the thioether complexes for the absence of the  $\sim 5000$  and  $\sim 7000 \text{ cm.}^{-1}$  bands, which appear to be characteristic of five coordinate vanadium(III).

The ultraviolet spectra are summarised in table 5.5. It can be seen once again that, whereas the spectra of the trimethylamine adducts are very similar in solution and solid, the spectra of the thioether complexes differ in these media. The solution spectra of all the compounds in non-polar solvents are different from the u.v. spectra observed for six-coordinate vanadium(III) adducts (see preceding chapter). The most apparent difference is the considerable shift of the lowest energy band from  $\sim 29,000 \text{ cm.}^{-1}$  in six-coordinate chloro complexes ( $\sim 23,000 \text{ cm.}^{-1}$  for bromo compounds) to  $\sim 38,000 \text{ cm.}^{-1}$  for solutions of  $\text{VCl}_3 \cdot 2\text{L}$  in non-polar solvents ( $\sim 30,000 \text{ cm.}^{-1}$  for the analogous  $\text{VBr}_3 \cdot 2\text{L}$ ). The bands are probably halogen( $\pi$ ) $\rightarrow$ metal(d) in character, and since the ground electronic configuration of vanadium(III) in a  $D_{3h}$  ligand field is  $(e'')^2$ , the shift in the bands may be accounted for by the increase in repulsion energy associated with the transfer of a halogen( $\pi$ ) electron to the half-filled level. This rationale is consistent





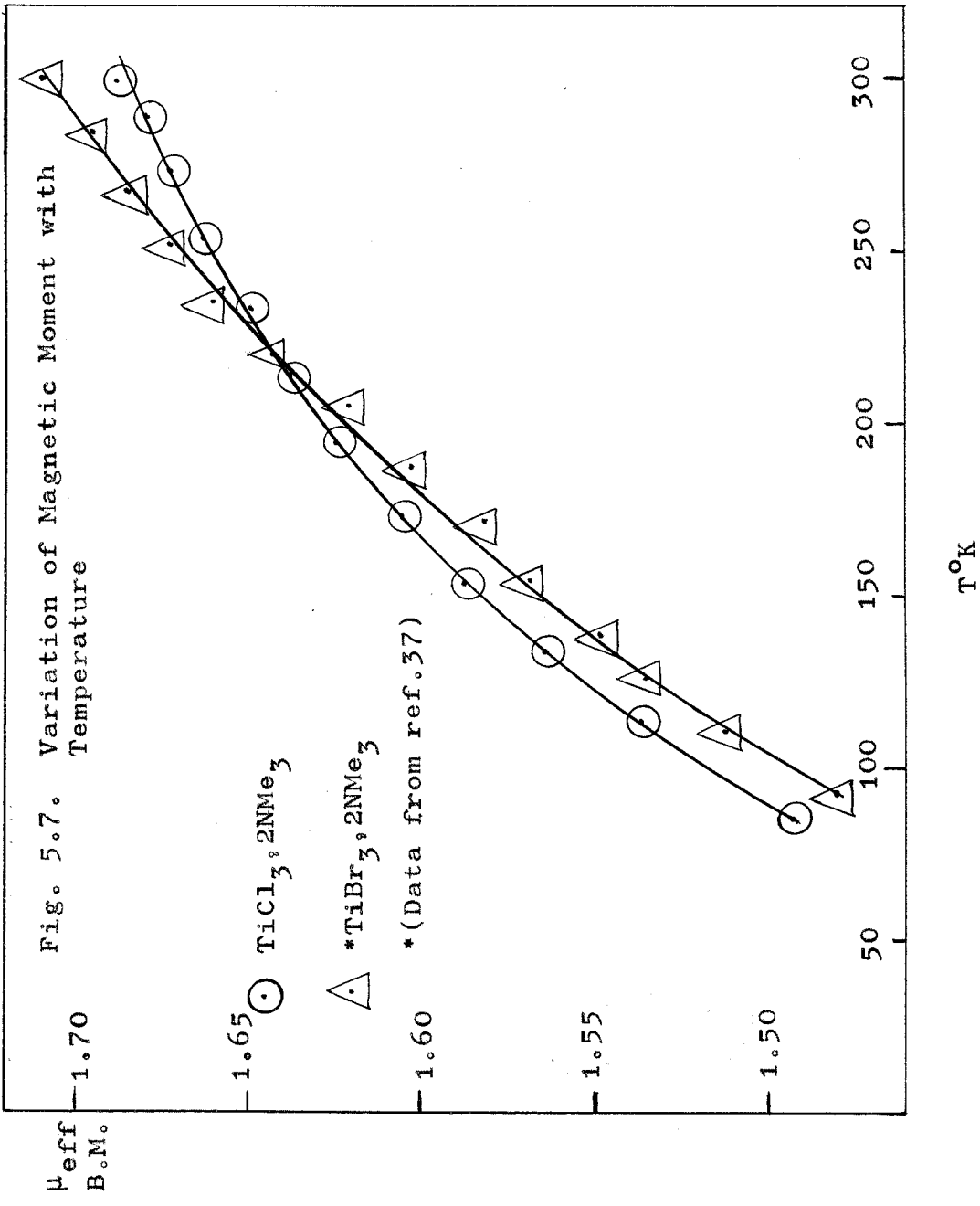


with the spectra of  $\text{TiX}_3 \cdot 2\text{NMe}_3$ ,<sup>101</sup> where the first charge-transfer band is found at a lower energy than in the vanadium analogues, even though on chemical grounds the reverse order is expected, as is observed in the spectra of the six-coordinate adducts. The intensities of the charge-transfer bands are also appreciably greater than those observed in the spectra of the six-coordinate complexes.

The ultraviolet spectra of the thioether complexes in the solid state and in thioether solution are similar to the spectra of other six-coordinate vanadium(III) species.

The magnetic properties of some of the complexes have been studied over a temperature range; all the compounds investigated obey the Curie-Weiss law over the range 80-300°K. Graphs of  $1/\chi'_m$  vs T, and the variation of  $\mu_{\text{eff}}$  with temperature are shown in figs. 5.5 and 5.6.

The magnetic behaviour of the trimethylamine complexes is consistent with the predictions made in chapter 2;  $\text{VCl}_3 \cdot 2\text{NMe}_3$  has a room temperature moment of 2.66 B.M. falling to 2.53 B.M. at 90°K<sup>30</sup> and the moment of  $\text{VBr}_3 \cdot 2\text{NMe}_3$  falls from a room temperature value of 2.76 B.M. to 2.63 B.M. at 83°K. In contrast, the



dimethylsulphide derivatives have magnetic moments which are considerably temperature dependent, falling from room temperature values of  $\sim 2.7$  B.M. to  $\sim 2.2$  B.M. at  $\sim 80^\circ\text{K}$ . Although this is the expected behaviour for  $\text{V}^{3+}$  in an octahedral field, complexes with essentially  $\text{O}_h$  symmetry have moments which are independent of temperature (see chapter 2). The analogous complex,  $\text{TiCl}_3 \cdot 2\text{SMe}_2$  is strongly antiferromagnetic with a Néel temperature  $\sim 320^\circ\text{K}$  and a susceptibility which falls with decreasing temperature.<sup>101</sup>  $\text{TiBr}_3 \cdot 2\text{SMe}_2$  and  $\text{TiI}_3 \cdot 2\text{SMe}_2$  obey a Curie-Weiss law with large values of  $\theta$ , which suggests that they are also antiferromagnetic, but with Néel points at very low temperatures. It is tentatively suggested that the strong temperature dependence of the magnetic moments of these dimethylsulphide/vanadium(III) complexes is due to some form of magnetic exchange involving either direct metal-metal interactions or some 'superexchange' mechanism via bridging atoms.

The temperature dependence of the five-coordinate titanium(III) complexes is shown in fig. 5.7. The moments exhibit a temperature dependence expected for a  ${}^2\text{E}''$  ground term split by spin-orbit coupling (see chapter 2). A deviation from regular  $\text{D}_{3h}$  symmetry found in the molecular structure of  $\text{TiBr}_3 \cdot 2\text{NMe}_3$  has been attributed to a Jahn-Teller distortion, expected for the degenerate

${}^2E''$  term.<sup>126</sup> The distortion produced must be insufficient to affect the temperature dependence of the magnetic moment appreciably. In contrast, the chromium complex obeys the Curie-Weiss law with  $\theta = 7^\circ$ , giving a temperature-independent moment of 3.88 B.M., although the  ${}^4E'$  ground term is expected to give rise to a temperature-dependent moment. To produce a spin-only moment, the expected Jahn-Teller distortion of the ground term will have to be  $\gg kT$ .

CHAPTER SIX

THE CRYSTAL AND MOLECULAR STRUCTURE  
OF  
TRICHLOROBISTRIMETHYLAMINECHROMIUM(III)

## Introduction

Although a number of pentacoordinate complexes of cobalt and nickel with multidentate ligands have been structurally characterised by X-ray diffraction,<sup>136</sup> little crystallographic data are available for potential five coordinate systems involving the early transition elements. Five coordinate complexes stabilized by the monodentate ligand, trimethylamine, are now known (see preceeding chapter) and molecular structure determinations of  $\text{AlH}_3, 2\text{NMe}_3$ <sup>137</sup> and  $\text{TiBr}_3, 2\text{NMe}_3$ <sup>126</sup> have revealed that the geometry<sub>^</sub><sup>of</sup> these complexes is essentially trigonal bipyramidal. The molecular structure of  $\text{TiBr}_3, 2\text{NMe}_3$  showed evidence of a Jahn-Teller distortion which was predicted because its electronic ground term in a ligand field of  $D_{3h}$  symmetry is  ${}^2E''$ . The complex  $\text{CrCl}_3, 2\text{NMe}_3$  with a  $d^3$  configuration gives rise to a  ${}^4E'$  ground term (in  $D_{3h}$ ) which is again orbitally degenerate and the molecule should be subject to a Jahn-Teller distortion. The crystal and molecular structure of  $\text{CrCl}_3, 2\text{NMe}_3$  were determined to investigate this prediction and to verify that the molecule does indeed possess five coordinate geometry.

### Experimental Data

Full details of the experimental procedure may be found in appendix B.

The lattice constants determined from precession photographs using Zr filtered MoK $\alpha$  radiation ( $\lambda = 0.7107\text{\AA}$ ) are  $a = 9.69 \pm 0.01$ ,  $b = 10.12 \pm 0.02$ ,  $c = 13.05 \pm 0.01\text{\AA}$ . Systematic absences [(Ok1) when  $k + 1 \neq 2n$ , (hk0) when  $h \neq 2n$ , (h00) when  $h \neq 2n$ , (Ok0) when  $k \neq 2n$  and (001) when  $l \neq 2n$ ] imply the space groups  $Pna2_1(C_{2v}^9)$  No. 33 or  $Pnma(D_{2h}^{16})$  No.62.<sup>138</sup> The calculated density, assuming four molecules per unit cell, of  $1.43 \text{ gm. ml.}^{-1}$  agrees well with the observed value of  $1.43 \text{ gm.ml.}^{-1}$ .

Intensity data were collected by the equi-inclination Weissenberg technique as described in appendix B. Of the 748 visually estimated reflexions, 256 were accidentally absent and were given an intensity of  $\frac{1}{2}$  the minimum observable. Three observed reflexions were later eliminated from the data as their intensities were affected by the beam-stop shadow, so that a total of 745 reflexions were used in the subsequent analysis. Lorentz, polarization and spot-shape<sup>141</sup> corrections were applied graphically<sup>139</sup> to the measured intensities, but no correction for absorption was made ( $\mu \sim 15 \text{ cm.}^{-1}$  for MoK $\alpha$  radiation).



Determination of the structure

Examination of the layer photographs showed that, qualitatively, the intensity distribution amongst the reflexions was similar to the distribution found in photographs of the analogous  $\text{TiBr}_3 \cdot 2\text{NMe}_3$  (with which the chromium complex is isomorphous), which crystallizes in the space group Pnma; this suggested that crystals of  $\text{CrCl}_3 \cdot 2\text{NMe}_3$  also belonged to this space group.

The following 'general' and 'special' positions [of type (c)] are generated by the space group Pnma.<sup>138</sup>

(i) 'general':  $x, y, z; \frac{1}{2}+x, \frac{1}{2}-y, \frac{1}{2}-z; \bar{x}, \frac{1}{2}+y, \bar{z};$

$\frac{1}{2}-x, \bar{y}, \frac{1}{2}+z;$

$\bar{x}, \bar{y}, \bar{z}; \frac{1}{2}-x, \frac{1}{2}+y, \frac{1}{2}+z; x, \frac{1}{2}-y, z;$

$\frac{1}{2}+x, y, \frac{1}{2}-z.$

(ii) 'special' :  $x, \frac{1}{4}, z; \bar{x}, \frac{3}{4}, \bar{z}; \frac{1}{2}-x, \frac{3}{4}, \frac{1}{2}+z; \frac{1}{2}+x, \frac{1}{4}, \frac{1}{2}-z.$

As there are four molecules per unit cell, the four chromium atoms must lie in 'special' positions on the mirror planes, at  $y=\frac{1}{4}$  and  $y=\frac{3}{4}$ . The twelve chlorine atoms must lie in eight 'general' and four 'special' positions in the unit cell.

The structure was solved by assuming initially a trans trigonal bipyramidal model, consisting of three chlorine atoms (two related by the mirror plane) and two nitrogen atoms surrounding a central chromium atom.

Atomic coordinates assigned to these atoms were those found for the analogous atoms in  $\text{TiBr}_3 \cdot 2\text{NMe}_3$ .<sup>142</sup> A full matrix least-squares refinement of these coordinates was performed, with inter-layer scale factors and isotropic thermal parameters as additional variables, giving unit weight to all the intensity data. R (based on observed and unobserved data) fell from an initial value of 0.423 to 0.297. A three dimensional Fourier synthesis based on the structure factors calculated during the refinement was computed, and the resulting electron density map was examined in the  $y = \frac{1}{4}$  region. The two nitrogen and two of the carbon atoms were found to lie on the mirror plane; there was no evidence of statistical disorder of the carbon atoms about the Cr-N bond.<sup>137</sup> A search of the other sections of the Fourier map revealed the two other carbon atoms in 'general' positions. Two cycles of full matrix least-squares refinement using all the atomic coordinates (except the mirror plane), inter-layer scale factors and isotropic thermal parameters as variables caused R to converge rapidly to 0.155. A Fourier synthesis was computed and the section through the electron density map at  $y = \frac{1}{4}$  was examined. In addition to the 'special' chromium and 'special'

chlorine atoms, the two nitrogen and two carbon atoms lay accurately on the mirror plane; the remaining carbon and chlorine atoms were found in 'general' positions. The space group is therefore confirmed as Pnma.

At this stage, the following weighting scheme was introduced: reflexions for which  $|F_o| < 22$  were given a weight  $\sqrt{w} = 22[116.1 - 4.28 |F_o|]^{-1}$  and those for which  $|F_o| > 22$  were given unit weight (i.e.  $\sqrt{w} = 1$ ). The effect of this scheme was to give reflexions with  $|F_o| \leq 10$  (i.e. the accidentally absent reflexions) a very low weight. As the reliability of reflexions with  $10 < |F_o| < 22$  increased as  $|F_o|$  increased, a steadily increasing weight was given to these reflexions. Reflexions for which  $|F_o| > 22$  were considered to be equally reliable and were given unit weight.

Two further cycles of full matrix least-squares refinement using this weighting scheme with fixed scale factors and anisotropic thermal parameters reduced R (for observed and unobserved data) to 0.116 and gave a weighted residual,  $R^1$ , (defined as  $\frac{\sum_w [ |F_o| - |F_c| ]^2}{\sum_w |F_o|^2}$ ) of 0.063. As the shifts in the atomic coordinates on the last cycle were less than their respective standard deviations, the refinement

Table 6.1 Final fractional Atomic Coordinates\*

	x	y	z
Cr	0.2955 (0003)	0.2500	0.0213 (0002)
Cl(1)	0.2113 (0003)	0.0686 (0003)	0.0941 (0002)
Cl(2)	0.4478 (0005)	0.2500	0.8908 (0003)
N(1)	0.1270 (0016)	0.2500	0.9132 (0009)
N(2)	0.4655 (0012)	0.2500	0.1256 (0008)
C(1)	0.4857 (0015)	0.2500	0.5312 (0014)
C(2)	0.4184 (0014)	0.2500	0.2371 (0009)
C(3)	0.0519 (0011)	0.1259 (0012)	0.3873 (0008)
C(4)	0.1403 (0014)	0.1276 (0012)	0.8406 (0008)

\* estimated standard deviations  
in parentheses

Table 6.2

Anisotropic Thermal Parameters\*

	$\beta_{11}$	$\beta_{22}$	$\beta_{33}$	$\beta_{12}$	$\beta_{13}$	$\beta_{23}$
Cr	0.0097 (0003)	0.0074 (0003)	0.0039 (0001)	0	0.0001 (0002)	0
Cl(1)	0.0146 (0004)	0.0112 (0004)	0.0082 (0002)	-0.0034 (0004)	-0.0020 (0003)	0.0029 (0002)
Cl(2)	0.0179 (0008)	0.0226 (0009)	0.0054 (0003)	0	0.0036 (0004)	0
N(1)	0.0247 (0025)	0.0122 (0020)	0.0054 (0009)	0	-0.0050 (0013)	0
N(2)	0.0101 (0017)	0.0109 (0018)	0.0044 (0008)	0	0.0000 (0009)	0
C(1)	0.0067 (0018)	0.0194 (0029)	0.0133 (0016)	0	-0.0012 (0016)	0
C(2)	0.0147 (0027)	0.0148 (0023)	0.0028 (0008)	0	-0.0014 (0012)	0
C(3)	0.0115 (0015)	0.0139 (0017)	0.0096 (0008)	0.0052 (0013)	0.0028 (0010)	0.0011 (0010)
C(4)	0.0252 (0021)	0.0139 (0017)	0.0089 (0009)	-0.0021 (0015)	-0.0066 (0011)	-0.0036 (0009)

\* estimated standard deviations in parentheses

The anisotropic thermal parameters are defined by:

$T = \exp[-\beta_{11}h^2 + \beta_{22}k^2 + \beta_{33}l^2 + 2\beta_{12}hk + 2\beta_{13}hl + 2\beta_{23}kl]$ . For atoms on the mirror plane,  $\beta_{12}$  and  $\beta_{23}$  are required to be zero.

was terminated. The final positional and anisotropic thermal parameters are given in tables 6.1 and 6.2, and the observed and calculated structure factors constitute appendix C.

The calculations were performed on the IBM.7090 computer of Imperial College, London, using the X-RAY 63 program system; atomic scattering factors used were those listed in "International Tables."<sup>140</sup> The ORFLS full matrix least-squares program of the X-RAY 63 system minimizes the function  $\sum w [ |F_o| - |F_c| ]^2$  and computes the standard deviations in the coordinates from the inverted least-squares matrix. As the inter-layer scale factors were not correlated on to the same relative scale and no absorption correction was applied to the intensities, the magnitudes of the thermal parameters have little significance.

### Results and discussion

The bond lengths and angles and their respective standard deviations are given in table 6.3 and fig. 6.1 shows the molecular geometry of  $\text{CrCl}_3 \cdot 2\text{NMe}_3$ . The projection of half the unit cell down (010) on to the mirror plane at  $y = \frac{1}{4}$  is reconstructed in fig. 6.2; the molecules on the  $y = \frac{3}{4}$  mirror plane are related to those drawn in fig. 6.2 by a centre of symmetry, but to

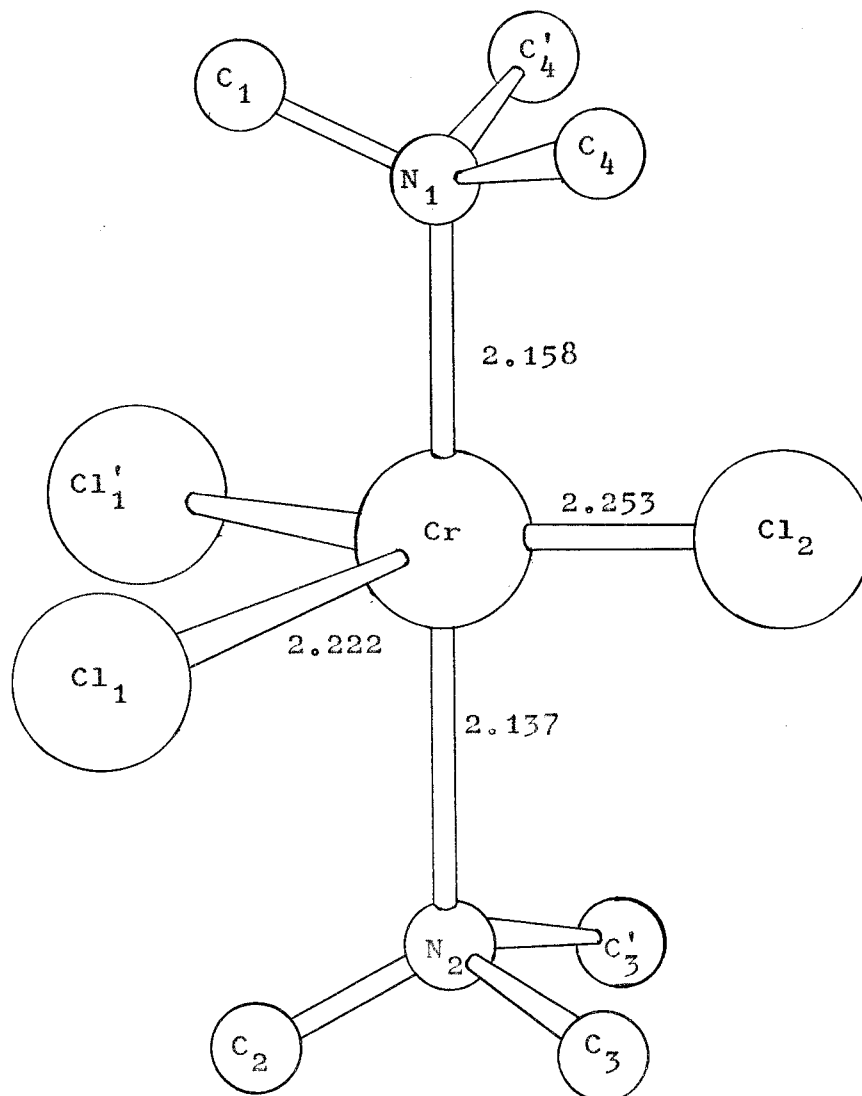


Fig. 6.1. The Molecular Geometry of  
 $\text{CrCl}_3 \cdot 2\text{NMe}_3$ .  
 (Bond lengths in Å)

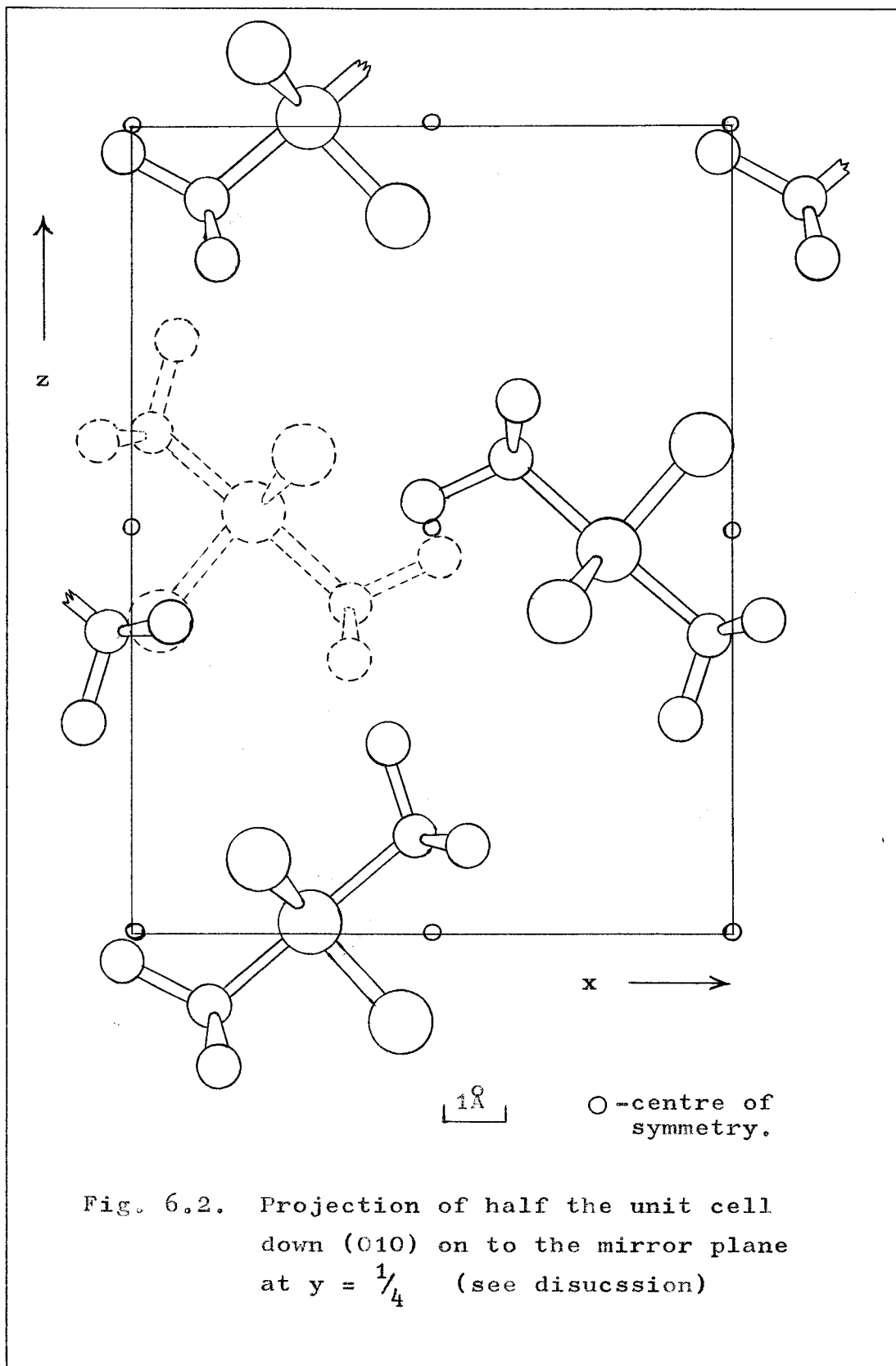
Table 6.3

Inter-atomic distances and angles\*

Bond lengths (Å)		Bond angles (°)	
C(1)-N(1)	1.549 (.021)	C(1)-N(1)-C(4)	110.9 (1.1)
C(4)-N(1)	1.565 (.014)	C(4)-N(1)-C(4)'	104.7 (1.2)
N(1)-Cr	2.158 (.014)	C(2)-N(2)-C(3)	105.7 (0.9)
Cl(1)-Cr	2.222 (.003)	C(3)-N(2)-C(3)'	111.6 (1.0)
Cl(2)-Cr	2.253 (.005)	C(1)-N(1)-Cr	111.3 (0.9)
N(2)-Cr	2.137 (.011)	C(4)-N(1)-Cr	109.5 (0.8)
C(3)-N(2)	1.519 (.013)	C(2)-N(2)-Cr	112.2 (0.8)
C(2)-N(2)	1.525 (.016)	C(3)-N(2)-Cr	110.8 (0.7)
Mean C-N	1.540 <sup>o</sup>	N(1)-Cr-Cl(1)	90.1 (0.4)
		N(1)-Cr-Cl(2)	90.1 (0.4)
		N(2)-Cr-Cl(1)	90.6 (0.3)
		N(2)-Cr-Cl(2)	88.65 (0.33)
		Cl(1)-Cr-Cl(1)'	111.4 (0.2)
		Cl(1)-Cr-Cl(2)	124.3 (0.2)
Intramolecular Contacts (Å)			
C(1)-Cl(1)	3.290		
C(4)-Cl(2)	3.293		
C(2)-Cl(1)	3.299		
C(3)-Cl(2)	3.314		
Shortest Intermolecular Contact			
C(3)'-Cl(2)	3.804 Å		

\* estimated standard deviations in  
parentheses.





preserve clarity, only one molecule (drawn with dotted lines) on the  $y = \frac{3}{4}$  plane has been included.

To fulfil the space group requirements, the molecule need only possess a mirror plane on which the atoms C(1), N(1), Cr, Cl(2), N(2) and C(2) must lie and which bisects the angles Cl(1)'-Cr-Cl(1), C(4)-N(1)-C(4)' and C(3)-N(2)-C(3)'. Although the two trimethylamine molecules are crystallographically independent, the two Cr-N distances are virtually identical with N-Cr-Cl angles of almost  $90^\circ$ . The equation of the "best" least-squares plane containing the chromium and chlorine atoms was calculated using a program written by Dr. J.S. Wood and modified for the 'Atlas' computer by Mrs. Christina Greene. The equation calculated is of the form  $lX+mY+nZ-p=0$  where  $l, m, n$  are the direction cosines of a line drawn perpendicular to the plane, passing through the origin, and  $p$  is the perpendicular distance of the origin from the plane. The equation of the plane is:

$$0.7568X + 0.6536Z - 2.3511 = 0$$

With the molecule drawn as in fig. 6.1, the chromium atom lies  $0.003\text{\AA}$  above and the chlorine atoms  $0.001\text{\AA}$  and  $0.002\text{\AA}$  below this plane: i.e. within the present standard deviations, the chromium and chlorine atoms are coplanar. As the Cl(1)-Cr-Cl(1)' angle is  $111.4^\circ$ ,

which is much lower than the value of  $120^\circ$  expected if the molecule possessed idealized  $D_{3h}$  symmetry, the molecular point group of  $\text{CrCl}_3 \cdot 2\text{NMe}_3$  is  $C_{2v}$ . The Cl(1)-Cr bond length is slightly shorter than the Cl(2)-Cr distance ( $2.222\text{\AA}$  compared with  $2.253\text{\AA}$ ), but both bond lengths are significantly shorter than the Cr-Cl distances observed in six coordinate chromium(III) complexes. For example, in p-tolyl,  $\text{CrCl}_2 \cdot 5\text{THF}$ , Cr-Cl bond lengths of  $2.307 \pm 0.003\text{\AA}$  and  $2.331 \pm 0.003\text{\AA}$  are found,<sup>143</sup> whilst in  $[\text{Cr}(\text{H}_2\text{O})_4\text{Cl}_2]\text{Cl} \cdot 2\text{H}_2\text{O}$ , the Cr-Cl distance is  $2.286 \pm 0.001\text{\AA}$ .<sup>144</sup>

There is no statistical disorder of the trimethylamine groups about their three-fold axes as in  $\text{AlH}_3 \cdot 2\text{NMe}_3$ .<sup>137</sup> Free rotation about the Cr-N bond is probably restricted by the interaction of the methyl carbon and the chlorine atoms, since the intra-molecular C-Cl distances are  $\sim 3.3\text{\AA}$ . The average C-N bond length,  $1.54\text{\AA}$ , is slightly longer than is observed in free trimethylamine ( $1.472 \pm 0.008\text{\AA}$ ),<sup>146</sup> and the C-N-C and C-N-Cr angles all deviate from the 'expected' tetrahedral angle of  $109^\circ 28'$ . These small bond and angular deviations which occur on coordination are consistent with methyl-chlorine interactions. The infrared spectrum of  $\text{CrCl}_3 \cdot 2\text{NMe}_3$  is also compatible with a lengthening of the C-N bonds since a substantial decrease in the frequency of the asymmetric

and symmetric C-N stretching modes occurs on coordination.

As the electronic ground state of  $\text{CrCl}_3 \cdot 2\text{NMe}_3$  is  $(e'')^2(e')$  in a ligand field of  $D_{3h}$  symmetry, a Jahn-Teller distortion is expected as the  $\sigma$  antibonding  $e'$  orbital is only singly occupied. The angular distortion from  $120^\circ$  and the differing Cr-Cl bond lengths are believed to arise from this configurational instability. A similar but somewhat smaller distortion was observed in  $\text{TiBr}_3 \cdot 2\text{NMe}_3$  where the Br-Ti-Br' angle was found to be  $117.5^\circ$ .<sup>126</sup> The smaller distortion in this complex results from the single occupation of the  $e''$  orbital which is weakly  $\pi$  antibonding in a molecular orbital scheme.

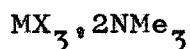
The large distortion in  $\text{CrCl}_3 \cdot 2\text{NMe}_3$  raises the degeneracy of the  ${}^4E'$  electronic ground term sufficiently to cause the magnetic moment of the complex to approach the spin-only value of 3.88 B.M. and to become temperature-independent. In  $C_{2v}$ , the ground term becomes  ${}^4A_1$  or  ${}^4B_2$ , either of which would give rise to the observed magnetic behaviour. Reduction of the symmetry of  $\text{TiX}_3 \cdot 2\text{NMe}_3$  ( $X = \text{Cl}, \text{Br}$ ) to  $C_{2v}$  causes the orbital degeneracy of the  ${}^2E''$  ground term to be removed, and the new ground term will be either  ${}^2A_2$  or  ${}^2B_1$ . In these complexes, the smaller distortion is insufficient to render the magnetic moment temperature-independent,

but the observed variation with temperature is much less than predicted for  $Ti^{3+}$  in a ligand field of  $D_{3h}$  symmetry.<sup>77</sup>

$CrCl_3 \cdot 2NMe_3$  is isomorphous with its titanium and vanadium analogues and also with  $TiBr_3 \cdot 2NMe_3$  (see table 6.4).

Table 6.4

Unit Cell Dimensions of the Complexes



Compound	a(Å)	b(Å)	c(Å)	ref.
$TiCl_3 \cdot 2NMe_3$	9.8	10.2	13.1	125
$VCl_3 \cdot 2NMe_3$	9.84	10.14	13.14	145
$CrCl_3 \cdot 2NMe_3$	9.69	10.12	13.05	this work
$TiBr_3 \cdot 2NMe_3$	10.23	10.28	13.46	120

The complexes are probably all isostructural. Although the density of  $VCl_3 \cdot 2NMe_3$  has been reported as  $2.9 \text{ gm.ml.}^{-1}$ , implying eight molecules per unit cell,<sup>145</sup> this value is probably in error since a highly distorted vanadium species would be expected in order to achieve such a high packing density in a unit cell of the given dimensions. As the ground state configuration of vanadium(III) in a ligand field of  $D_{3h}$  symmetry is  $(e'')^2$  no

Jahn-Teller distortion is anticipated, and it has been shown that the spectroscopic and magnetic properties of the pentacoordinate vanadium(III) compounds are consistent with a regular trans trigonal bipyramidal geometry for these molecules.<sup>77</sup> The measured densities of  $\text{TiCl}_3 \cdot 2\text{NMe}_3$ <sup>125</sup> and  $\text{TiBr}_3 \cdot 2\text{NMe}_3$ <sup>120</sup> are those expected for unit cells containing four monomers.

APPENDIX A

STARTING MATERIALS AND ANALYTICAL METHODS

I. Preparation and purification of starting materials

(a) Gases

Nitrogen, Oxygen-free nitrogen (B.O.C.) was dried by passage through two drying tubes, the first containing anhydrous magnesium perchlorate and the second phosphoric oxide. Towards the end of this work, a communal supply of oxygen-free nitrogen was installed, and the gas was dried with B.D.H. 4a molecular sieves.

Hydrogen, (B.O.C.) was dried by bubbling through concentrated sulphuric acid.

Chlorine, The gas was obtained from a cylinder (I.C.I.) and dried by bubbling through concentrated sulphuric acid.

Bromine, Liquid bromine (May and Baker) was allowed to stand over phosphoric oxide in a bubbler overnight. Dry oxygen-free nitrogen was then passed through, and the resulting mixture of bromine vapour and nitrogen was further dried by passage through a bubbler containing concentrated sulphuric acid.

(b) Liquids, (All distillations were performed on the vacuum line)

Benzene, 2,2,4-trimethylpentane ("iso-octane"), cyclohexane and chloroform were allowed to stand for



24 hours over  $P_2O_5$ , followed by repeated distillations from  $P_2O_5$ , and storage over B.D.H. 4a molecular sieves.

Acetonitrile was refluxed with calcium hydride for 24 hours, and transferred to the vacuum line where it was repeatedly distilled off  $P_2O_5$  and finally stored over molecular sieves.

Nitromethane was dried by repeated distillation from  $P_2O_5$ .

Ethers (Tetrahydrofuran (THF), dioxan, 1,2-dimethoxyethane) were distilled from calcium hydride and molecular sieves and finally condensed on to a potassium mirror for storage.

Thioethers (Tetrahydrothiophen (THT), dimethylsulphide, thioxan) were distilled from calcium hydride and molecular sieves.

Pyridine was repeatedly distilled off freshly crushed barium oxide.

Trimethylamine. This amine has a low boiling point ( $4^\circ C/760$  mm.) and therefore special precautions had to be observed whilst handling it in the vacuum system. It was dried by repeated distillation off  $P_2O_5$  (which also removed any primary or secondary amine impurities), the trap containing the liquid being surrounded at all times by an acetone/'drikold' slush bath. Final drying was effected by condensing titanium(IV) chloride

Fig. A.1a.

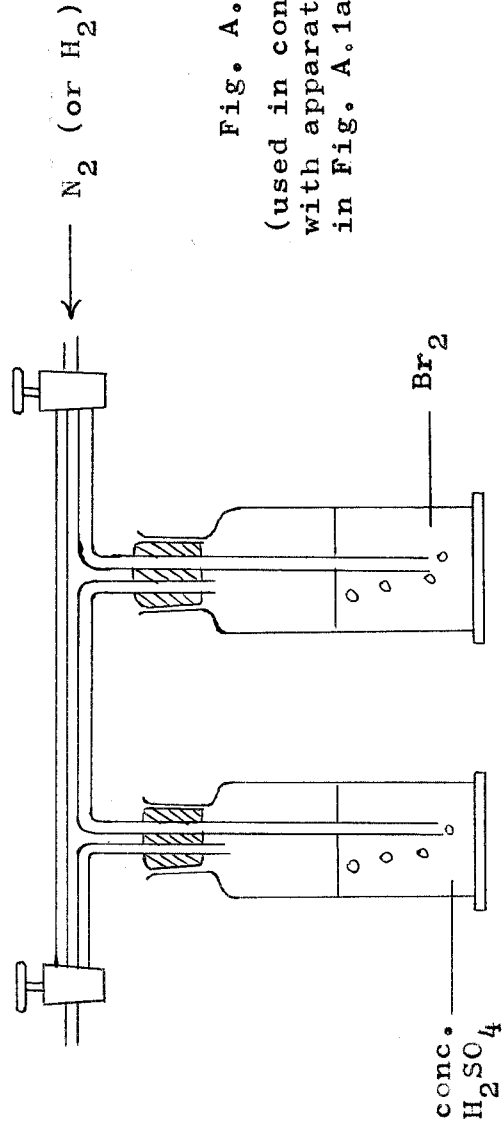
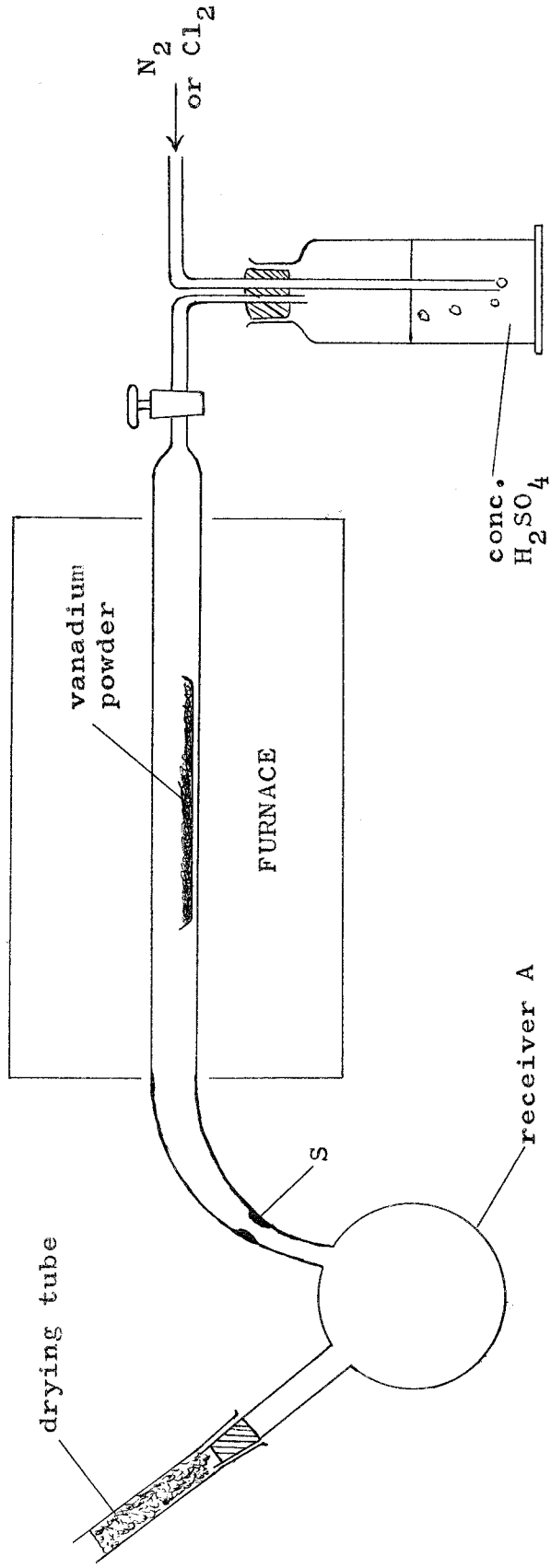


Fig. A.1b.

(used in conjunction  
with apparatus shown  
in Fig. A.1a.)

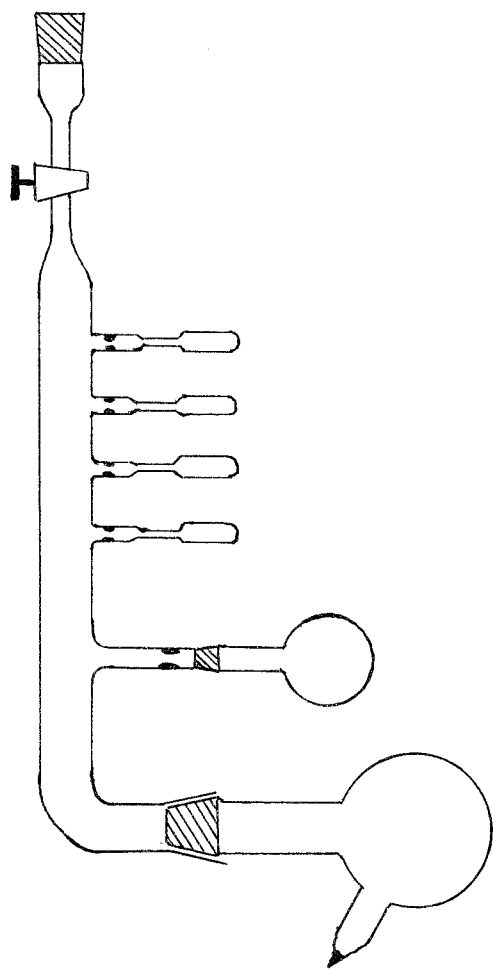


Fig. A.2. Ampoule train ('pig')

on to the amine.

B.D.H. 4a Molecular Sieves were regenerated by heating them in vacuo to 250°C overnight.

(c) Halides

(i) Vanadium(IV) chloride

Vanadium powder (Magnesium Electron Limited) was heated in a current of dry nitrogen to 400°C in the apparatus shown in Fig. A1a. When all the air had been displaced, the nitrogen flow was stopped and replaced by dry hydrogen which removed any surface oxide on the metal. After three hours, hydrogen was displaced by nitrogen and then dry chlorine gas was passed over the metal. Vanadium(IV) chloride was collected as an oily, brown liquid in the ice-cooled receiver, A. When the reaction was complete (after about three hours), the flask was sealed off at S and transferred to an ampoule train ("pig") (Fig. A2) which had previously been evacuated on the vacuum line. The halide was frozen in liquid nitrogen and the "pig" evacuated and removed from the line. Approximately 1-2 ml. of halide were condensed into each ampoule; these were removed as they were filled by freezing the contents with liquid nitrogen and sealing off at the constriction. The ampoules were stored in a refrigerator to

minimise the decomposition of their contents to vanadium(III) chloride.

(ii) Vanadium(III) chloride was supplied by Union Carbide and used without further purification.

Found: Cl, 67.7; V, 32.45%

Calc. for  $VCl_3$ : Cl, 67.6; V, 32.4%

(iii) Vanadium(III) bromide was prepared in the apparatus shown in Fig. A1a using the bubbler system incorporating liquid bromine (Fig. A1b). Vanadium metal was reduced with hydrogen as before at  $400^{\circ}C$ . After displacement of hydrogen with nitrogen, the taps on the bubblers were adjusted to give a slow stream of bromine vapour, carried in nitrogen, which was passed over the metal at  $400^{\circ}C$ . The neck of the reaction tube N was heated with a Bunsen burner during the preparation to prevent its being obstructed by the halide as it formed. It was found that a slow stream of bromine vapour was also essential if clogging at the neck of the tube was to be prevented. The halide was collected as a black, finely powdered solid in the ice-cooled receiver, A, which was sealed off at S and transferred to the vacuum line. The solid was pumped at room temperature for half-an-hour to remove excess bromine, whereupon it was split up into convenient quantities (1-2 gm) in a "pig" which had jointed specimen

tubes connected to each leg. These tubes were sealed off under nitrogen at atmospheric pressure. Analysis confirmed the purity of the product.

Found: Br, 82.3; V, 17.2%

Calc. for  $VBr_3$ : Br, 82.5; V, 17.5%

(iv) Chromium(III) chloride (anhydrous) was prepared by the method of Heisig et al.<sup>147</sup>

(d) Solid Ligands

1,10-phenanthroline monohydrate (Koch Light) was heated in vacuo to remove water, and then recrystallized from benzene.

2,2'-bipyridyl (I.C.I.) was used without further purification.

(e) Complex compounds

(i) Trichlorotriscetonitrilevanadium(III) was prepared as described previously.<sup>68</sup>

(ii) Trichlorobistrimethylaminevanadium(III) was prepared by the reduction of vanadium(IV) chloride with trimethylamine diluted with benzene.<sup>90,128</sup>

Found: Cl, 38.0; V, 18.1%

Calc. for  $VCl_3 \cdot 2N(CH_3)_3$ : Cl, 38.6; V, 18.5%

(iii) Tribromobistrimethylaminevanadium(III) was prepared by the direct reaction of liquid trimethylamine

on vanadium(III) bromide in a double ampoule (see later). The purple-pink trimethylamine-soluble complex was collected and extracted with benzene on the vacuum line.

Found: Br, 58.0; V, 12.6%

Calc. for  $VBr_3 \cdot 2N(CH_3)_3$ : Br, 58.6; V, 12.5%.

## II Analytical Procedures

### (a) Vanadium analysis

Organic ligands were found to interfere with the standard volumetric procedure for vanadium estimation,<sup>148</sup> and their complete removal from hydrolysis solutions with organic solvents (e.g.  $CCl_4$ ) was not always successful.

Vanadium was estimated gravimetrically as  $V_2O_5$ . A platinum crucible was heated to constant weight with a 'Meker' burner and a weighed quantity of the complex (0.1—0.2 gm.) was introduced into the crucible via a bent, jointed adaptor. The compound was covered with 2 or 3 layers of filter paper to prevent mechanical loss of products when acid was added. The complex was decomposed by the addition of 2-3 ml. of concentrated nitric acid and the liquid phase was slowly evaporated with a small flame to complete the degradation. The analysis was completed by stronger heating with a 'Meker' burner for about fifteen

minutes (until the crucible reached constant weight); excessive heating for longer periods resulted in some loss of  $V_2O_5$ . The crucible was allowed to cool prior to re-weighing.

(b) Chromium analysis

Chromium was estimated by direct ignition of a weighed quantity of complex to  $Cr_2O_3$ , following the same procedure given above for vanadium.

(c) Halogen analysis

A small quantity (0.1—0.2 gm.) of complex was transferred under nitrogen into a weighed, jointed tube (whose stopper had also been weighed). The tube was re-weighed and compound was hydrolysed with about 20 ml. of 4M sulphuric acid in a stoppered 250 ml. conical flask. The solution was washed quantitatively into a beaker with distilled water, and halogen was estimated gravimetrically in the usual way by the precipitation of the appropriate silver halide with a solution of silver nitrate.

When complexes containing chromium were analysed, a weighed sample was hydrolysed with approximately 10 ml. of 4M sodium hydroxide. Addition of 1-2 ml. of 100 volume hydrogen peroxide followed by boiling



yielded a yellow solution which was made just acid to litmus by the careful addition of concentrated nitric acid. After the quantitative transfer of the solution to a beaker, the halogen was estimated gravimetrically as above.

(d) Carbon, hydrogen, sulphur, nitrogen and occasional halogen analyses were performed by a professional analyst (Bieler, Vienna).

APPENDIX B

EXPERIMENTAL TECHNIQUES

## I Vacuum Line Techniques

Many complexes studied in this research were unstable to aerial oxidation and hydrolysis. A convenient way of handling such complexes is to use a vacuum line (Fig. B1) which is particularly suitable for the examination of soluble and insoluble reaction products, and the preparation of solutions of unstable complexes for physical measurements. A description of the most frequently used manipulations is given below.

### (a) Drying and storage of solvents and liquid reagents.

The empty traps, A, B and C (Fig. B1) were pumped and flamed to remove moisture. They were removed under nitrogen, a suitable drying agent (cf. Appendix A) added and then re-evacuated. The vessel containing the solvent or liquid ligand which had had preliminary drying treatment was attached to the line with the appropriate adaptor and the tap opened and closed quickly. The liquid was then frozen in an acetone/'drikold' slush bath or liquid nitrogen, and the tap was opened again until a vacuum had been established. The solid was then melted and the liquid condensed on to a fresh batch of drying agent by cooling the trap

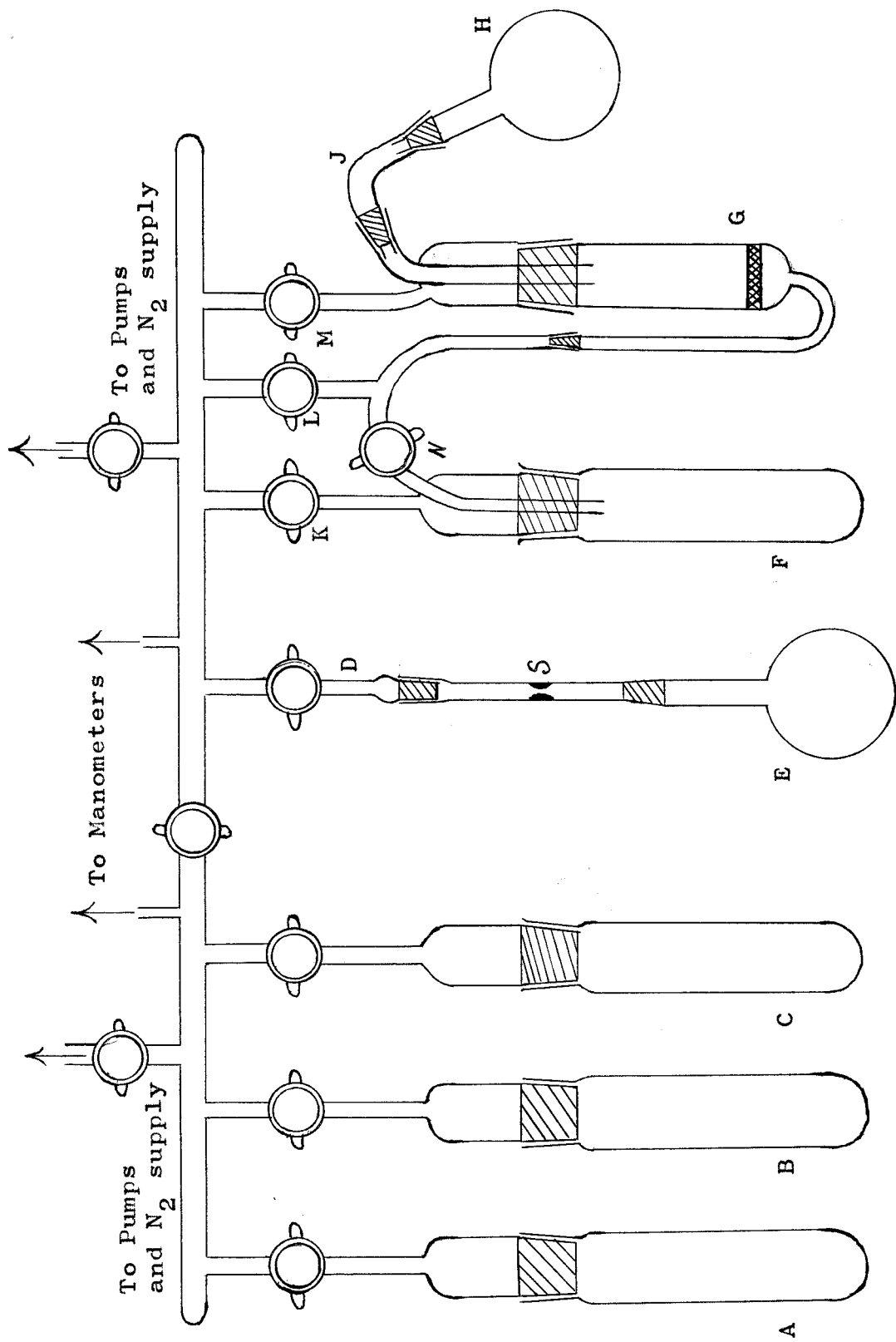


Diagram of the Vacuum System. Fig. B.1.

in liquid nitrogen. Usually, three distillations from the drying agent were performed before the liquid was finally distilled on to and stored over molecular sieves.

(b) Reactions in ampoules

All reactions were performed in ampoules - a 100 ml. round bottom flask with a long neck terminated by an extended B19 ground glass joint. An ampoule was attached to the line via a constriction and a B14 socket (E in Fig. B1) and was flamed and pumped to remove moisture in the usual way. Nitrogen was admitted to the line and the ampoule removed, whereupon the halide, contained in a storage tube made from an extended B14 cone, was introduced by plugging the two joints together and tipping the solid out of its tube. The ampoule was quickly returned to the line and evacuated. About 20 ml. of solvent or liquid ligand were then condensed on to the halide, and, whilst the contents were frozen out in liquid nitrogen, the ampoule was sealed off at the constriction, S. The structure of vanadium(III) halides (see Chapter 1) is such that fast reactions are inhibited, and therefore in most cases the ampoule's contents had to be gently refluxed on a heating mantle to initiate a reaction.

Solid ligands were added in a similar manner to the halide itself, and either benzene or acetonitrile was used as the reaction medium.

Vanadium(IV) chloride was introduced into an ampoule in the apparatus shown in Fig. B2.<sup>149</sup> The tube of halide was placed in the "breaker" which was then pumped and flamed, and solid ligand, solvent or liquid ligand were introduced into the ampoule in the usual way. With the ampoule surrounded by refrigerant, the breaker was twisted through 180° so that the weight, W, fell and broke the tube containing the liquid halide, which immediately distilled into the ampoule, L, which was then sealed off.

(c) Examination of Reaction Products

(i) Insoluble or partially soluble products

This normal filtration technique is illustrated in Fig. B.1. After flaming and evacuation, dry nitrogen was admitted to the appropriate sections of the line. An ampoule, whose contents had been frozen in liquid nitrogen, was opened under nitrogen by "hot-spotting" a scratch mark in the glass just above the B19 cone, and plugged into the bent adaptor, J. The line was re-evacuated, and with tap M closed, the

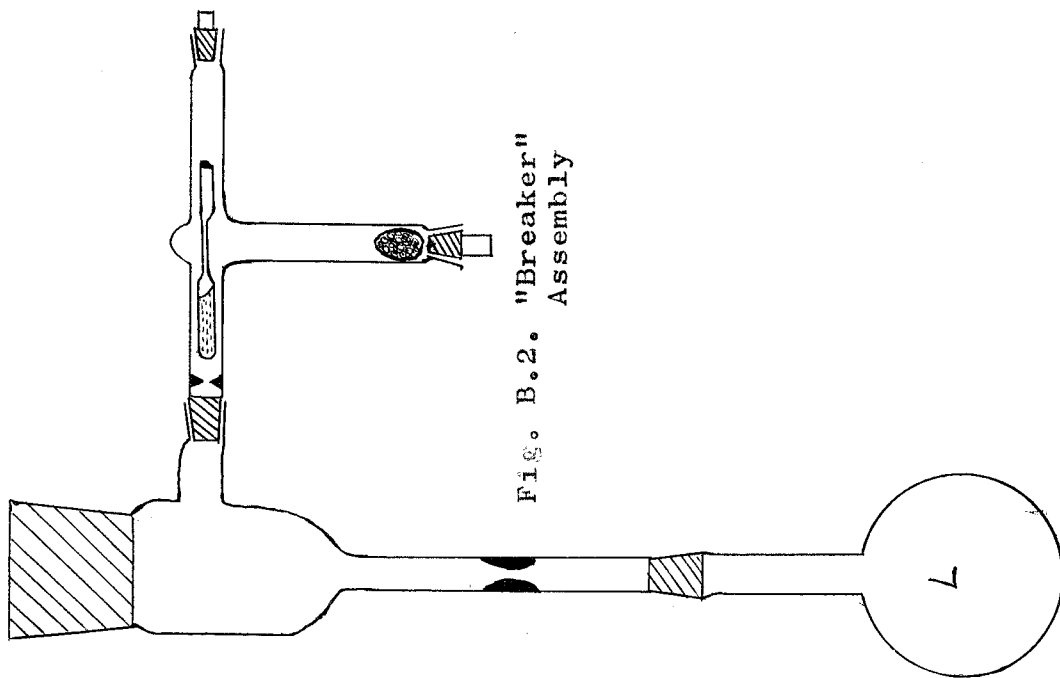


FIG. B.2. "Breaker"  
Assembly

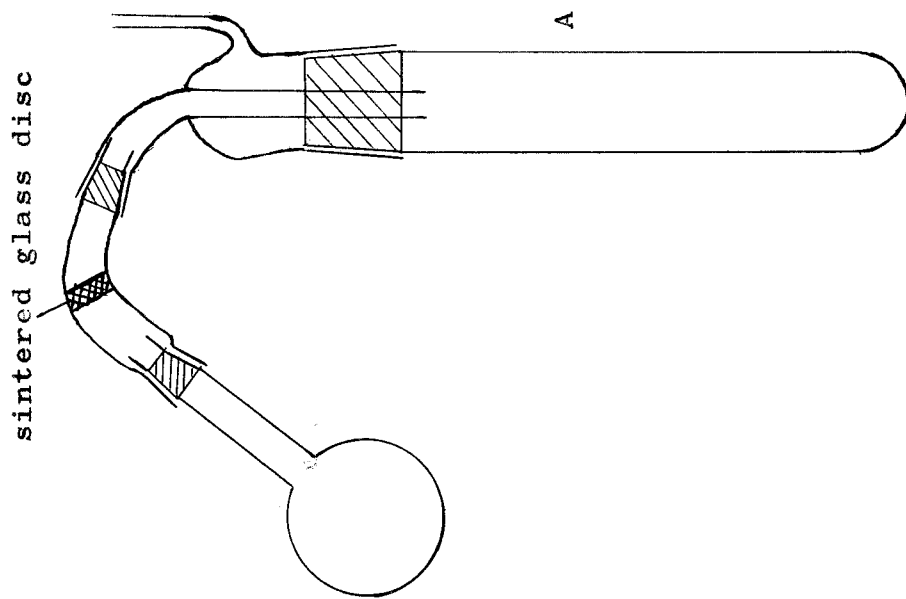


FIG. B.3. Filtration Apparatus

ampoule was allowed to attain room temperature. Tap N was opened, trap F gently cooled, and the bent adaptor was rotated through  $180^{\circ}$  so that the solid could be collected on the sintered glass filter and the liquid collected in trap F. Tap N was closed and with the tap to the main vacuum system closed, taps K and M were opened. The ampoule was moved back to its normal position and liquid was distilled in from trap F. This solvent was used to wash the insoluble product on the filter pad free of excess ligand; alternatively, fresh solvent from a storage trap could have been used for the washing. This sequence of operations could be repeated as often as possible, but, in practice, six consecutive washings were found to be adequate. The solid was then pumped free of solvent for several hours at room temperature prior to its transference to a jointed storage tube.

(ii) Isolation of soluble products

The bent adaptor shown in Fig. B1 was replaced by one containing a sintered glass disc, and the filter vessel by a single trap as indicated in Fig. B3; the use of extended joints provides a greaseless filtration system. An ampoule was plugged into the filter adaptor in the manner described above, and, on warming to room temperature, the contents of the ampoule were



allowed to filter into trap A. The liquid phase was removed by slow, careful distillation and the remaining solute was pumped at room temperature for several hours. Under nitrogen, the compound was scraped from the walls of the trap, powdered, and transferred to a jointed storage tube.

In preparative routes involving the use of liquid trimethylamine a double ampoule arrangement (Fig. B4) was found useful. The ampoule was attached to the vacuum line by a constriction and B14 socket and after flaming and pumping, the halide was introduced into ampoule A under nitrogen. After re-evacuation, trimethylamine was distilled into A and the ampoule sealed off at T. Periodically, as the reaction proceeded, the trimethylamine-soluble compound was filtered through the sintered glass filter into ampoule B, after which the solvent was carefully distilled back on to unreacted halide in A. This cycle of operations could be repeated until the reaction appeared to be complete, at which point the trimethylamine was finally distilled back into A, frozen, and the two halves of the system severed by sealing the constriction S. The product in B could be further purified by extraction with solvents on the line or shaken out under nitrogen via an adaptor

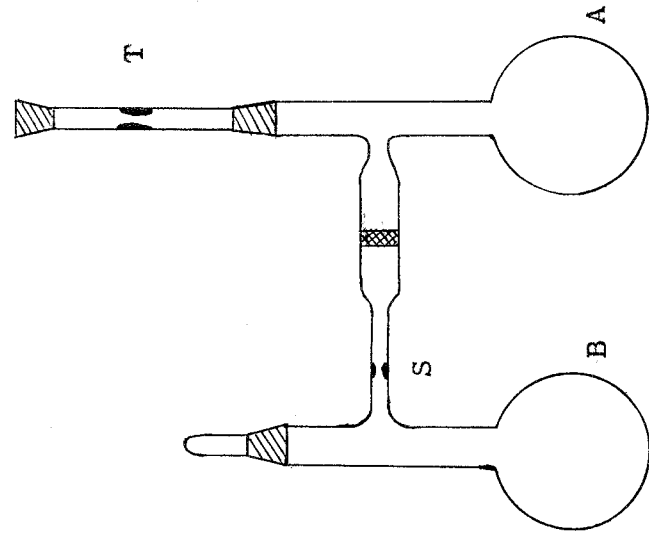


Fig. B.4. Double Ampoule

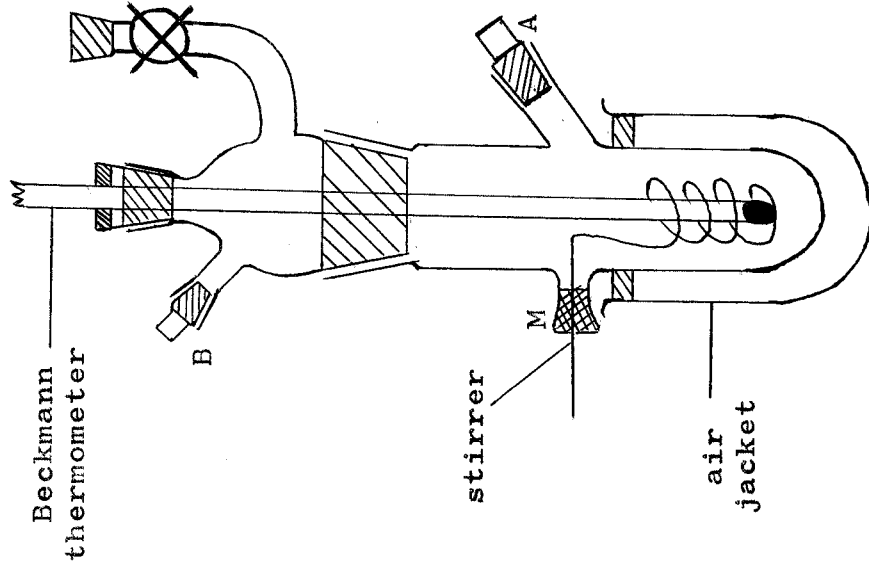


Fig. B.5. Molecular Weight Apparatus

into a jointed tube.

## II Experimental Aspects of Structural Investigations

### (a) Molecular weight determinations

Molecular weights were determined cryoscopically in benzene in an apparatus depicted in Fig. B5, specially designed for use in conjunction with the vacuum line. A standard Beckmann thermometer was fitted with a B24 cone, an effective vacuum-tight seal being provided by a rubber collar which fitted round the thermometer inside the joint, with a layer of 'araldite' adhesive round the outside of the rubber. A stainless steel rod to which a stainless steel spiral stirrer was attached was secured in a rubber collar, M, and sealed with 'araldite' in such a way that the rod could be agitated with a stirring motor.

After the apparatus had been evacuated and flamed, it was removed from the line under nitrogen and weighed on a torsion balance. It was returned to the line, re-evacuated, approximately 25 gm. of dry benzene distilled in and then re-weighed. The molecular weight determination followed the standard procedure<sup>150</sup> except for the introduction of the solute, which was stored under nitrogen in a thin tube, some 10 cm. long.

When the complex had to be added to the benzene, the top of the storage tube was cut off and replaced with a small rubber bung. The tube was weighed, the stopper quickly removed and the complex tipped at A into the solvent against a flow of nitrogen delivered through B. The tube and stopper were re-weighed to determine the quantity of compound which had been added.

The molecular weight was calculated from the expression:

$$M.W. = \frac{K.m. 1000}{\Delta T. M}$$

where K = molal depression constant for benzene  
(5.07)

m = mass (in gm) of compound used

M = mass (in gm) of benzene

$\Delta T$  = depression in freezing point

(b) Measurement of conductivity

Acetonitrile was chosen as the solvent in which the majority of conductivity measurements were made because it has a fairly high dielectric constant, low viscosity and is easily purified on the vacuum line.

Conductance data were obtained at a concentration of approximately  $10^{-3}M$  in the apparatus shown in Fig. B6. The actual conductance cell was purchased ready

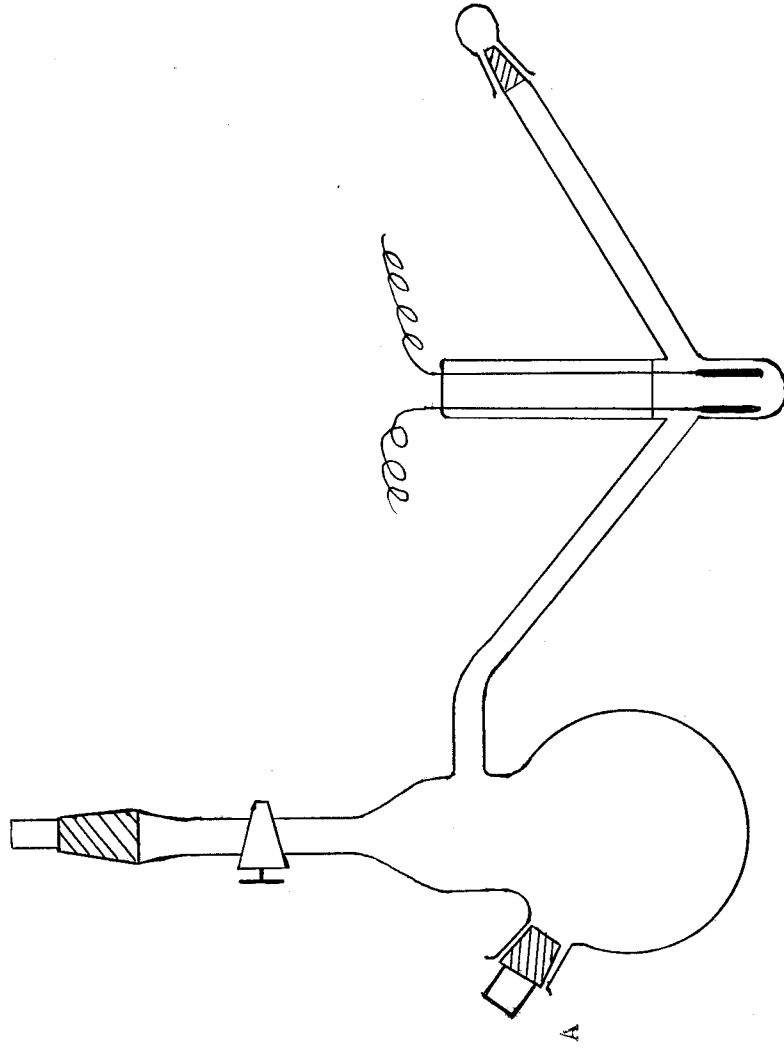


Fig. B6. Conductivity Cell

calibrated from Mullard's and the conductance was measured on a Pye Conductance Bridge (No. 11700).

Initially, the apparatus was cleaned with chromic acid, steamed out for several hours and rinsed with a small quantity of spectroscopic ethanol to remove most of the water. Final drying was effected by prolonged evacuation on the vacuum line. A weighed quantity of sample was then inserted, with the cell filled with nitrogen, via joint A. The cell was re-evacuated, weighed and returned to the line where acetonitrile was distilled into the reservoir. The cell (under vacuum) was detached from the line and re-weighed; the volume of acetonitrile used was thus determined from the weight used and its density at 25°C. After ensuring that the solid had completely dissolved in the solvent, the solution was tipped from the reservoir into the conductivity cell; the apparatus was placed in a constant temperature bath (at 25°C) where it was allowed to attain the temperature of the bath before any measurements were made. The variation of conductivity over a range of concentrations was studied by successive dilutions of the original solution with acetonitrile, re-weighing the cell each time to determine the concentration of the solution.

The molar conductivity,  $\Delta_m$ , may be computed from the following expression:

$$\Delta_m = \frac{C \cdot V \cdot M \cdot K}{m}$$

where C = cell constant

V = volume of solvent (ml.)

m = mass of compound (gm.) in V ml.  
of solvent.

M = Mol. weight of solute

K = Conductivity of solution ( $\text{ohm}^{-1}$ ).

(c) Magnetic Susceptibility Measurements

(i) The susceptibilities of solid products were determined at room temperature by the standard Gouy procedure.<sup>151</sup> An electromagnet providing a field of approximately 8000 gauss was used in conjunction with a Stanton, air-damped, semi-microbalance. Sample tubes were constructed from B7 sockets such that they had a flat base with an internal diameter of 3-4 mm. and were 12-14 cm. in length. They were suspended between the poles of the magnet with a 'nylon' thread attached to a rubber collar which was situated around the lip of the socket. The length of sample in the tube was approximately 10 cm.; a permanent scratch mark on the tube ensured that the same sample length was used in

each determination. The Gouy method yields only the relative susceptibility of a substance, and therefore the tube was calibrated for a given field strength with a compound of known susceptibility. Mercury tetrathiocyanatocobaltate(II)<sup>151</sup> (gram. susceptibility,  $\chi_g = 16.44 \times 10^{-6}$  c.g.s.u. at 20°C.) was chosen as the calibrant because it could be readily prepared pure and had exceptional packing properties.

The tube used for the susceptibility determinations was calibrated with six separate measurements using the standard substance. After the tube had been evacuated, the complex whose susceptibility was to be measured was introduced into the tube under nitrogen via a bent adaptor a little at a time, and packed to the mark. The net pull on the sample suspended in the magnetic field was noted; the tube was emptied, repacked and the measurement repeated until the pull-to-weight ratio for successive packings agreed to within 1%.



Calculation of the magnetic susceptibility and  
magnetic moment

It may be shown that<sup>151</sup>

$$K_{\text{sample}} = \frac{f_{\text{sample}}}{f_{\text{cal}}} \cdot [K_{\text{cal}} - K_{\text{air}}] + K_{\text{air}}$$

$$= f_{\text{sample}} \cdot T_{\text{tube}} + K_{\text{air}}$$

where  $K_{\text{sample}}$  = volume susceptibility of the sample (cgsu)

$K_{\text{cal}}$  = " " " " calibrant (cgsu)

$K_{\text{air}}$  = " " " " air (cgsu)

$f_{\text{sample}}$  = net pull on sample (gm)

$f_{\text{cal}}$  = net pull on calibrant (gm)

$T_{\text{tube}}$  = Tube constant

If  $\chi_g$  = gram susceptibility of sample (cgsu)

$\chi_m$  = molar " " " (cgsu)

$\chi'_m$  = " " " " corrected for the diamagnetism of all other atoms.

then:  $\chi_g = \frac{K_{\text{sample}}}{\text{density}}$  and  $\chi_m = \chi_g \times (\text{empirical Mol. wt.})$

$\chi'_m = \chi_m - (\text{diamagnetic correction for all the other atoms}).$

= Molar susceptibility of the paramagnetic ion.

The diamagnetic corrections were calculated from the values of Pascall's constants listed in reference 151.

The effective magnetic moment,  $\mu_{\text{eff}}$ , is given by:

$$\mu_{\text{eff}} = 2.828 \sqrt{\chi'_m \cdot T} \quad \text{Bohr Magnetons where}$$

T is the absolute temperature.

(ii) Measurement of the variation of magnetic susceptibility with temperature

The temperature dependence of the magnetic susceptibility of a complex was determined using a Newport Instruments Variable Temperature Gouy Balance. Accurate temperature control ( $\pm 0.3^\circ$ ) to  $77^\circ\text{K}$  was achieved with a cryostat similar in design to the one described by Figgis and Nyholm.<sup>152</sup> A 12 cm. Gouy tube was constructed from a B5 socket so that it could be filled in the usual way on the vacuum line. "Pyrex" glass, from which the tube was constructed, contains traces of paramagnetic materials and hence the variation with temperature of the net push on the empty tube due to the presence of the magnetic field was measured. The solid under investigation was packed into the tube to give a sample length of approximately 10 cm., and the variation of the net pull on the compound was determined as a function of temperature and the results displayed graphically. All measurements were performed in an atmosphere of dry nitrogen, and at two or more differing field strengths to check for the absence of

ferromagnetic impurities.

The susceptibility at different temperatures was deduced as follows:

From (i) above

$$K_{\text{sample}} = f_{\text{sample}} \cdot T_{\text{tube}} + K_{\text{N}_2}$$

but,  $K_{\text{N}_2}$ , the volume susceptibility of nitrogen is negligible.

$$\therefore K_{\text{sample}} = f_{\text{sample}} \cdot T_{\text{tube}}$$

$$\therefore \chi_g = \frac{f_{\text{sample}} \cdot T_{\text{tube}}}{(\text{density})}$$

$$\therefore \chi_m = \frac{f_{\text{sample}} \cdot T_{\text{tube}} \cdot \text{Mol.wt.}}{(\text{density})}$$

$$\text{i.e. } \chi_m = f_{\text{sample}} \cdot (\text{const.})$$

Hence, the molar susceptibility is proportional to the net pull on the sample. An accurate value of the molar susceptibility of the complex was determined as in (i) above at room temperature. From the net pull vs. temperature graph measured above, the pull corresponding to the room temperature susceptibility was noted and the constant of proportionality evaluated. The susceptibility at other temperatures was then computed and the corrected susceptibility,  $\chi'_m$  for the paramagnetic ion was evaluated by subtracting the

corrections for all the other atoms; these diamagnetic corrections are temperature independent.

(d) Spectral Measurements

(i) Infrared region

Measurements were made on Nujol mulls using Unicam SP.200 or Perkin-Elmer 337 spectrophotometers. The complex, sealed in a small tube under nitrogen, was quickly tipped into some Nujol (dried over molecular sieves) on a KBr disc in an atmosphere of dry air. Another disc was placed on top and rotated to distribute the mull evenly. This procedure was satisfactory for all but the most unstable compounds whose mulls were prepared in a dry-box.

The low infrared region between  $500\text{ cm.}^{-1}$  and  $200\text{ cm.}^{-1}$  was scanned with a Grubb-Parsons DM.4 spectrophotometer. Spectra were run on Nujol mulls, prepared in a dry-box, between polythene plates. Solution spectra were run as thin liquid films in specially constructed polythene cells shown in Fig. B7a. These were made by heat-sealing two pieces of polythene sheet together, one of which contained a polythene tube cemented in with 'araldite', the other end being joined with 'araldite' to a piece of glass tubing.

Fig. B.7a. Construction of  
Cells for measurement  
of the Far i.r. spectra of  
liquid films

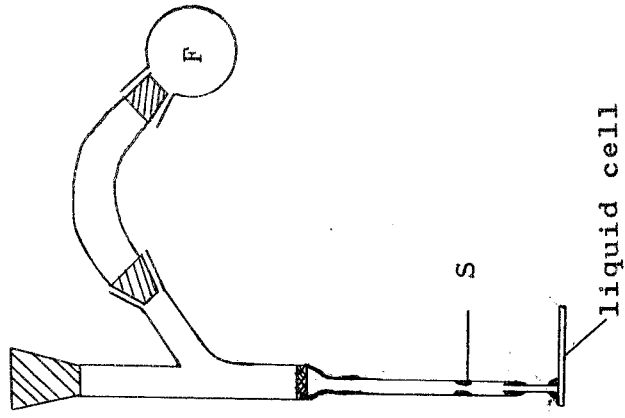
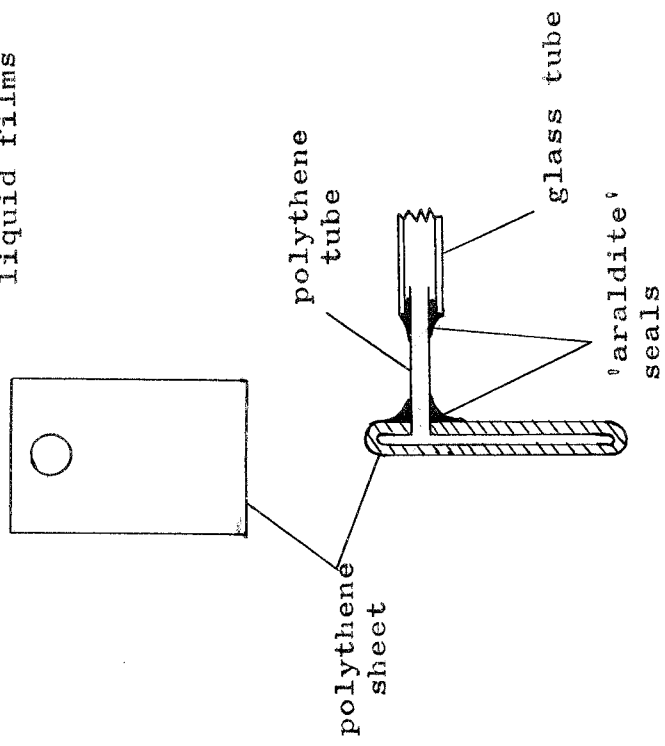


Fig. B.7b.

The cells were first tested for leaks by inflation with compressed air under water, joined to the rest of the apparatus shown in Fig. B7b and evacuated for twenty four hours. Every few hours, nitrogen was forced into the cells and removed by pumping to facilitate the removal of traces of moisture. The sample was placed in flask F and a small quantity of solvent condensed in. When the complex had dissolved, a few drops of the solution were poured on to the sintered glass filter, and about three-quarters of an atmosphere of nitrogen was admitted into the apparatus. The solution was forced into the polythene cell by the sudden rise in pressure, and the cell was carefully sealed off at S. The film thickness was controlled to give the best spectrum by gently warming or cooling the glass tube above the polythene tube, and then clamping the latter with a Mohr's clip. The cell was slotted into a holder, specially made in the Departmental Workshop to fit inside the spectrometer.

(ii) Visible and ultraviolet region

Diffuse reflectance spectra

In the region  $28,500 \text{ cm.}^{-1}$  to  $10,000 \text{ cm.}^{-1}$ , spectra were measured on solid samples using a Unicam SP.500 spectrophotometer fitted with a standard reflectance

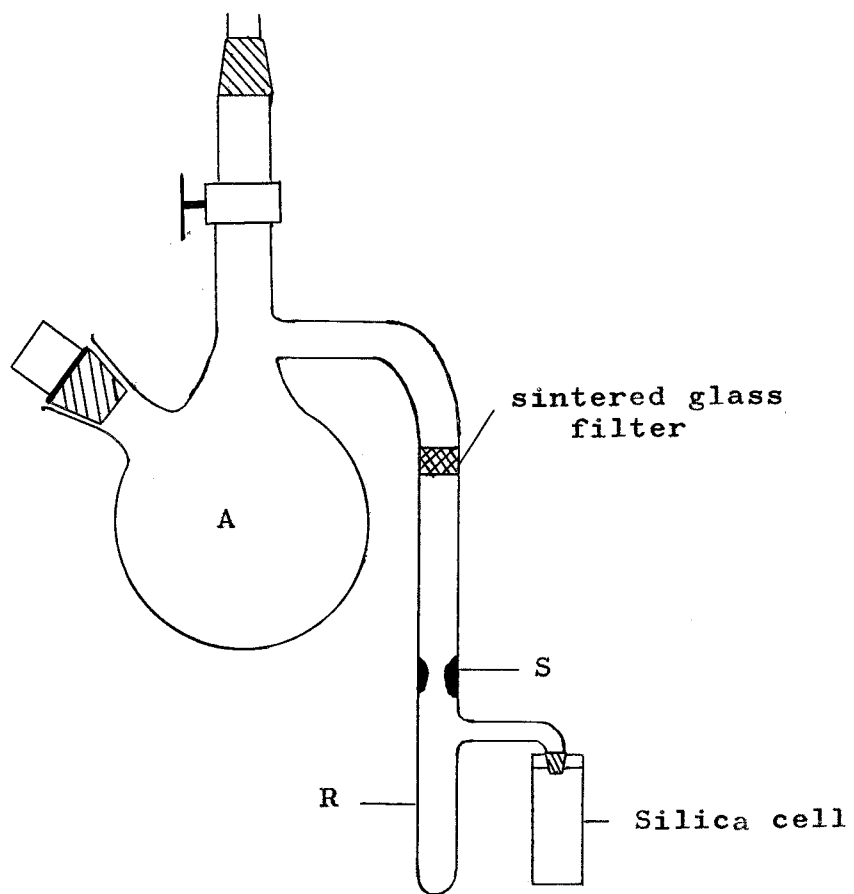
attachment. Samples were prepared in the dry-box under nitrogen between circular glass plates sealed with silicone grease to minimise hydrolysis and oxidation whilst the spectrum was being taken. Sometimes, a drop of dry Nujol, mixed with the compound between the discs, was used in addition to the above precautions when the spectra of very unstable complexes were run. Magnesium oxide or anhydrous calcium carbonate were used as references.

Spectra were recorded automatically on a Unicam SP.700C spectrophotometer fitted with a standard reflectance attachment in the range  $50,000 \text{ cm.}^{-1}$  to  $14,000 \text{ cm.}^{-1}$ . A special holder, fitted with a silica disc was filled with the compound under investigation in the dry-box.

#### Solution Spectra

The spectra were measured in sealed 1 cm. silica cells using Unicam SP.500, SP.700C and SP.800 spectrophotometers. The most useful instrument was found to be the SP.700C as spectra could be recorded automatically on a linear wave number scale from  $50,000 \text{ cm.}^{-1}$  to  $2,800 \text{ cm.}^{-1}$ . Solutions were prepared in the apparatus shown in Fig. B8, the principle of making up a solution of known concentration in reservoir A being precisely

Fig. B.8.





the same as in (b) above.

Concentrations of  $\sim 10^{-2}$  M. were used in the visible region; some complexes were only slightly soluble in the solvent chosen and in these circumstances, the concentration of the solution could not be estimated. The solution was filtered into the cell reservoir, R, and cooled in liquid nitrogen before sealing off at constriction S. The reference cell was filled with a pure sample of solvent distilled from the vacuum line.

To record the spectrum in the ultra-violet region, the solution as prepared above had to be diluted by pouring it from the cell into reservoir R and distilling solvent back into the cell using cotton wool soaked in acetone/"drikold" mixture. In this case, only estimates of the molar extinction coefficients were possible.

The molar extinction coefficient,  $\epsilon_{\max}$ , for a particular spectral band is given by the following expression:

$$\epsilon_{\max} = \frac{E}{C \cdot l.}$$

where E = optical density =  $\log_{10} \frac{I}{I_0}$

C = concentration of the solution in gm. mol. litre<sup>-1</sup>.

l = cell path length (usually 1 cm.)

(e) X-ray Diffraction Techniques<sup>82,153</sup>

(i) Source of X-rays

A stable X-ray beam was supplied by a General Electric X.R.D.6 generator unit fitted with an X-ray tube containing either a copper or molybdenum target. The accelerating potential used was 50 kilovolts and the tube current 30mA.

(ii) Single crystal photographs

This section refers specifically to work carried out on single crystals of trichlorobis(trimethylamine)chromium(III).

Crystals of the complex were grown by slowly evaporating a trimethylamine solution of trichlorobis(trimethylamine)chromium(III) contained in one half of a double ampoule, using ice water as the coolant. The crystals grew as beautiful, purple-blue coloured, elongated rectangular blocks. Several crystals were tipped under nitrogen into hand-drawn 'pyrex' glass capillaries of wall thickness  $\sim 0.15$  mm. Unfortunately, all the crystals were fairly long and the one finally selected by inspection under a microscope had dimensions  $1.68 \times 0.2 \times 0.2$  mm. The tube containing the crystal was sealed off and mounted in plasticine on a goniometer which was then affixed to a Nonius

Weissenberg camera. The crystal was centred optically by arc and translation adjustments so that its long axis was co-incident with the axis of rotation of the camera. A  $10^{\circ}$  oscillation photograph with zirconium filtered  $\text{MoK}\alpha$  radiation revealed a series of layer lines almost perpendicular to the rotation axis, containing single spots. The crystal was thus very nearly mounted about a crystallographic axis.

The goniometer was transferred to a Buerger Precession camera (Charles Supper Incorporated) and the crystal was accurately aligned using unfiltered molybdenum radiation with a  $10^{\circ}$  precession angle, using the method described in the camera manual. A principal reciprocal net was located and photographed with a  $30^{\circ}$  precession angle, using zirconium filtered  $\text{MoK}\alpha$  radiation and a four hour exposure. The spots on this photograph formed a rectangular net. The crystal axis was rotated through  $90^{\circ}$  where another principal net was found and photographed. The spots on this photograph also formed a rectangular net, and therefore the crystal belongs to the orthorhombic system. Measurement of the high angle spots from both photographs gave the following cell dimensions:

$a = 9.69\text{\AA}$ ;  $b = 10.12\text{\AA}$ ;  $c = 13.05\text{\AA}$ . The crystal was mounted about its b axis.

Molybdenum radiation was chosen to take the intensity photographs as the absorption correction for the crystal was negligible ( $\mu \sim 15 \text{ cm.}^{-1}$ ). Copper radiation would have been preferable, but the absorption correction was fairly high and would have been difficult to apply as the crystal was rectangular rather than spherical or rod-shaped. Integrated Weissenberg photographs were taken with filtered  $\text{MoK}\alpha$  radiation, but the fog level on the film was very high owing to the long exposures necessary to produce spots of adequate density.

Unintegrated photographs of the reciprocal planes  $h0l$  to  $h9l$  were taken with a  $116^\circ$  oscillation angle using the equi-inclination Weissenberg camera arrangement and the multiple film technique. Zirconium filtered  $\text{MoK}\alpha$  radiation was used with exposures of fifteen hours for the levels  $h0l$  to  $h6l$ , forty hours for  $h7l$  and thirty hours for  $h8l$  and  $h9l$ . After exposure, each film pack, made from Ilford "G", "B" and "Cx" X-ray film (with "G" nearest the crystal) was carefully developed for five minutes, washed, fixed for ten minutes and washed with water for a least an hour. The films were allowed to dry slowly in a drying cabinet.

A standard intensity wedge was prepared by selecting a well-shaped, strong spot on the zero level

and isolating it on the film with a narrow ( $4^{\circ}$ ) oscillation angle and the Weissenberg arrangement. A series of timed exposures was taken on "B" film to determine the weakest intensity observable with the eye. Twenty-two separate timed exposures were then recorded for the reflexion on the same piece of film, increasing the exposure time from that required to produce the weakest spot so that the ratio between consecutive times was 1.2. The intensities of the spots on the films were then estimated by comparison with this standard wedge; those spots which were too intense on the upper film were measured on the lower films, and the scaling factors obtained by the measurement of spots which appeared on both films were used to correct the intensities to the upper film. The exposure times for the standard spots were taken as an indication of the relative intensity and a set of 'raw' data was thus collected for each reciprocal lattice level. The intensities of reflexions on films exposed for thirty and forty hours were corrected to fifteen hour exposures by the appropriate scaling factors.

The density of the complex was determined by flotation in a mixture of dry 'iso-octane' and dry di-iodomethane, and found to be  $1.43 \text{ gm.ml.}^{-1}$

## APPENDIX C

OBSERVED AND CALCULATED

STRUCTURE AMPLITUDES

FOR

TRICHLOROBISTRIMETHYLAMINECHROMIUM(III)

h	k	l	F <sub>o</sub>	F <sub>c</sub>	h	k	l	F <sub>o</sub>	F <sub>c</sub>
4	0	0	70.67	70.22	4	0	1	5.67	0.97
6	0	0	7.02	-3.50	4	0	2	61.14	59.31
8	0	0	32.09	-35.70	4	0	3	17.57	-13.19
10	0	0	16.32	15.90	4	0	4	6.33	-3.82
0	0	4	104.31	-102.27	4	0	5	12.38	-5.95
0	0	6	52.04	-49.97	4	0	6	14.25	-14.06
0	0	8	61.10	61.32	4	0	7	40.95	-40.12
0	0	10	48.36	48.69	4	0	8	7.80	10.86
0	0	12	8.90	9.28	4	0	9	37.85	-35.57
0	0	14	23.24	-22.45	4	0	10	21.05	21.12
1	0	3	25.12	25.06	4	0	11	29.03	-31.17
1	0	4	97.60	-95.66	4	0	12	9.48	-0.45
1	0	5	31.45	29.48	4	0	13	12.81	-12.80
1	0	6	37.76	-36.32	5	0	1	6.38	-6.31
1	0	7	22.94	-20.99	5	0	2	6.48	-5.27
1	0	8	7.02	0.38	5	0	3	44.42	-45.45
1	0	9	37.96	-39.95	5	0	4	6.90	-0.95
1	0	10	28.14	-25.08	5	0	5	57.28	-59.28
1	0	11	8.46	8.30	5	0	6	16.72	-20.74
1	0	12	34.46	-29.95	5	0	7	36.13	-35.07
1	0	13	13.32	15.05	5	0	8	8.19	-10.23
1	0	14	25.31	-25.09	5	0	9	8.57	7.06
2	0	1	10.82	2.37	5	0	10	8.94	9.55
2	0	2	79.29	-76.14	6	0	1	39.18	-39.88
2	0	3	60.56	-54.44	6	0	2	11.05	8.49
2	0	4	48.61	-46.35	6	0	3	53.16	-50.34
2	0	5	22.24	20.06	6	0	4	11.58	9.98
2	0	6	8.85	-9.74	6	0	5	20.60	18.37
2	0	7	53.67	57.90	6	0	6	19.57	19.00
2	0	8	12.15	13.90	6	0	7	55.20	57.39
2	0	9	35.35	32.82	6	0	8	8.63	-3.83
2	0	10	16.51	-16.12	6	0	9	37.99	39.55
2	0	11	8.57	-8.67	7	0	1	25.99	23.42
2	0	12	20.25	-19.51	7	0	2	7.77	-1.33
3	0	1	51.40	-47.59	7	0	3	23.12	21.55
3	0	2	133.78	135.60	7	0	4	8.07	-5.10
3	0	3	118.10	115.63	7	0	5	33.38	35.66
3	0	4	79.56	79.02	7	0	6	8.52	-8.78
3	0	5	112.14	112.99	7	0	7	25.78	27.12
3	0	6	25.40	-22.60	7	0	8	16.94	-14.94
3	0	7	27.00	26.63	8	0	1	8.35	7.15
3	0	8	18.16	-17.56	8	0	2	13.03	-14.82
3	0	9	21.02	-18.32	8	0	3	8.52	10.31
3	0	10	15.54	11.71	8	0	4	8.67	5.89
3	0	11	16.32	-16.78	8	0	5	13.74	-12.93
3	0	12	35.57	34.00	8	0	6	9.08	3.21
3	0	13	9.69	1.03	8	0	7	15.81	-17.82
3	0	14	13.09	14.95	8	0	8	19.52	-16.99
					8	0	9	18.45	-19.23

h	k	l	F <sub>o</sub>	F <sub>c</sub>	h	k	l	F <sub>o</sub>	F <sub>c</sub>
9	0	1	13.90	16.12	3	1	8	24.14	-24.12
9	0	2	14.02	14.88	3	1	9	7.95	-2.47
9	0	3	14.16	-15.37	3	1	10	14.20	-12.36
9	0	4	17.28	11.15	3	1	11	12.46	10.31
9	0	5	27.73	-29.12	3	1	12	15.68	-18.86
10	0	1	9.64	-2.70	4	1	1	24.49	-25.12
10	0	2	16.42	16.97	4	1	2	47.57	-48.59
					4	1	3	37.21	-33.39
0	1	5	53.32	-51.88	4	1	4	74.12	-72.94
0	1	7	23.23	-21.36	4	1	5	6.75	5.97
0	1	9	41.86	-41.10	4	1	6	47.33	-50.16
0	1	11	22.78	-24.14	4	1	7	7.46	-5.66
0	1	13	15.96	-17.15	4	1	8	7.85	3.75
0	1	15	16.07	-14.44	4	1	9	8.25	-7.69
2	1	0	14.54	20.36	4	1	10	8.66	8.78
4	1	0	18.49	18.22	4	1	11	9.08	-7.20
6	1	0	51.92	53.86	5	1	1	17.41	-17.81
8	1	0	8.38	-3.40	5	1	2	6.59	-6.30
1	1	3	25.11	-28.89	5	1	3	6.76	1.53
1	1	4	5.10	-1.31	5	1	4	6.99	8.94
1	1	5	5.63	-5.46	5	1	5	7.25	14.60
1	1	6	25.95	26.84	5	1	6	29.22	30.12
1	1	7	19.44	-19.88	5	1	7	7.88	-1.33
1	1	8	30.02	28.44	5	1	8	41.80	44.55
1	1	9	29.18	-27.96	5	1	9	14.56	-18.30
1	1	10	12.46	10.31	5	1	10	28.88	30.30
1	1	11	12.04	-12.85	5	1	11	9.39	0.32
1	1	12	8.98	-8.57	5	1	12	16.59	15.69
2	1	1	19.58	19.59	6	1	1	7.15	4.26
2	1	2	23.15	24.44	6	1	2	40.17	38.10
2	1	3	75.39	79.63	6	1	3	7.37	-7.36
2	1	4	57.24	54.56	6	1	4	22.12	23.89
2	1	5	47.23	47.62	6	1	5	7.79	8.91
2	1	6	18.70	18.84	6	1	6	25.91	24.94
2	1	7	16.68	16.13	6	1	7	8.35	1.12
2	1	8	30.69	29.57	6	1	8	17.63	17.59
2	1	9	11.96	12.06	6	1	9	9.01	-5.61
2	1	10	8.18	0.42	7	1	1	20.77	-19.13
2	1	11	30.47	32.72	7	1	2	17.53	15.35
2	1	12	9.08	-11.23	7	1	3	7.96	-2.81
2	1	13	28.01	27.04	7	1	4	8.14	-3.12
3	1	1	38.24	33.97	7	1	5	8.33	2.55
3	1	2	5.27	-6.54	7	1	6	25.15	-25.64
3	1	3	64.23	62.53	7	1	7	8.84	-6.67
3	1	4	5.90	-10.04	7	1	8	20.43	-20.34
3	1	5	34.88	33.91	8	1	1	8.41	7.57
3	1	6	28.27	-28.67	8	1	2	8.47	-6.51
3	1	7	10.99	8.52	8	1	3	8.58	10.24



h	k	l	F <sub>o</sub>	F <sub>c</sub>	h	k	l	F <sub>o</sub>	F <sub>c</sub>
8	1	4	23.28	-25.49	3	2	8	27.67	-27.48
8	1	5	8.92	12.35	3	2	9	8.28	-1.40
8	1	6	18.54	-19.61	3	2	10	23.45	-22.66
9	1	1	16.80	18.51	3	2	11	9.16	-3.96
9	1	2	9.08	0.57	3	2	12	21.53	-20.42
9	1	3	14.21	16.65	4	2	1	34.00	30.60
9	1	4	9.33	4.75	4	2	2	22.12	-22.43
9	1	5	16.05	12.28	4	2	3	73.97	74.85
					4	2	4	28.50	-26.19
0	2	4	60.94	-52.32	4	2	5	24.99	24.13
0	2	6	39.74	-40.88	4	2	6	31.41	-33.30
0	2	8	49.39	-50.20	4	2	7	7.79	1.79
0	2	10	8.35	-5.59	4	2	8	15.26	-14.14
0	2	12	9.31	13.18	4	2	9	8.60	7.43
2	2	0	80.74	-74.06	4	2	10	9.01	0.97
4	2	0	6.06	-6.12	4	2	11	30.29	33.88
6	2	0	7.43	-6.01	4	2	12	9.87	9.93
8	2	0	17.74	17.67	4	2	13	27.62	24.89
1	2	2	58.38	-63.83	5	2	1	71.49	70.63
1	2	3	32.16	-30.05	5	2	2	18.52	-16.57
1	2	4	20.88	-19.14	5	2	3	32.73	31.13
1	2	5	32.98	-32.23	5	2	4	16.36	-11.76
1	2	6	56.54	59.46	5	2	5	7.57	-0.58
1	2	7	11.75	13.77	5	2	6	13.35	14.54
1	2	8	68.31	69.91	5	2	7	8.22	5.22
1	2	9	33.41	34.12	5	2	8	17.46	16.79
1	2	10	38.81	40.74	5	2	9	16.66	12.73
1	2	11	8.85	-0.72	5	2	10	9.34	5.63
1	2	12	9.34	9.22	5	2	11	16.52	16.36
2	2	1	33.40	-31.50	6	2	1	7.46	-12.03
2	2	2	24.72	23.03	6	2	2	18.47	-17.60
2	2	3	18.70	-23.66	6	2	3	22.56	-22.89
2	2	4	95.41	100.91	6	2	4	7.88	-6.35
2	2	5	37.88	-37.62	6	2	5	19.83	-19.15
2	2	6	76.97	75.68	6	2	6	8.40	-3.73
2	2	7	15.96	-10.86	6	2	7	19.46	-16.14
2	2	8	7.60	-0.56	6	2	8	9.02	7.76
2	2	9	12.48	-8.88	6	2	9	19.04	-16.33
2	2	10	14.42	-14.84	7	2	1	59.07	-57.98
2	2	11	8.97	-4.10	7	2	2	8.19	3.15
2	2	12	9.45	-3.54	7	2	3	14.06	-17.90
3	2	1	62.09	-55.92	7	2	4	8.48	6.00
3	2	2	5.59	-2.06	7	2	5	8.67	2.39
3	2	3	61.92	-61.99	7	2	6	8.92	11.70
3	2	4	13.92	-10.66	7	2	7	9.20	-4.72
3	2	5	40.31	-38.82	7	2	8	9.50	14.82
3	2	6	15.67	-11.76	8	2	1	12.38	11.95
3	2	7	12.57	-11.83	8	2	2	12.46	10.20

h	k	l	F <sub>o</sub>	F <sub>c</sub>	h	k	l	F <sub>o</sub>	F <sub>c</sub>
8	2	3	19.95	20.66	3	3	11	10.00	11.48
8	2	4	11.70	7.58	3	3	12	30.76	31.51
8	2	5	17.26	20.47	4	3	1	21.81	-22.69
8	2	6	9.48	6.94	4	3	2	60.79	57.21
9	2	1	9.39	9.57	4	3	3	22.83	-18.47
9	2	2	9.45	3.80	4	3	4	34.46	33.91
9	2	3	9.54	10.01	4	3	5	7.79	3.16
					4	3	6	8.15	15.72
0	3	3	125.27	-119.97	4	3	7	25.03	22.37
0	3	5	15.89	16.58	4	3	8	8.96	-7.25
0	3	7	95.71	97.61	4	3	9	17.48	17.30
0	3	9	68.90	73.43	4	3	10	12.70	10.70
0	3	11	9.65	2.63	5	3	1	16.77	18.30
2	3	0	132.06	-130.73	5	3	2	55.46	-54.47
4	3	0	44.72	44.86	5	3	3	19.02	-19.39
6	3	0	102.81	-103.95	5	3	4	44.61	-43.55
8	3	0	27.95	23.81	5	3	5	11.74	-5.66
1	3	3	75.05	72.44	5	3	6	8.63	-4.62
1	3	4	23.27	-20.18	5	3	7	16.73	18.58
1	3	5	75.85	76.77	5	3	8	13.26	-8.94
1	3	6	33.02	-32.98	5	3	9	15.12	14.67
1	3	7	38.69	39.73	5	3	10	24.89	-22.42
1	3	8	11.53	-9.49	5	3	11	10.63	-6.67
1	3	9	8.65	8.81	5	3	12	27.06	-25.09
1	3	10	9.17	-4.81	6	3	1	8.20	4.37
1	3	11	14.98	-14.84	6	3	2	55.21	-55.04
2	3	1	19.06	16.14	6	3	3	14.25	12.98
2	3	2	33.36	-31.53	6	3	4	14.61	15.30
2	3	3	5.91	5.62	6	3	5	8.88	-5.40
2	3	4	22.51	18.48	6	3	6	14.25	16.66
2	3	5	20.18	-17.67	6	3	7	9.51	1.14
2	3	6	7.38	0.47	6	3	8	22.02	-21.96
2	3	7	47.76	-50.88	6	3	9	10.20	-1.21
2	3	8	32.12	-33.34	6	3	10	28.35	-27.88
2	3	9	39.05	-39.95	7	3	1	19.81	18.49
2	3	10	14.42	-12.80	7	3	2	21.85	21.27
2	3	11	26.17	-25.82	7	3	3	12.83	2.22
3	3	1	43.79	40.05	7	3	4	22.64	20.08
3	3	2	65.38	62.49	7	3	5	9.47	-2.78
3	3	3	62.83	-63.70	7	3	6	9.75	13.49
3	3	4	60.32	60.72	7	3	7	10.02	8.59
3	3	5	88.24	-90.84	8	3	1	9.56	7.49
3	3	6	7.72	-0.63	8	3	2	19.56	18.31
3	3	7	34.46	-33.36	8	3	3	9.75	8.76
3	3	8	20.99	-18.07	8	3	4	9.90	11.42
3	3	9	24.18	24.32	8	3	5	17.11	-16.30
3	3	10	17.74	14.76	8	3	6	10.33	-3.36

h	k	l	F <sub>o</sub>	F <sub>c</sub>	h	k	l	F <sub>o</sub>	F <sub>c</sub>
8	3	7	19.74	-21.83	4	4	1	6.12	-1.77
9	3	1	10.23	-4.99	4	4	2	21.98	22.49
9	3	2	17.44	-21.82	4	4	3	32.37	-31.86
9	3	3	17.60	-19.28	4	4	4	6.68	8.78
9	3	4	16.35	-16.96	4	4	5	20.42	-20.10
9	3	5	21.82	-24.30	4	4	6	19.49	19.79
					4	4	7	7.63	-13.07
0	4	4	51.57	54.85	4	4	8	8.01	5.31
0	4	6	6.35	4.84	4	4	9	15.60	-16.36
0	4	8	25.64	27.05	4	4	10	8.76	0.13
0	4	10	15.17	11.99	4	4	11	26.80	-27.88
2	4	0	4.63	-5.43	5	4	1	44.86	-43.55
4	4	0	36.89	33.66	5	4	2	6.82	-4.46
6	4	0	7.30	-2.31	5	4	3	29.55	-29.20
8	4	0	8.50	-8.97	5	4	4	7.20	-9.41
1	4	1	24.29	-29.44	5	4	5	15.14	-12.18
1	4	3	19.14	19.14	5	4	6	7.72	-4.20
1	4	4	5.47	-6.75	5	4	7	12.43	-10.45
1	4	5	5.94	1.90	5	4	8	8.37	0.12
1	4	6	42.72	-41.56	5	4	9	13.47	-11.15
1	4	7	18.31	-16.81	6	4	1	7.34	12.18
1	4	8	44.44	-44.96	6	4	2	10.49	12.57
1	4	9	17.28	-16.51	6	4	3	10.67	13.35
1	4	10	21.87	-22.12	6	4	4	7.71	6.16
1	4	11	8.62	3.17	6	4	5	7.95	4.37
2	4	1	8.83	8.85	6	4	6	8.20	4.48
2	4	2	43.97	-42.60	6	4	7	15.77	16.47
2	4	3	22.74	17.48	6	4	8	8.76	-0.73
2	4	4	53.21	-51.92	6	4	9	24.24	24.16
2	4	5	34.39	33.50	7	4	1	27.87	29.75
2	4	6	36.77	-32.42	7	4	2	7.99	-2.80
2	4	7	7.03	1.10	7	4	3	18.13	21.90
2	4	8	7.46	-0.59	7	4	4	8.26	-2.17
2	4	9	7.88	10.99	7	4	5	8.44	11.69
2	4	10	8.31	2.34	7	4	6	8.68	-7.84
2	4	11	14.76	12.10	8	4	1	8.52	-3.74
3	4	1	43.56	45.60	8	4	2	8.58	-6.67
3	4	2	5.63	1.73	8	4	3	8.68	-4.79
3	4	3	32.75	31.31	8	4	4	8.81	-10.96
3	4	4	26.19	26.56	8	4	5	8.99	-13.81
3	4	5	39.86	38.63	8	4	6	9.19	-10.94
3	4	6	20.30	20.67					
3	4	7	23.46	22.89	0	5	3	25.08	-25.73
3	4	8	7.68	12.09	0	5	5	33.01	-30.96
3	4	9	8.10	-0.56	0	5	7	26.42	-24.08
3	4	10	8.51	9.04	0	5	9	20.65	-18.19
3	4	11	8.90	-0.18	0	5	11	9.41	-8.85

h	k	l	F <sub>o</sub>	F <sub>c</sub>	h	k	l	F <sub>o</sub>	F <sub>c</sub>
0	5	13	21.04	-20.08	5	5	2	7.52	-8.95
2	5	0	45.73	40.68	5	5	3	13.03	14.24
4	5	0	28.33	24.90	5	5	4	7.92	-1.77
6	5	0	28.28	24.85	5	5	5	21.82	19.06
8	5	0	9.30	8.65	5	5	6	15.79	19.47
1	5	1	99.94	-105.81	5	5	7	8.81	-1.08
1	5	3	37.16	-37.08	5	5	8	38.68	39.42
1	5	4	6.10	1.58	5	5	9	9.53	-12.13
1	5	5	23.21	19.17	5	5	10	26.48	26.19
1	5	6	26.17	27.11	6	5	1	8.07	-0.90
1	5	7	7.55	2.59	6	5	2	21.79	23.87
1	5	8	17.96	18.22	6	5	3	8.29	-3.02
1	5	9	29.91	-29.30	6	5	4	22.65	22.23
1	5	10	8.96	8.55	6	5	5	8.71	8.69
1	5	11	17.56	-16.15	6	5	6	21.96	21.80
2	5	1	35.58	36.64	6	5	7	9.27	-1.93
2	5	2	8.70	7.63	6	5	8	16.24	17.92
2	5	3	68.92	72.83	7	5	1	16.17	-15.52
2	5	4	17.16	18.01	7	5	2	21.39	20.78
2	5	5	34.73	31.09	7	5	3	8.88	0.45
2	5	6	33.83	28.60	7	5	4	9.06	10.27
2	5	7	7.75	0.05	7	5	5	9.24	3.14
2	5	8	21.89	21.08	7	5	6	23.21	-22.87
2	5	9	8.65	-1.08	7	5	7	9.76	-9.88
2	5	10	9.10	-4.70	7	5	8	24.59	-26.87
2	5	11	23.32	23.13	8	5	1	9.32	-0.50
2	5	12	10.01	7.06	8	5	2	9.39	-3.85
2	5	13	25.62	24.72	8	5	3	9.50	1.64
3	5	1	33.63	34.81	8	5	4	23.54	-25.20
3	5	2	13.97	10.73	8	5	5	9.84	12.05
3	5	3	36.30	34.64	8	5	6	17.01	-18.15
3	5	4	12.76	-11.45					
3	5	5	21.22	17.57	0	6	4	13.20	10.58
3	5	6	18.64	-17.76	0	6	6	22.16	16.84
3	5	7	8.01	1.43	0	6	8	30.25	-32.33
3	5	8	15.70	-18.06	0	6	10	25.54	-25.78
3	5	9	8.86	-5.33	2	6	0	45.55	43.41
3	5	10	18.92	-19.53	4	6	0	36.66	-36.05
4	5	1	18.07	-9.70	6	6	0	8.62	-5.21
4	5	2	24.28	-21.39	8	6	0	16.83	19.70
4	5	3	32.64	-30.76	1	6	2	40.16	40.95
4	5	4	64.50	-63.71	1	6	3	6.08	-3.80
4	5	5	17.17	-13.63	1	6	4	33.54	34.40
4	5	6	48.85	-50.16	1	6	5	11.03	5.41
4	5	7	8.37	5.17	1	6	6	13.66	14.39
4	5	8	8.77	5.90	1	6	7	14.57	12.39
4	5	9	9.17	3.90	1	6	8	8.62	5.67
5	5	1	34.30	-32.87	1	6	9	12.88	10.27

h	k	l	F <sub>o</sub>	F <sub>c</sub>	h	k	l	F <sub>o</sub>	F <sub>c</sub>
1	6	10	16.25	17.73	6	6	8	10.26	-1.13
1	6	11	10.08	-5.20	6	6	9	25.91	-24.48
1	6	12	19.69	22.43	7	6	1	9.31	-9.00
2	6	1	5.83	4.45	7	6	2	9.39	6.25
2	6	2	40.76	41.01	7	6	3	19.33	-19.77
2	6	3	6.52	10.11	7	6	4	9.69	6.10
2	6	4	16.98	15.78	7	6	5	24.13	-24.23
2	6	5	18.07	-17.35					
2	6	6	7.88	4.82	0	7	5	13.14	13.37
2	6	7	22.23	-20.58	0	7	7	20.68	19.07
2	6	8	8.80	4.09	0	7	9	30.38	30.56
2	6	9	15.68	-18.21	0	7	11	20.33	20.22
2	6	10	15.08	12.98	2	7	0	19.54	-18.27
3	6	1	6.59	2.17	4	7	0	15.62	13.56
3	6	2	34.43	-35.30	6	7	0	31.60	-31.63
3	6	3	39.28	-41.97	8	7	0	11.04	13.74
3	6	4	31.34	-32.72	1	7	3	22.65	20.80
3	6	5	47.56	-54.43	1	7	4	5.28	-4.87
3	6	6	8.20	0.46	1	7	5	24.03	21.08
3	6	7	19.27	-17.03	1	7	6	8.57	-7.24
3	6	8	9.04	4.57	1	7	7	24.89	22.61
3	6	9	14.70	11.13	1	7	8	11.52	-8.87
3	6	10	9.96	-8.70	1	7	9	16.20	12.75
3	6	11	10.41	6.95	2	7	1	4.69	2.78
3	6	12	19.45	-19.99	2	7	2	16.81	-15.54
4	6	1	14.87	-10.91	2	7	3	8.12	-8.06
4	6	2	21.84	-21.97	2	7	4	19.59	-20.13
4	6	3	7.61	-2.72	2	7	5	14.39	-14.10
4	6	4	7.94	2.33	2	7	6	8.82	-6.58
4	6	5	15.41	11.47	2	7	7	17.68	-17.62
4	6	6	8.62	-1.64	2	7	8	10.82	-8.38
4	6	7	31.70	30.24	2	7	9	16.48	-17.05
4	6	8	9.40	-6.58	2	7	10	7.64	-2.08
4	6	9	21.93	22.99	2	7	11	19.62	-18.92
5	6	1	13.54	9.81	3	7	1	5.25	-6.45
5	6	2	8.09	5.21	3	7	2	8.44	7.39
5	6	3	29.14	29.57	3	7	3	21.80	-23.32
5	6	4	8.51	5.27	3	7	4	14.39	13.12
5	6	5	33.83	32.91	3	7	5	23.88	-25.20
5	6	6	9.09	3.44	3	7	6	14.49	15.88
5	6	7	15.97	17.26	3	7	7	18.29	-14.28
6	6	1	8.67	11.62	3	7	8	11.11	10.91
6	6	2	8.76	-7.99	4	7	1	5.82	3.36
6	6	3	18.09	17.52	4	7	2	30.25	28.19
6	6	4	9.08	0.27	4	7	3	6.05	4.32
6	6	5	9.33	-8.10	4	7	4	29.27	27.17
6	6	6	9.63	-4.36	4	7	5	6.52	-4.40
6	6	7	31.87	-31.81	4	7	6	16.65	14.65

h	k	l	F <sub>o</sub>	F <sub>c</sub>	h	k	l	F <sub>o</sub>	F <sub>c</sub>
4	7	7	7.08	5.91	4	8	2	7.70	6.67
5	7	1	6.32	-1.70	4	8	3	31.51	-32.87
5	7	2	6.39	-8.83	4	8	4	18.93	15.32
5	7	3	6.54	1.72	4	8	5	11.34	-11.09
5	7	4	15.00	-13.23	4	8	6	12.98	14.98
5	7	5	6.91	4.22	5	8	1	36.05	-36.27
5	7	6	14.73	-14.83	5	8	2	8.31	8.28
5	7	7	7.41	4.79	5	8	3	13.63	-12.99
5	7	8	18.85	-16.64	6	8	1	8.82	6.31
5	7	9	7.99	5.78	6	8	2	8.94	5.33
5	7	10	12.95	-11.67	6	8	3	16.03	15.10
6	7	1	6.81	2.31	7	8	1	26.45	30.48
6	7	2	21.37	-23.80					
6	7	3	7.00	9.54	0	9	5	15.48	-14.86
6	7	4	11.16	-11.35	0	9	7	20.94	-22.70
7	7	1	15.09	11.57	0	9	9	21.22	-22.41
					2	9	0	15.51	19.17
0	8	4	27.24	23.48	4	9	0	25.08	-25.15
0	8	6	34.36	31.56	6	9	0	29.27	29.93
0	8	8	20.33	20.41	1	9	3	21.49	-21.62
4	8	0	7.51	-4.89	1	9	4	7.58	4.97
6	8	0	8.82	5.15	1	9	5	27.02	-27.75
1	8	2	25.84	27.79	1	9	6	8.61	1.19
1	8	3	6.39	1.35	1	9	7	13.40	-12.15
1	8	4	6.91	5.96	2	9	1	6.80	-7.85
1	8	5	11.88	10.33	2	9	2	13.69	13.12
1	8	6	26.35	-26.54	2	9	3	7.47	-3.00
1	8	7	8.36	-2.65	2	9	4	7.91	5.80
1	8	8	32.30	-32.94	2	9	5	16.18	13.20
1	8	9	16.42	-14.17	2	9	6	8.84	-0.34
1	8	10	20.66	-22.47	2	9	7	19.60	21.75
2	8	3	15.79	13.91	3	9	1	7.55	3.09
2	8	4	41.64	-42.19	3	9	2	17.95	-16.88
2	8	5	11.27	10.18	3	9	3	18.64	19.06
2	8	6	35.65	-36.04	3	9	4	13.46	-12.55
2	8	7	8.53	5.29	3	9	5	18.48	19.04
3	8	1	24.14	23.39	4	9	1	8.27	-1.03
3	8	2	7.05	-2.96	4	9	2	21.46	-21.74
3	8	3	24.54	25.57	5	9	1	8.94	-1.74
3	8	4	7.66	-1.26	5	9	2	14.54	14.21
3	8	5	8.04	8.56	6	9	1	9.58	3.25
3	8	6	8.42	7.16	6	9	2	15.62	17.11
4	8	1	17.55	-17.15					

## REFERENCES

1. J. Selbin, Chem. Rev., 65 (1965) 153.
2. J. Selbin, Coord. Chem. Rev. 1 (1966) 293.
3. N.V. Sidgwick, "The Chemical Elements and their Compounds". Oxford U.P. 1962.
4. D. Nicholls, Coord. Chem. Rev. 1 (1966) 379.
5. J.H. Canterford and T.A.O'Donnell, Inorg. Chem. 6 (1967) 541
6. W.E. Dasent, "Nonexistent Compounds". E. Arnold (London) 1965 page 133.
7. R.E.McCarley and J.W. Roddy, Inorg. Chem., 3 (1964) 54
8. R.G. Cavell and H.C. Clarke, J.C.S. (1962) 2692.
9. Y. Morino and H. Uehara, J. Chem. Phys. 45 (1966) 4543.
10. J.A. Creighton, J. Green, W. Kynaston, J.C.S.(A) (1966) 208.
11. R.J.H. Clark and D.J. Machin, J.C.S. (1963) 4430.
12. F.A.Cotton and G. Wilkinson, "Advanced Inorganic Chemistry", Second Ed. Interscience 1966.
13. A.F. Wells, "Structural Inorganic Chemistry", Oxford 1962.
14. B.N. Figgis and J. Lewis, "Prog. Inorg. Chem". Vol. 6. Ed. Cotton, Interscience 1964 p.111.
15. W. Klemm and L. Grimm, Z. anorg. Chem., 249 (1941) 198.
16. H. Selig and H.H. Claasen, J. Chem. Phys., 44 (1966) 1404.

17. F.A. Miller and L.R. Cousins, J. Chem. Phys.,  
26 (1957) 329.
18. F.A. Miller and W.K. Baer, Spect. Acta. 17 (1961)  
112.
19. H. Funk, W. Weiss and M. Zeising, Z. anorg. Chem.,  
296 (1958) 36.
20. C.N. Caughlan, H.M. Smith and K. Watenpaugh,  
Inorg. Chem., 5 (1966) 2131.
21. G.J. Moody and H. Selig, J. Inorg. Nucl. Chem.,  
28 (1966) 2429.
22. R.J.H. Clark, M.L. Greenfield and R.S. Nyholm,  
J.C.S.(A) (1966) 1254.
23. R.J.H. Clark, J. Lewis and R.S. Nyholm, J.C.S.  
(1962) 2460.
24. R.J.H. Clark, J. Lewis, R.S. Nyholm, P. Pauling  
and G.B. Robertson, Nature, 192 (1961) 222.
25. R.J.H. Clark, J.C.S. (1965) 5699.
26. M.W. Duckworth and G.W.A. Fowles, J. Less-Common  
Metals, 4 (1962) 338.
27. D.C. Bradley, R.K. Multani and W. Wardlaw.  
J.C.S. (1958) 4647.
28. R.K.Y. Ho, S.E. Livingstone and T.N. Lockyer,  
Aust. J. Chem., 19 (1966) 1179.
29. G.W.A. Fowles and R.A. Walton, J. Inorg. Nucl.  
Chem., 27 (1965) 735.
30. P.A. Kilty and D. Nicholls, J.C.S. (1965) 4915.
31. P.A. Kilty and D. Nicholls, J.C.S.(A) (1966) 1175.
32. M.H.L. Pryce and W.A. Runciman, Disc. Far. Soc.,  
26 (1958) 34.



33. S.C. Furman and C.S. Garner, J.A.C.S. 72 (1950) 1785.
34. B.N. Figgis, J. Lewis and F. Mabbs, J.C.S. (1960) 2480.
35. G.W.A. Fowles and W.R. McGregor, J.C.S. (1958) 136.
36. R.J.H. Clark and M.L. Greenfield, J.C.S.(A) (1967) 409.
37. D.J. Machin, K.S. Murray and R.A. Walton, to be published.
38. D.C. Bradley and M.L. Mehta, Can. J. Chem., (1962) 40 1710.
39. G.W.A. Fowles, P.G. Lanigan and D. Nicholls, Chem. Ind. (London) 1961 1167.
40. D. Nicholls, J. Inorg. Nucl. Chem., 24 (1962) 1001
41. N.N. Greenwood, P.V. Parish and P. Thornton, J.C.S.(A) (1966) 320.
42. H. Böhlend and P. Malitzke, Z. Naturforsch, 20 (11) 1126 (1965).
43. H. Böhlend and P. Malitzke, Z. anorg. Chem., 350 (1967) 70.
44. G.W.A. Fowles and B.J. Russ, J.C.S.(A) (1967) 517.
45. J. Lewis, R.S. Nyholm and P.W. Smith, J.C.S. (1961) 4590.
46. J. Burmeister and L.E. Williams, J. Inorg. Nucl. Chem., 29 (1967) 839
47. D.M. Adams, J. Chatt, J.M. Davidson and J. Gerratt, J.C.S. (1963) 2189.
48. G.J. Wessel and D.J.W. Ijdo, Acta. Cryst., 10 (1957) 466.

49. R.J.H. Clark, R.S. Nyholm. and D.E. Scaife, J.C.S.(A) (1966) 1296.
50. R.H. Fenn, A.J. Graham and R.D. Gillard, Nature, 213 (1967) 1012.
51. S. Herzog, Z. anorg. Chem., 294 (1958) 155.
52. W.A. Hieber et al., Chem. Ber., 94 (1961) 2572.
53. H. Funk, G. Mohaupt and A. Paul, Z. anorg. Chem., 302 (1959) 199.
54. G.W.A. Fowles and P.G. Lanigan, J. Less-Common Metals, 6 (1964) 396.
55. D.M. Gruen and R.L. McBeth, J. Phys. Chem. 66 (1962) 57.
56. F. Calderazzo, Inorg. Chem., 5 (1966) 429.
57. A. Davison, N. Edelstein, R.H. Holm and A.H. Maki, Inorg. Chem., 4 (1965) 55.
58. R. Eisenberg, E.I. Stiefel, R.C. Rosenberg, and H.B. Gray, J.A.C.S., 88 (1966) 2874.
59. H. Montgomery et al., Acta Cryst., 22 (1967) 775.
60. G.W.A. Fowles and R.A. Hoodless, J.C.S. (1963) 33.
61. P. Walden and E.J. Birr, Z. phys. Chem. A, 144 (1929) 269.
62. A.C. Harkness and H.M. Daggett, Can. J. Chem., 43 (1965) 1215.
63. R.D. Feltham and R.G. Hayter, J.C.S. (1964) 4587.
64. F.A. Cotton, "Chemical Applications of Group Theory", Interscience 1963.
65. R.S. Drago, "Physical Methods in Inorganic Chemistry", Reinhold 1965.

66. J.P. Clark, V.M. Langford and C.J. Wilkins, J.C.S.(A) (1967) 792.
67. R.J. Kern, J. Inorg. Nucl. Chem., 1962 24 1105.
68. M.W. Duckworth, G.W.A. Fowles, R.A. Hoodless, J.C.S. (1963) 5665.
69. K.F. Purcell, R.S. Drago, J.A.C.S., 88 (1966) 919.
70. K.F. Purcell, J.A.C.S., 89 (1967) 247.
71. F.A. Cotton, C. Oldham, R.A. Walton, Inorg. Chem., 6 (1967) 214.
72. R.J.H. Clark, Spect. Acta., (1965) 21 955.
73. I.R. Beattie and T. Gilson, J.C.S. (1964) 3528.
74. I.R. Beattie and F.W. Parrett, J.C.S.(A) (1966) 1784.
75. B.N. Figgis, "Introduction to Ligand Fields", Wiley 1966.
76. C.J. Balhausen, "Introduction to Ligand Field Theory", McGraw Hill 1962.
77. J.S. Wood, private communication
78. C.K. Jørgensen, "Absorption Spectra and Chemical Bonding in Complexes", Pergamon 1962.
79. G. Dyer and D.W. Meek, Inorg. Chem., 6 (1967) 149.
80. B.N. Figgis, Nature, 182 (1958) 1568.
81. J.C.D. Brand and J.C. Speakman, "Molecular Structure", Arnold 1950.
82. H. Lipson and W. Cochran, "The Determination of Crystal Structures" Bell 1966.

83. W.W. Brandt, F.P. Dwyer and E.C. Gyarfas, Chem. Rev., 54 (1954) 959.
84. C.K. Jørgensen, "Inorganic Complexes", Academic Press 1963, p.70.
85. G.W.A. Fowles and R.A. Walton, J. Less-Common Metals, 5 (1963) 510.
86. R.J.H. Clark, J.C.S., (1963) 1377.
87. G.W.A. Fowles, R.A. Hoodless and R.A. Walton, J. Inorg. Nucl. Chem., 27 (1965) 391.
88. G.R. Willey, private communication.
89. P.G. Lanigan, Ph.D. Thesis, University of Southampton 1962.
90. M.W. Duckworth, Ph.D. Thesis, University of Southampton 1962.
91. R.A. Hoodless, Ph.D. Thesis, University of Southampton 1962.
92. G.W.A. Fowles and R.A. Walton, J. Less-Common Metals, 2 (1965) 457.
93. N.S. Gill et al., J. Inorg. Nucl. Chem., 18 (1961) 79.
94. J.R. Durig et al., Spect. Acta, 23A (1967) 1121.
95. N.N. Greenwood and K. Wade, J.C.S. (1960) 1130.
96. R.J.H. Clark and C.S. Williams, Inorg. Chem., (1965) 4 350.
97. R.A. Walton, Q. Rev., (1965) 19 126.
98. A.A. Schilt and R.C. Taylor, J. Inorg. Nucl. Chem., 2 (1959) 211.
99. R.G. Inskeep, J. Inorg. Nucl. Chem., 24 (1962) 763.

100. N.S. Gill and R.S. Nyholm, J.C.S. (1959) 3997.
101. T.E. Lester, private communication
102. D. Hall, A.D. Rae and T.N. Waters, Acta Cryst., 22 (1967) 258.
103. K. Watenpaugh and C N. Caughlan, Inorg. Chem., 6 (1967) 963.
104. W.M. Carmichael, D.A. Edwards and R.A. Walton, J.C.S.(A) (1966) 97.
105. S.E. Livingston and B. Wheelahan, Aust. J. Chem., 17 (1964) 219.
106. F.P. Dwyer, H.A. Goodwin, E.C. Gyarfas, Aust. J. Chem., 16 (1963) 544.
107. R.J.H. Clark, and C.S. Williams, Spect. Acta., 21 (1965) 1861.
108. R.J.H. Clark and C.S. Williams, *ibid.* 23A (1967) 1055.
109. W.R. McWhinnie, J. Inorg. Nucl. Chem., 27 (1965) 1063.
110. J.R. Ferraro et al., Inorg. Chem., 5 (1966) 391.
111. C.K. Jørgensen, Acta. Chem. Scand., 9 (1955) 1362.
112. K. Nakamoto, J. Phys. Chem., 64 (1960) 1420.
113. B.E. Bridgland, G.W.A. Fowles and R.A. Walton, J. Inorg. Nucl. Chem., 27 (1965) 383.
114. G.W.A. Fowles, R.A. Hoodless and R.A. Walton, J.C.S. (1963) 5873.
115. R.J.H. Clark, J. Lewis, D.J. Machin, and R.S. Nyholm, J.C.S. (1963) 379.

116. E. Kurras, *Naturewiss.*, 46 (1959) 171.
117. B.E. Bridgland, M.Sc. Thesis, University of Southampton 1964.
118. W. Herwig and H.H. Zeiss, *J. Org. Chem.*, 23 (1958) 1404.
119. A. Palm and E.R. Bissell, *Spect. Acta*, 16 (1960) 459.
120. B.J. Russ, Ph.D. Thesis, University of Southampton 1966.
121. A. Miyake, *J.A.C.S.*, 82 (1960) 3040.
122. R.J.H. Clark and W. Errington, *Inorg. Chem.*, 5 (1966) 650.
123. B.J. Brisdon, T.E. Lester and R.A. Walton, *Spect. Acta.*, 23A (1967) 1969.
124. I.R. Beattie and T. Gilson, *J.C.S.*, (1965) 6595.
125. M. Antler and A.W. Laubengayer, *J.A.C.S.*, 77 (1955) 5250.
126. B.J. Russ and J.S. Wood, *Chem. Comm.*, (1966) 745.
127. K. Issleib and G. Bohn, *Z. anorg. Chem.*, 301 (1959) 188.
128. G.W.A. Fowles and C.M. Pleass, *Chem. and Ind.*, (1955) 1743; *J.C.S.*, (1957) 1674.
129. M.W. Duckworth, G.W.A. Fowles and R.G. Williams, *Chem. and Ind.*, (1962) 1285.
130. H. Yada, T. Tanaka and S. Nagakura, *J. Mol. Spect.* (1962) 9 461.
131. J.R. Alkins and P.J. Hendra, *Spect. Acta.*, (1966) 22 2075.
132. L.J. Bellamy, "The Infrared Spectra of Complex Molecules", Methuen London 1960, p.353.

133. J. Lewis, J.R. Miller, R.L. Richards, and A. Thompson, J.C.S. (1965) 5850.
134. C.K. Jørgensen, private communication to G.W.A. Fowles.
135. M. Ciampolini, N. Nardi and G.P. Speroni, Coord. Chem. Rev. (1966) 1 222.
136. See for example, M. DiVaira and P.L. Orioli, Inorg. Chem., (1967) 6 955.
137. C.W. Heitsch, C.E. Nordman and R.W. Parry, Inorg. Chem., 2 (1963) 508.
138. International Tables for X-ray Crystallography, Kynoch Press 1952, Vol.1.
139. ibid. Vol.3, page 136.
140. ibid. Vol.3, page 202.
141. D.C. Phillips, Acta. Cryst., 7 (1954) 746.
142. B.J. Russ and J.S. Wood, unpublished observations.
143. J.J. Daley, J.C.S.(A) (1967) 739.
144. B. Morosin, Acta. Cryst. 21 (1966) 280.
145. L.D. Calvert and C.M. Pleass, Can. J. Chem., (1962) 40 1473.
146. D.R. Lide and D.E. Mann, J. Chem. Phys., 28 (1958) 572.
147. G.B. Heisig et al., Inorg. Syntheses, 2 (1946) 193.
148. L.W. McCay and W.T. Anderson, J.A.C.S. 44 (1922) 1018.
149. G.W.A. Fowles and C.M. Pleass, J. Chem. Ed. 33 (1956) 640.
150. A. Findlay, "Practical Physical Chemistry", Longman (1960) p.107.

151. B.N. Figgis and J. Lewis, "Modern Coordination Chemistry", Interscience 1960.
152. B.N. Figgis and R.S. Nyholm, J.C.S., (1959) 331.
153. N.F.M. Henry, H. Lipson and W.A. Wooster, "Interpretation of X-ray Diffraction Photographs", Macmillan 1960, p.82.